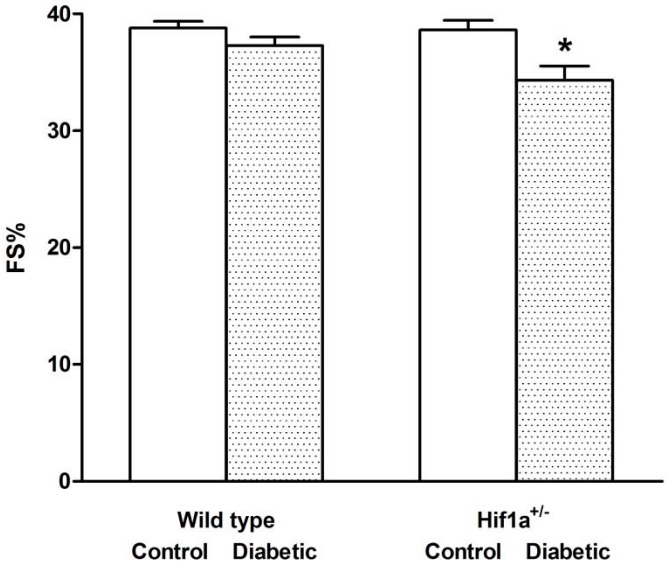


**Figure 1.** Echocardiographic assessment of cardiac function in *wt* and *Hif1a*$^{+/-}$ mice. Systolic dysfunction was calculated from LV dimensions as fractional shortening. The exposure to diabetic environment resulted in a significant decrease of LV fractional shortening (FS) in *Hif1a*$^{+/-}$ mice but not in *wt* animals.

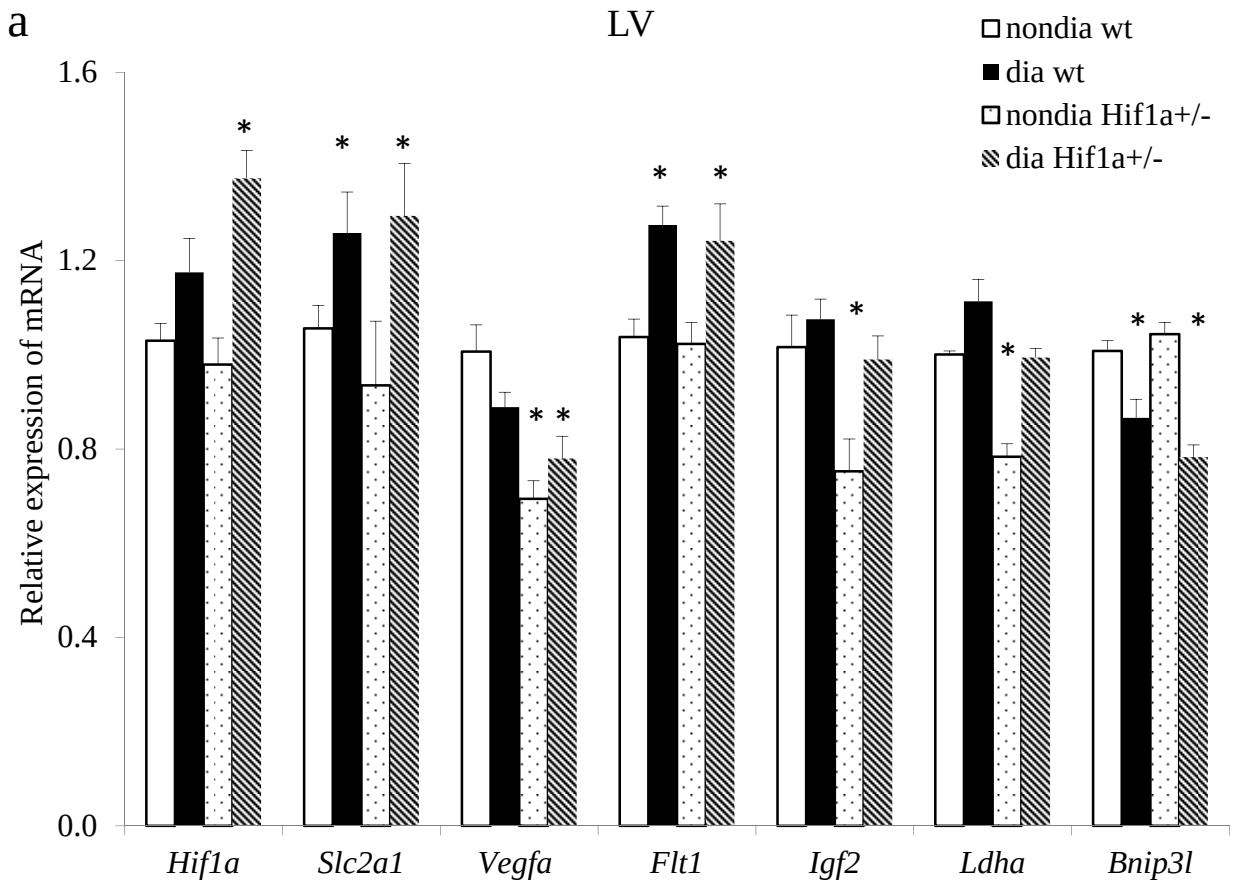
a
LV
nondia wt
dia wt
nondia Hif1a+/-
dia Hif1a+/-
Relative expression of mRNA
1.6
1.2
0.8
0.4
0.0
Hif1a
Slc2a1
Vegfa
Flt1
Igf2
Ldha
Bnip3l

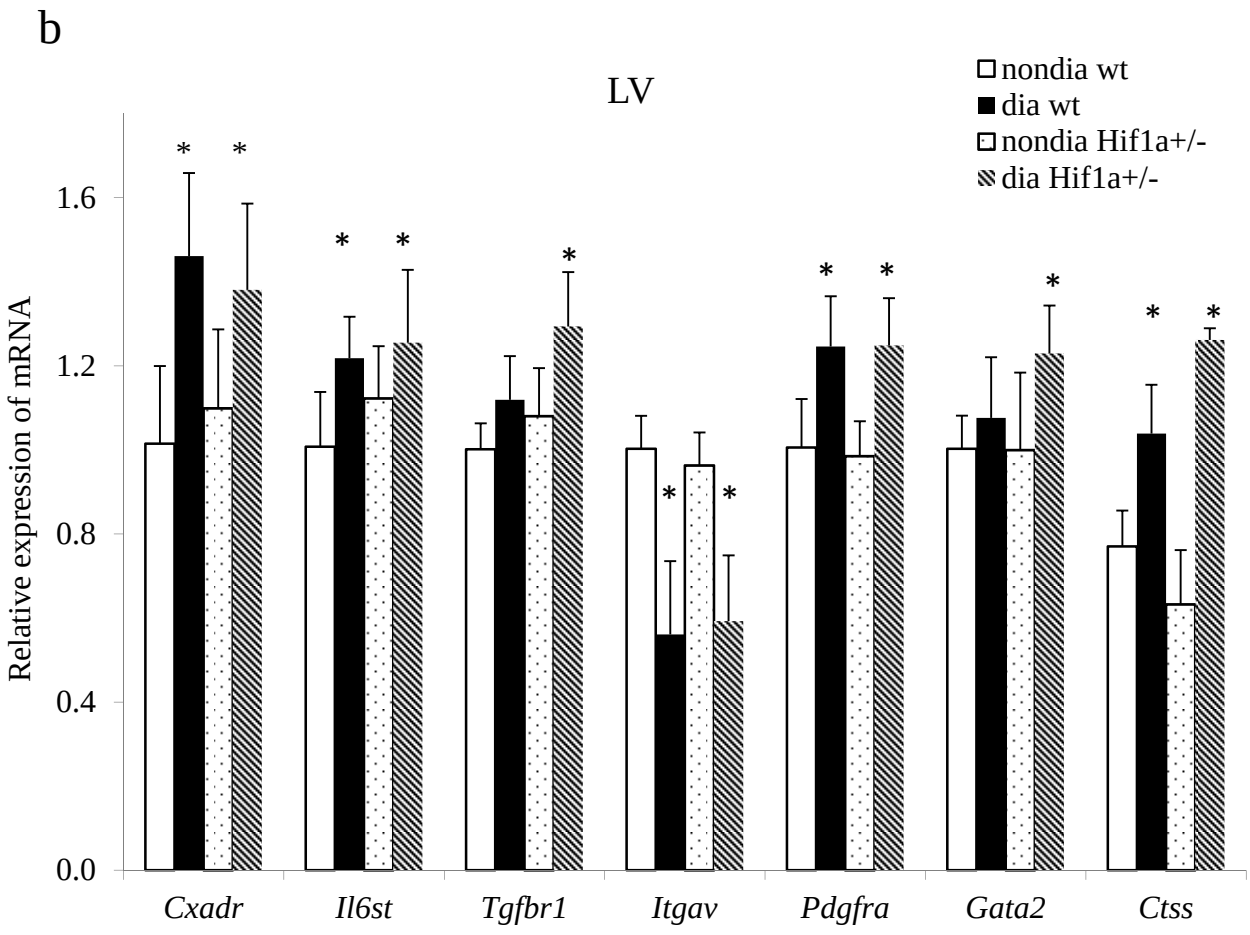
b
LV
nondia wt
dia wt
nondia Hif1a+/-
dia Hif1a+/-
Relative expression of mRNA
1.6
1.2
0.8
0.4
0.0
Cxadr
Il6st
Tgfbr1
Itgav
Pdgfra
Gata2
Ctss

**Figure 2.** Gene expression profile of *wt* and *Hif1a*$^{+/-}$ mice. The expression of selected genes was analyzed using RT-qPCR. The relative expression levels were quantified using ΔΔCT method. The data represent an expression of mRNA relative to non-diabetic *wt* expression of mRNA, normalized by the housekeeping mRNA of *Hprt1*. The values are means ± STDEV (each experiment in duplicate; n = 8). Differences in normalized Ct values were tested for statistical significance by one-way ANOVA followed by Bonferroni's multiple comparison post-test. *, $P < 0.05$, **, $P < 0.01$, ***, $P < 0.001$.

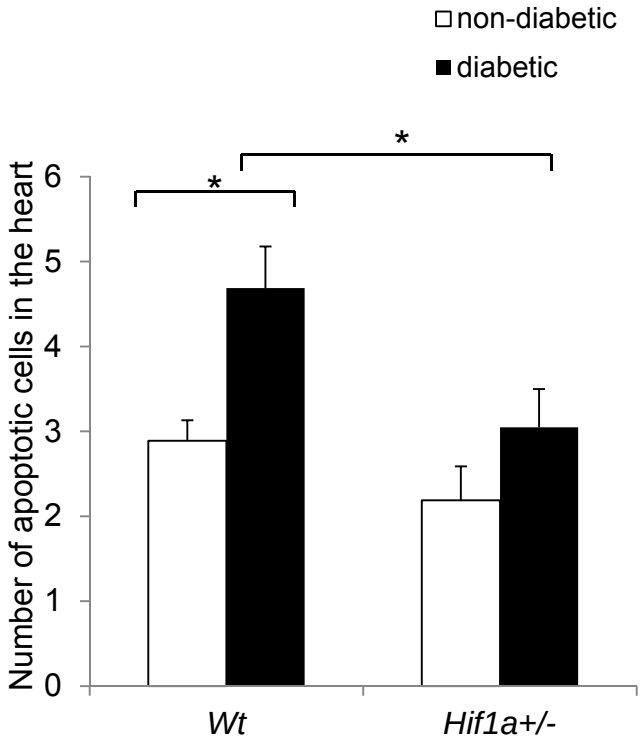


**Figure 3.** Apoptosis in the diabetic and non-diabetic hearts of *Wt* and *Hif1a*$^{+/-}$ embryos. The apoptotic cells were detected with TUNEL assay. The apoptotic cells were counted in the myocardium of left and right ventricles, and atrioventricular septum. The quantitative analysis showed that the number of apoptotic cells was significantly increased in the *wt* diabetic hearts. The values represent means ± SEM. Differences were tested for statistical significance by one-way ANOVA followed by Bonferroni's multiple comparison post-test. *, $P < 0.05$.

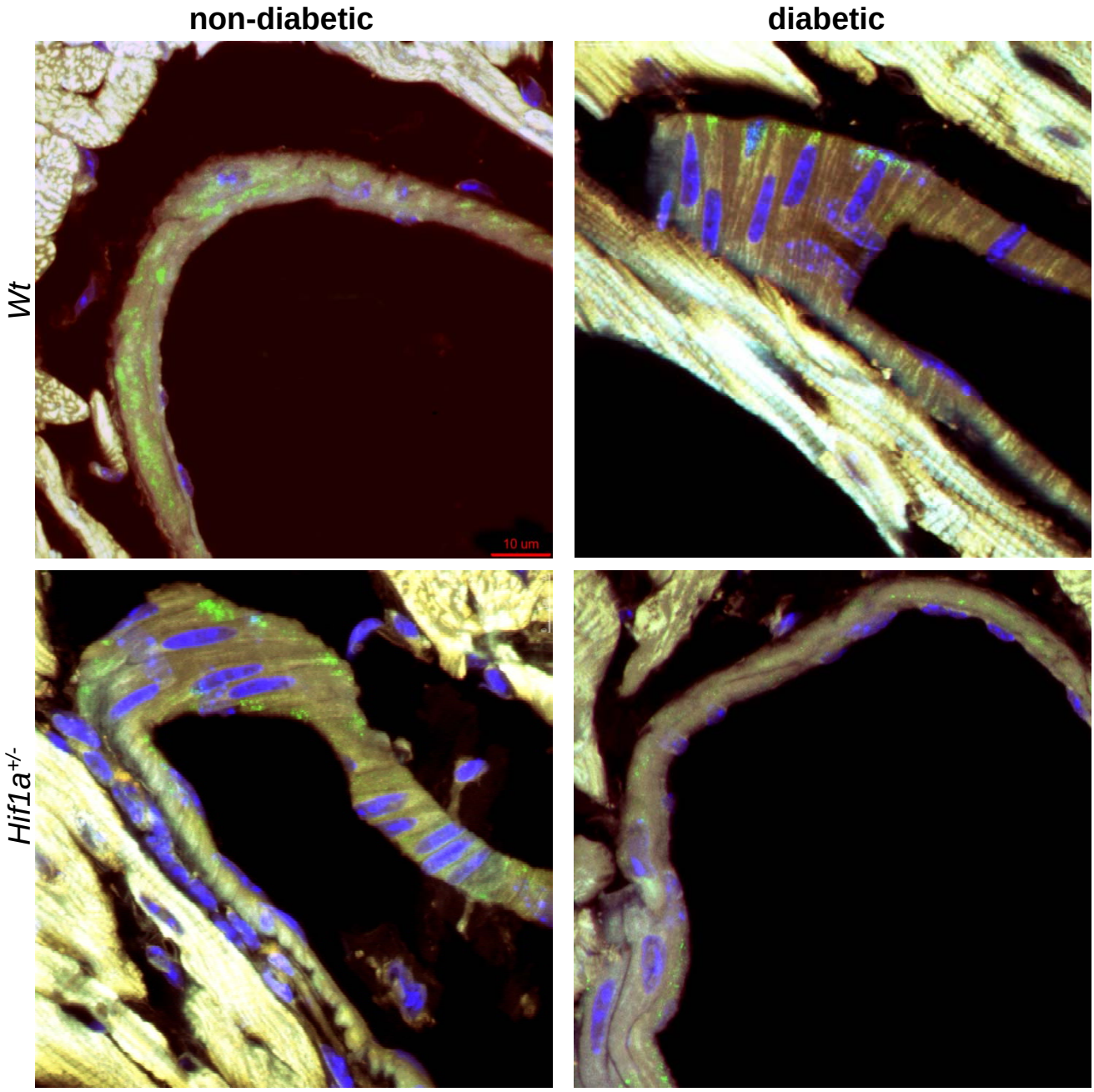


**Figure 4.** Diabetes-induced changes in cardiac VEGF expression. Confocal imaging of transverse sections of *wt* and *Hif1a*$^{+/-}$ heart s stained with anti-VEGF-A antibody (green) showed VEGF-A expression in blood vessels of the heart. Hoechst 33342 (blue) was used as a nuclear counterstain. Images are stacked Z-plane sections from confocal microscopy. Scale bar: 10 μm

**Table 1.** *Changes in body and heart mass.*

| Parameter | | non-diabetic *wt* | diabetic *wt* | non-diabetic *Hif1a*$^{+/-}$ | diabetic *Hif1a*$^{+/-}$ |
|---|---|---|---|---|---|
| n | males | 7 | 8 | 10 | 8 |
| BW (g) | | 28.00 ± 0.4 | 24.66 ± 0.9* | 28.42 ± 0.6 | 22.93 ± 0.8*$^{+}$ |
| RV/BW | | 0.77 ± 0.03 | 0.74 ± 0.04 | 0.76 ± 0.04 | 0.73 ± 0.02 |
| LV/BW | | 2.18 ± 0.03 | 1.98 ± 0.06* | 2.07 ± 0.04 | 1.96 ± 0.03* |
| n | females | 7 | 12 | 10 | 8 |
| BW (g) | | 22.0 ± 0.68 | 22.1 ± 0.57 | 22.1 ± 0.5 | 20.5 ± 0.4 |
| RV/BW | | 0.8 ± 0.04 | 0.8 ± 0.02 | 0.74 ± 0.02 | 0.73 ± 0.03 |
| LV/BW | | 2.34 ± 0.07 | 2.31 ± 0.08 | 2.26 ± 0.05 | 2.34 ± 0.14 |

Values are means ± SEM from indicated number of animals in each group. Abbreviations: BM, body mass; HM, heart mass; LV, left ventricular mass; RV, right ventricular mass. Statistical significance was assessed by one-way ANOVA followed by Bonferroni's multiple comparison post-test (GraphPad Prism 4). *P < 0.05 vs. non-diabetic wt; +P < 0.05 vs. non-diabetic Hif1a+/-.

**Table 2.** Mean systemic arterial blood pressure (MAP), heart rate (HR) and basal left ventricular echocardiographic parameters in non-diabetic and diabetic *wt* and *Hif1a*$^{+/-}$ mice.

| Parameter | | non-diabetic *wt* | diabetic *wt* | non-diabetic *Hif1a*$^{+/-}$ | diabetic *Hif1a*$^{+/-}$ |
|---|---|---|---|---|---|
| n | male | 7 | 8 | 10 | 8 |
| MAP (mmHg) | | 83.0 ± 2.1 | 87.5 ± 1.5 | 84.1 ± 1.4 | 88.2 ± 1.6 |
| HR (beats/min) | | 496 ± 21 | 471 ± 12 | 449 ± 38 | 440 ± 34 |
| LVDd (mm) | | 3.59 ± 0.08 | 3.59 ± 0.04 | 3.47 ± 0.10 | 3.65 ± 0.06 |
| LVDs (mm) | | 2.22 ± 0.06 | 2.27 ± 0.05 | 2.16 ± 0.08 | 2.42 ± 0.06* |
| AWTd (mm) | | 0.83 ± 0.02 | 0.76 ± 0.01* | 0.88 ± 0.02 | 0.74 ± 0.02* |
| PVTd (mm) | | 0.84 ± 0.02 | 0.76 ± 0.01* | 0.91 ± 0.04 | 0.69 ± 0.03* |
| AWTs (mm) | | 1.29 ± 0.03 | 1.20 ± 0.04 | 1.27 ± 0.03 | 1.10 ± 0.04* |
| PWTs (mm) | | 1.21 ± 0.02 | 1.09 ± 0.03* | 1.20 ± 0.03 | 1.00 ± 0.04* |
| n | female | 7 | 12 | 10 | 8 |
| MAP (mmHg) | | 84.6 ± 2.1 | 88.5 ± 2.2 | 84.8 ± 0.04 | 88.1 ± 1.3 |
| HR (beats/min) | | 504 ± 7 | 478 ± 14 | 484 ± 15 | 448 ± 16 |
| LVDd (mm) | | 3.52 ± 0.08 | 3.52 ± 0.05 | 3.45 ± 0.04 | 3.46 ± 0.04 |
| LVDs (mm) | | 2.33 ± 0.06 | 2.37 ± 0.06 | 2.30 ± 0.04 | 2.43 ± 0.06 |
| AWTd (mm) | | 0.74 ± 0.02 | 0.75 ± 0.01 | 0.72 ± 0.01 | 0.72 ± 0.01 |
| PVTd (mm) | | 0.79 ± 0.01 | 0.74 ± 0.02 | 0.78 ± 0.03 | 0.74 ± 0.02 |
| AWTs (mm) | | 1.12 ± 0.04 | 1.05 ± 0.02 | 1.06 ± 0.01 | 0.97 ± 0.02*$^{+}$ |
| PWTs (mm) | | 1.10 ± 0.02 | 1.05 ± 0.02 | 1.09 ± 0.02 | 0.99 ± 0.02*$^{+}$ |

Values are means ± SEM from indicated number of animals in each group. LVDD – diastolic cavity diameter, LVDS – systolic diameter, AWTD – diastolic anterior wall thickness, PWTD – diastolic posterior wall thickness, AWTS – systolic anterior wall thickness, PWTS – systolic posterior wall thickness, RWT – relative wall thickness. Statistical significance was assessed by one-way ANOVA followed by Bonferroni's multiple comparison post-test (GraphPad Prism 4). *P < 0.05 vs. non-diabetic wt; +P < 0.05 vs. non-diabetic Hif1a+/-.

DEV Elsevier Editorial System for Journal of Molecular and Cellular Cardiology
Manuscript Draft

Manuscript Number: JMCC7092

Title: Increased susceptibility of HIF-1α heterozygous-null mice to cardiovascular malformations associated with maternal diabetes

Article Type: Resubmission of Rejected Manuscript

Keywords: diabetic embryopathy; heart defect; hypoxia-inducible factor 1 alpha

Corresponding Author: Dr. Gabriela Pavlinkova, Ph.D.

Corresponding Author's Institution: Institute of Biotechnology AS CR

First Author: Romana Bohuslavova

Order of Authors: Romana Bohuslavova; Lada Skvorova; David Sedmera, M.D., Ph.D.; Gregg L Semenza, M.D., Ph.D.; Gabriela Pavlinkova, Ph.D.

Abstract: ABSTRACT
Cardiovascular malformations are the most common manifestation of diabetic embryopathy. The molecular mechanisms underlying the teratogenic effect of maternal diabetes have not been fully elucidated. Using genome-wide expression profiling, we previously demonstrated that exposure to maternal diabetes resulted in dysregulation of the hypoxia-inducible factor 1 (HIF-1) pathway in the developing embryo. We thus considered a possible link between HIF-1-regulated pathways and the development of congenital malformations. HIF-1α heterozygous-null (Hif1a+/-) and wild type (Wt) littermate embryos were exposed to the intrauterine environment of a diabetic mother to analyze the frequency and morphology of congenital defects, and assess gene expression changes in Wt and Hif1a+/- embryos. We observed a decreased number of embryos per litter and an increased incidence of heart malformations, including atrioventricular septal defects and reduced myocardial mass, in diabetes-exposed Hif1a+/- embryos as compared to Wt embryos. We also detected significant differences in the expression of key cardiac transcription factors, including Nkx2.5, Tbx5, and Mef2C, in diabetes-exposed Hif1a+/- embryonic hearts compared to Wt littermates. Thus, partial HIF-1α deficiency alters gene expression in the developing heart and increases susceptibility to congenital cardiac defects in a mouse model of diabetic pregnancy.

ABSTRACT

Cardiovascular malformations are the most common manifestation of diabetic embryopathy. The molecular mechanisms underlying the teratogenic effect of maternal diabetes have not been fully elucidated. Using genome-wide expression profiling, we previously demonstrated that exposure to maternal diabetes resulted in dysregulation of the hypoxia-inducible factor 1 (HIF-1) pathway in the developing embryo. We thus considered a possible link between HIF-1-regulated pathways and the development of congenital malformations. HIF-1$\alpha$ heterozygous-null (*Hif1a*$^{+/-}$) and wild type (*Wt)* littermate embryos were exposed to the intrauterine environment of a diabetic mother to analyze the frequency and morphology of congenital defects, and assess gene expression changes in *Wt* and *Hif1a*$^{+/-}$ embryos. We observed a decreased number of embryos per litter and an increased incidence of heart malformations, including atrioventricular septal defects and reduced myocardial mass, in diabetes-exposed *Hif1a*$^{+/-}$ embryos as compared to *Wt* embryos. We also detected significant differences in the expression of key cardiac transcription factors, including Nkx2.5, Tbx5, and Mef2C, in diabetes-exposed *Hif1a*$^{+/-}$ embryonic hearts compared to *Wt* littermates. Thus, partial HIF-1$\alpha$ deficiency alters gene expression in the developing heart and increases susceptibility to congenital cardiac defects in a mouse model of diabetic pregnancy.

# Increased susceptibility of HIF-1α heterozygous-null mice to cardiovascular malformations associated with maternal diabetes

Running title: Partial HIF-1α deficiency in diabetic embryopathy

Romana Bohuslavova[1], Lada Skvorova[1], David Sedmera[2], Gregg L. Semenza[3], and Gabriela Pavlinkova[1].

[1]Institute of Biotechnology AS CR, Prague, Czech Republic

[2]Institute of Anatomy, First Faculty of Medicine, Charles University, Prague, and Institute of Physiology AS CR, Prague, Czech Republic

[3]Vascular Program, Institute for Cell Engineering; Departments of Pediatrics, Medicine, Oncology, Radiation Oncology, and Biological Chemistry; and McKusick-Nathans Institute of Genetic Medicine, The Johns Hopkins University School of Medicine, Baltimore, Maryland, USA.

Corresponding author:

Gabriela Pavlinkova
Laboratory of Molecular Pathogenetics
Institute of Biotechnology AS CR, v.v.i.
Vídenská 1083
Prague 4
CZ-142 20
Czech Republic
phone: (+420) 241 063 415
fax: (+420) 244 471 707
email: gpavlinkova@img.cas.cz

## 1. Introduction

Diabetic pregnancy is associated with an increased incidence of congenital malformations compared with non-diabetic pregnancy [1, 2]. Diabetic embryopathy can affect any developing organ system, although congenital heart defects are the most frequent malformations in the offspring of diabetic women [1]. Atrioventricular septal (AVS) defects, hypoplastic left heart syndrome, and persistent truncus arteriosus are the most frequent cardiac malformations detected in clinical studies [1, 3-5]. The same types of heart malformations that are associated with diabetic pregnancies in humans have been reported in animal models [4, 6-8]. Animal studies have indicated that hyperglycemia, hypoxia, fetal acidemia, and abnormal maternal/fetal fuel metabolism are responsible for changes in embryonic development [9-15]. Recent studies suggest that a major teratogenic effect of the diabetic-hyperglycemic milieu is mediated by increased oxidative stress and that administration of anti-oxidants reduces the occurrence of developmental defects [13-16]. However, the molecular mechanisms by which hyperglycemia or oxidative stress lead to the dysregulated gene expression that ultimately results in malformations have not yet been elucidated.

Using global gene expression profiling, we previously showed that maternal diabetes alters embryonic gene expression [17, 18]. In particular, twenty genes regulated by hypoxia-inducible factor 1 (HIF-1) exhibited increased expression in diabetes-exposed embryos at E10.5, possibly reflecting an adaptive embryonic response to the diabetic environment of increased oxidative stress and hypoxia [17]. HIF-1 activates over 800 target genes that are involved in cell proliferation, angiogenesis, erythropoiesis, metabolism, and apoptosis [19]. Oxygen tension plays a key role in the regulation of HIF-1$\alpha$ expression, stabilization, and activation [19].

The amplitude of this response is also modulated by growth factor and cytokine-dependent signaling pathways [20, 21]. Furthermore, emerging evidence indicates that mitochondrial reactive oxygen species (ROS) are both necessary and sufficient to initiate the stabilization and activation of HIF-1α, and that treatment with antioxidants prevents HIF-1α protein stabilization [22].

The critical role of HIF-1 in development is demonstrated by the consequences of homozygosity for a null allele at the *Hif1a* locus encoding the HIF-1α subunit. *Hif1a*$^{-/-}$ knockout mouse embryos die at mid-gestation due to cardiovascular and neural tube defects [23, 24]. HIF-1α is essential for proper cardiac looping and the modulation of neural crest cell (NCC) migration and survival [24, 25]. Interestingly, exposure of mouse embryos to increased ambient $O_2$ concentrations partially rescues development of the *Hif1a*$^{-/-}$ embryonic heart, specifically chamber formation. However, hyperoxia fails to rescue pharyngeal arch development and NCC migration. Noticeably, the global nature of the *Hif1a* deletion in these studies does not readily allow a definitive attribution of the noted effects to a single cell type. Furthermore, mice lacking HIF-1α in ventricular cardiomyocytes exhibit embryonic lethality due to abnormal cardiac development on embryonic day (E)8.5 to 10.0 [26]. Not only HIF-1α loss-of-function, but also excessive HIF-1 activity, may result in birth defects. CITED2 is a negative regulator of HIF-1 transcriptional activity and *Cited2*$^{-/-}$ mouse embryos manifest overexpression of HIF-1 target genes, such as *Vegfa*, *Glut1*, and *Pgk1*, as well as neural tube and cardiovascular defects [27]. Cardiac defects were partially rescued in *Cited2*$^{-/-}$*;Hif1a*$^{+/-}$ embryos [28]. Localized adenoviral overexpression of HIF-1α in the chick heart was sufficient to cause coronary artery anomalies [29]. Thus, increased or decreased HIF-

1 activity results in neural and cardiovascular defects, which are the most frequent developmental defects associated with diabetic embryopathy.

Based on our finding that the expression of HIF-1 target genesis induced by maternal diabetes [17], and the knowledge that *Hif1a*$^{-/-}$ embryos have major defects in cardiovascular development [23, 24], we hypothesized that HIF-1 transcriptional activity represents a protective response of the embryo to maternal diabetes and that loss of HIF-1 activity increases susceptibility to heart defects observed in diabetic embryopathy. *Hif1a*$^{+/-}$ heterozygous-null mice develop normally but demonstrate impaired responses when challenged with hypoxia after birth [30, 31]. We hypothesized that limiting levels of HIF-1$\alpha$ may compromise embryonic development under conditions of aggravated hypoxia, which may occur in the context of maternal diabetes. We tested this hypothesis by exposing *Hif1a*$^{+/-}$ embryos to maternal diabetes. We analyzed the frequency and morphology of heart defects in diabetes-exposed *Hif1a*$^{+/-}$ and wild type (*Wt*) littermate embryos. Our results suggest an important role for HIF-1 in embryonic responses to the diabetic environment, including regulation of the key cardiac transcription factors Nkx2.5, Tbx5, and Mef2C.

## 2. Methods

### *2.1. Experimental animals.*

This study was conducted in accordance with the Guide for the Care and Use of Laboratory Animals (NIH Publication No. 85-23, revised 1996). Diabetes was induced in female inbred FVB mouse strain (strain code 207, Charles River), aged 7-9 weeks, by 2 intraperitoneal injections of 100 mg/kg body weight of streptozotocin (STZ; Sigma, St. Louis, MO), as described [17]. Blood glucose levels were measured in

fasted animals by glucometer (COUNTOUR TS, Bayer, Switzerland). We analyzed embryos from 52 diabetic dams that maintained blood glucose levels above 13.9 mmol/L (classified as diabetic) with blood glucose levels (mean ± SD) of 10.0 ± 1.2; 18.3 ± 4.3; and 28.7 ± 6.36 mmol/L before STZ treatment, on the mating day, and at embryo harvest, respectively. Mouse embryos were isolated from diabetic or control dams between E10.5 –and E18.5. Noon of the day on which the vaginal plug was found was designated E0.5. Diabetic FVB *Wt* females were mated to *Hif1a*$^{+/-}$ males (with the *Hif1a*$^{tm1jhu}$ knockout allele [23] on an FVB background) to generate *Hif1a*$^{+/-}$ and *Wt* (*Hif1a*$^{+/+}$) littermate embryos. *Hif1a*$^{+/-}$ mice are defective in the induction of HIF-1α protein in response to hypoxia or ischemia [32, 33]. Offspring of *Wt x Hif1a*$^{+/–}$ matings were genotyped by PCR [23, 34]. Non-diabetic embryos were generated from crosses between mock-induced *Wt* females (i.e. no STZ treatment) to *Hif1a*$^{+/-}$ males. This breeding scheme minimized the potential influence of maternal genotype since the mutant allele was paternally contributed. The developmental stage was classified for each embryo by morphological criteria, including somite number as well as central nervous system, limb, and eye development. Embryonic and cardiac morphology was assessed using a Nikon SMZ dissection microscope. Digital images of whole embryos were captured with a Nikon DS-Fi1 camera. Measurements of the crown-rump length and relative heart area were obtained ex vivo by light microscopy using the NIS-elements software program (Nikon). We analyzed embryos that were comparable in their developmental progression.

*2.2. Morphological analysis and immunostaining.*

Dissected thoraxes from E14.5 embryos were fixed with 4% paraformaldehyde in PBS (pH 7.4) at 4$^{o}$C overnight, dehydrated, and embedded in paraffin. Quantification

of myocardial tissue area (ventricular compact myocardium and trabeculae) and the area of the ventricular lumens was performed in *Wt* and *Hif1a*$^{+/-}$ diabetes-exposed and control hearts (n = 5 each) using the threshold tool in the NIH ImageJ program (**http://imagej.nih.gov/ij/download.html**), as described [35]. We analyzed 3 consecutive sections of 7-µm thickness running through the atrioventricular (AV) junction with a four-chamber view. Immunohistochemistry was performed with anti-VEGF-A antibody at 1:50 dilution (#sc-7269, Santa Cruz Biotechnology, CA, USA), anti-α-smooth muscle actin (α-SMA) antibody at 1:500 dilution (#A2547, Sigma-Aldrich), and anti-phospho-histone H3 (pHH3) antibody (Merck Millipore; #06-570) at dilution 1:100; each analysis was repeated a minimum of 3 times on an average of 4 embryos per genotype and included appropriate controls. The sections were analyzed under a Nikon Eclipse 50i microscope with a 20x magnification objective using the NIS-elements program. α-SMA and pHH3 immunostaining was analyzed with a two-photon microscope (Zeiss MP7). VEGF-A and α-SMA expression was quantified using ImageJ software. Immunopositive pHH3$^{+}$ nuclei in compact myocardium were counted using Adobe Photoshop CS5.11.

*2.3. TUNEL Assay.*

For diabetes-exposed and control *Wt* and *Hif1a*$^{+/-}$ embryos, we analyzed 3 cardiac sections running through the AV junction with a four chamber view from 3 embryos of different litters for each genotype. Tissue sections (7 µm) of dissected E14.5 thoraxes were treated with 20 µg/ml Proteinase K for 20 min at room temperature. The sections were incubated with the TUNEL labeling kit (Roche) for 1 hour at 37$^{o}$C and Hoechst 33342 was used as a nuclear counterstain. The sections were analyzed under a Nikon Eclipse E400 fluorescent microscope.

*2.4. Real-time reverse-transcription PCR.*

Total RNA was isolated from hearts at E14.5 from experimental samples (EXP; diabetes-exposed *Wt,* diabetes-exposed *Hif1a*$^{+/-}$, and non-diabetic *Hif1a*$^{+/-}$) and from non-diabetic *Wt* (control). Following reverse transcription (RT), quantitative real-time PCR (qPCR) was performed with the initial AmpliTaq activation at 95°C for 10 min, followed by 40 cycles at 95°C for 15 s and 60°C for 60 s, as described [34]. The *Hprt1* gene was selected as the best reference gene for our analyses from a panel of 12 control genes (TATAA Biocenter AB, Sweden). The relative expression of a target gene was calculated, based on qPCR efficiencies (E) and the crossing point (Cp) difference (Δ) of an experimental sample versus control (ratio = $(E_{\text{target}})^{\Delta Cp\ Hif1a(Mean\ control - Mean\ EXP)}$ / $(E_{Hprt1})^{\Delta Cp\ Hprt1(Mean\ control - Mean\ EXP)}$ [36]. RT-qPCR data were analyzed using the GenEX5 program (http://www.multid.se/genex/). Primer sets were designed to exclude amplification of potentially contaminating genomic DNA by positioning the amplicons across exon-exon junctions. Primers were designed using Primer 3 software (http://frodo.wi.mit.edu/primer3/). Primers were selected according to the following parameters: length between 18 and 24 bases; melting temperature (Tm) between 58° and 60°C; and G+C content between 40 and 60% (optimal 50%). Primer sequences are presented in Supplemental Table S1.

*2.5. Western blotting.*

Western blotting was performed according to a standard protocol using a monoclonal antibody that specifically recognizes HIF-1α [23]. Dissected E10.5 whole embryos without hearts and E10.5 hearts were lysed and stored at –80°C until

analysis. Protein levels were quantified using the BCA assay. Protein samples (25 µg per lane for whole embryos; 8 µg per lane for embryonic hearts) were denatured, resolved using 8% SDS-PAGE, and transferred onto a nitrocellulose membrane. The membrane was blocked with 5% dry milk and incubated overnight with anti-HIF-1α IgG in TBS buffer at 1:750 dilution (#NB100-105; Novus Biologicals, Cambridge, UK). Anti-α-actin IgG (Santa Cruz Biotechnology) was used as a loading control. After incubation with a horseradish peroxidase–conjugated secondary IgG (Amersham, Arlington Heights, IL), the blots were developed using the ECL kit (Pierce, Rockford, IL), and quantified using ImageJ software.

*2.6. Statistical analysis.*

Fisher's exact test was used to compare the number of embryos and number of defects between two independent groups. A one-way analysis of variance (ANOVA) was used to investigate statistically significant differences among genotypes and experimental conditions. When a significant interaction was detected, the differences between subgroups were further compared using the post *t*-test (significance assigned at the $P < 0.05$ level; Graph Pad, 2005; Graph Pad, San Diego, CA)

## 3. Results

*3.1. Effects of diabetes-exposure on litter size, embryonic growth, and external morphology of Hif1a$^{+/-}$ and Wt mice*

*Wt* (n = 195) and *Hif1a*$^{+/-}$ (n = 163) embryos from 52 diabetic pregnancies, and *Wt* (n = 120) and *Hif1a*$^{+/-}$ (n = 117) embryos from 29 non-diabetic pregnancies were

collected between E10.5 and E18.5 (Supplemental Table S2). The number of resorbed embryos was significantly increased in diabetic pregnancies with severe hyperglycemia (blood glucose level > 30 mmol/L; 24% of embryos) compared to non-diabetic pregnancies (2% of embryos) or diabetic pregnancies with blood glucose levels < 30 mmol/L (3% of embryos; Supplemental Table S3). The average number of *Wt* embryos per litter was not significantly different in diabetic pregnancies with glucose levels > 30 mmol/L (severe hyperglycemia; 3.97 ± 0.4) and in diabetic pregnancies with blood glucose levels between 13.9 mmol/L and 30 mmol/L (moderate hyperglycemia; 3.37 ± 0.4) compared to non-diabetic pregnancies (4.1 ± 0.4; Fig. 1). However, compared to *Wt* non-diabetic pregnancies, the number of *Hif1a*$^{+/-}$ embryos per litter was significantly lower in diabetic pregnancies with moderate hyperglycemia (3.28 ± 0.4; $P < 0.05$) or with severe hyperglycemia (3.05 ± 0.3; $P < 0.001$) (one-way ANOVA followed by Bonferroni post-test). The number of *Hif1a*$^{+/-}$ embryos per litter (3.1 ± 1.9) was significantly lower than *Wt* littermates in diabetic pregnancies (3.7 ± 1.7; $P < 0.05$).

We detected a significant decrease in the average crown-rump length of *Wt* and *Hif1a*$^{+/-}$ diabetic embryos at E18.5 ($P < 0.0001$, one-way ANOVA; Supplemental Fig. S1A). The heart size of embryos from diabetic pregnancies was smaller than the sizes of embryonic hearts from non-diabetic pregnancies at E18.5 ($P < 0.0002$; Supplemental Fig. S1B).

Dissected embryos were examined for defects in gross morphology. Diabetes-exposed embryos displayed a variety of external developmental defects, including neural tube defects and cardiovascular anomalies (Fig. 2A-J). Cardiovascular anomalies were the most frequent and were manifested by hemorrhage, edema, and in some cases, anemia. The evaluation of external phenotype of diabetes-exposed

embryos demonstrated that *Hif1a*$^{+/-}$ embryos from diabetic pregnancies had an increased incidence of developmental defects of 22% (36 of 163) compared to 13% (26 of 195) of *Wt* littermate embryos (Fig. 2K; *P* = 0.03, Fisher's exact test). No significant effect of genotype on the frequency of developmental defects was detected in pregnancies with glucose levels > 30 mmol/L (severe hyperglycemia) with frequencies of 26% (15 of 58) and 28% (18 of 64) for *Hif1a*$^{+/-}$ and *Wt* embryos, respectively (*P* = 0.8, Fisher's exact test). However, a significant effect of genotype on the incidence of developmental defects was observed in diabetic pregnancies with blood glucose levels of moderate hyperglycemia, in which 20% (21 of 105) of *Hif1a*$^{+/-}$ embryos, as compared to only 6% (8 of 131) of *Wt* embryos, demonstrated developmental defects (*P* = 0.002, Fisher's exact test). Since we detected a significant effect of genotype on the incidence of developmental defects in embryos from diabetic pregnancies with moderate hyperglycemia, we used only embryos from pregnancies with moderate hyperglycemia for our subsequent analyses.

### *3.2. The frequency and morphology of cardiovascular defects*

To assess the morphology and frequency of cardiovascular defects, we examined heart development and heart morphology by histological analysis of thorax sections of E14.5 embryos (Fig. 3A-D). Since HIF-1$\alpha$ modulates NCC survival and migration [25], we have carefully analyzed morphology of the outflow tract and pharyngeal arch arteries, because NCCs contribute to their formation. We analyzed 6 litters from diabetic dams consisting of 17 *Hif1a*$^{+/-}$ and 18 *Wt* embryos and 4 litters from non-diabetic dams consisting of 13 *Hif1a*$^{+/-}$ and 15 *Wt* embryos. The *Hif1a*$^{+/-}$ embryos from diabetic pregnancies showed an increased incidence of cardiovascular defects of 47% (n = 8 with defects/17 embryos; *P* = 0.004, Fisher's exact test) and *Wt*

diabetes-exposed embryos showed an increased incidence of cardiac malformations of 28% (n = 5 with defects/18 embryos; $P$ = 0.048, Fisher's exact test) compared to *Hif1a*$^{+/-}$ and *Wt* embryos from non-diabetic pregnancies, respectively. The majority of heart defects associated with diabetic pregnancy were AVS defects (65% of cardiovascular defects). We also identified pericardial effusion (12% of cardiac defects) in association with AVS defects.

We closely observed the cardiovascular malformations involving cardiac outflow tract defects. In 35 analyzed *Hif1a*$^{+/-}$ and *Wt* embryos from diabetic pregnancies, we identified one case of persistent truncus arteriosus in a *Hif1a*$^{+/-}$ embryo. We did not observe any cases of transposition of the great vessels or double outlet right ventricle. However, histological analysis showed that ventricular myocardial mass was profoundly reduced and the compact ventricular myocardial walls were thinner in all diabetes-exposed embryos at E14.5 (Fig. 3A-D, E; one-way ANOVA, $P$ < 0.0001). Additionally, in diabetic pregnancies, the myocardial volume of the left ventricle (LV) of *Hif1a*$^{+/-}$ embryos was significantly decreased compared to *Wt* littermates (Fig. 3E). Interestingly, a sponge-like layer of myocardium (trabeculae) was increased in both diabetes-exposed *Wt* and *Hif1a*$^{+/-}$ embryos compared to non-diabetic *Wt* embryos (Fig. 3F). Since the ventricular trabeculae are thought to increase surface area to maximize oxygen uptake by the myocardium, our results are consistent with the hypothesis that the diabetic embryonic environment impairs tissue oxygen availability and may activate compensatory mechanisms to satisfy oxygen demands.

To investigate the mechanistic bases for the observed thin-walled myocardium, we quantified proliferation and apoptosis in the compact myocardium in both ventricles at E14.5. Isolated TUNEL-positive cells were seen in the endocardium, mesenchymal tissues of the forming cardiac skeleton, remodeling AV

and outflow tract valves, and the interventricular septum of control embryos. A higher frequency of apoptotic cells was detected, mainly in the endocardial cushions and AV septum, of diabetes-exposed embryos. Since the majority of heart defects observed in diabetes-exposed embryos were AVS defects, we also analyzed apoptosis specifically in hearts with AVS defects. We detected a significant increase in apoptotic cells in *Hif1a*$^{+/-}$ diabetes-exposed embryos with AVS defects as compared to *Hif1a*$^{+/-}$ embryos from non-diabetic pregnancies (Fig. 4A; one-way ANOVA, $P < 0.02$).

To further analyze cellular changes in the diabetes-exposed myocardium, we quantified cell proliferation by immunostaining for pHH3 in the hearts at E14.5 (Fig. 4B). Mitotic activity was increased in compact myocardium of diabetic *Wt* hearts relative to non-diabetic *Wt* hearts. Our analysis of mitotic activity also revealed a marked decrease in mitotic activity in the compact myocardium of both the LV and RV ventricles of diabetes-exposed hearts from *Hif1a*$^{+/-}$ embryos compared to *Wt* embryos at E14.5. Thus, cell proliferation in the compact myocardium of diabetes-exposed *Hif1a*$^{+/-}$ embryos is considerably impaired, which provides a cellular mechanism for the decreased thickness of compact myocardium in diabetic *Hif1a*$^{+/-}$ embryos compared to non-diabetic *Wt* embryos.

*3.3 Analysis of HIF-1$\alpha$ protein levels*

To understand the basis for the escalation of congenital defects in *Hif1a*$^{+/-}$ diabetic embryos, we analyzed HIF-1$\alpha$ protein levels. Protein lysates were prepared from *Wt* and *Hif1a*$^{+/-}$ whole embryos and hearts at E10.5 (Fig. 5). Quantitative Western blot analysis showed significantly decreased HIF-1$\alpha$ levels in whole *Hif1a*$^{+/-}$ embryos by 1.9 fold relative to *Wt* embryos. In contrast, HIF-1$\alpha$ protein levels in the

hearts of *Wt* and *Hif1a*$^{+/-}$ littermates from non-diabetic pregnancies were similar. HIF-1$\alpha$ levels were increased 2.9-fold in diabetes-exposed *Wt* hearts but only 1.8 fold in *Hif1a*$^{+/-}$ hearts, compared to non-diabetic *Wt* hearts.

*3.4 Analysis of cardiac VEGF-A and $\alpha$-SMA expression*

Next, we focused on cardiac expression of VEGF-A, a key HIF-1 target gene product. VEGF-A is an essential modulator of cardiovascular development and modest increases or decreases in VEGF-A levels lead to embryonic lethality [37, 38]. We analyzed histological sections of E14.5 hearts to establish the spatial expression of VEGF-A using immunohistochemistry. VEGF-A was detected in the interventricular septum, myocardial cells lining the endocardial cushions of both the inflow tract and the outflow tract, and in the ventricular myocardium (Fig. 6A-F). Diabetes significantly increased VEGF-A protein levels in *Wt* hearts but not in *Hif1a*$^{+/-}$ hearts (Fig. 6G). In diabetes-exposed *Hif1a*$^{+/-}$ hearts, the expression of VEGF-A was decreased in three of four analyzed embryos. We also used RT-qPCR to analyze *Vegfa* mRNA levels in the embryonic hearts at E14.5 (Fig. 6H). We detected a marked variability in *Vegfa* mRNA expression levels in the diabetes-exposed hearts. However, mean *Vegfa* mRNA levels in the hearts of diabetes-exposed *Hif1a*$^{+/-}$ embryos were markedly reduced compared to *Wt* littermates.

To further elucidate the roles of HIF-1$\alpha$ in cardiac responses to the diabetic environment, we analyzed spatial expression of $\alpha$-SMA, a marker of immature cardiomyocytes. The expression of $\alpha$-SMA in early cardiomyocytes is more prominent before E12.5 and its expression is decreased with cardiomyocyte maturation at E14.5 [39]. We observed a reduced number of $\alpha$-SMA$^{+}$ cardiomyocytes in both the LV and RV of diabetic *Hif1a*$^{+/-}$ embryos compared to non-diabetic

embryos at E14.5 (Fig. 7A and B). Although the RV myocardial volume in diabetes-exposed *Wt* embryos was significantly decreased compared to non-diabetic *Wt* embryos (Fig. 3), the expression of α-SMA was similar in diabetic and non-diabetic RVs. Since mature cardiomyocytes lose α-SMA expression, the differences in the number of α-SMA$^{+}$ cardiomyocytes may indicate dysregulated differentiation (maturation) of the ventricular cardiomyocytes in diabetic embryos.

*3.5 Analysis of cardiac gene transcription*

RT-qPCR was performed to analyze the expression of genes encoding molecules important for myofibrillogenesis, transcriptional regulation, differentiation, and proliferation, including T-box 5 (*Tbx5*), NK class homeodomain protein (*Nkx2.5*), atrial natriuretic peptide (*Nppa*), gap-junction gene connexin 43 (*Cx43*), myocyte enhancer factor 2C (*Mef2c*), skeletal α-actin 1 (*Acta1*), myosin light chain isoform (*Mlc2v*), and cardiac troponin I (*Tnni3*). Whereas expression of *Tbx5* was significantly decreased in non-diabetic *Hif1a*$^{+/-}$ compared to *Wt* hearts, it was markedly increased in diabetes-exposed *Hif1a*$^{+/-}$ hearts compared to non-diabetic and diabetic *Wt* hearts (Fig. 8). Expression of the cardiogenic factor *Nkx2.5* mRNA expression was also significantly increased in diabetes-exposed *Hif1a*$^{+/-}$ hearts. Tbx5 and Nkx2.5 can synergistically activate the *Nppa* gene promoter [40, 41]. Expression levels of *Nppa* were significantly increased in diabetes-exposed *Hif1a*$^{+/-}$ embryos in accordance with the expression patterns of *Tbx5* and *Nkx2.5*. Next, we analyzed the expression of *Mef2c*, which encodes another cardiac-specific transcription factor. *Mef2c* mRNA levels were also increased in diabetes-exposed *Hif1a*$^{+/-}$ hearts but not in diabetes-exposed *Wt* hearts at E14.5. In contrast, maternal diabetes modestly increased the

expression of a marker of myocardial cell differentiation, *Cx43*, in both *Wt* and *Hif1a*$^{+/-}$ hearts. The expression of *Acta1* was modestly decreased in both the *Wt* and *Hif1a*$^{+/-}$ diabetes-exposed hearts compared to non-diabetic hearts. The expression of myofilament genes, *Tnni3* and ventricle-specific *Mlc2v,* was not significantly affected by *Hif1a* genotype or the diabetic environment. Taken together, our data are consistent with the hypothesis that dysregulated gene expression in the hearts of *Hif1a*$^{+/-}$ embryos subjected to the diabetic environment underlies the increased incidence of congenital cardiac defects in these embryos.

## 4. Discussion

Our study revealed that compared to *Wt* littermates, mouse embryos heterozygous for a knockout allele at the *Hif1a* locus have a 3-fold increased incidence of malformations in the teratogenic environment of maternal diabetes. The reduction in functional *Hif1a* gene dosage decreased the number of embryos per litter and increased the incidence of heart malformations, including AVS defects and reduced ventricular myocardial mass, in diabetes-exposed *Hif1a*$^{+/-}$ compared to *Wt* embryos. In addition, we demonstrated that the levels of transcription factors of heart specification and differentiation, *Tbx5, Nkx2.5*, and *Mef2c*, are abnormally increased in *Hif1a*$^{+/-}$ hearts compared to *Wt* littermates from diabetic pregnancies.

Previous studies have documented that HIF-1$\alpha$ expression is necessary for normal heart development. *Hif1a*$^{-/-}$ knockout embryos die by E10.5 displaying severe cardiovascular and neural tube defects [23, 24]. Furthermore, excessive HIF-1 activity in the absence of negative regulation by CITED2 is also detrimental and leads to numerous developmental defects, including cardiac defects [27, 28]. In the present

study, we have demonstrated increased HIF-1α levels in diabetes-exposed hearts compared to non-diabetic hearts at E14.5. However, cardiac HIF-1α levels were reduced by 40% in diabetes-exposed hearts from *Hif1a*$^{+/-}$ embryos compared to *Wt* littermates, reflecting *Hif1a* haploinsufficiency. Indeed, the incidence of cardiovascular defects in diabetes-exposed *Hif1a*$^{+/-}$ embryos was higher than in *Wt* littermates, but we did not identify any particular defects associated only with the *Hif1a*$^{+/-}$ genotype. Interestingly, we found that the LV myocardial volume in diabetes-exposed *Hif1a*$^{+/-}$ hearts was significantly reduced compared to *Wt* littermates at E14.5. We detected significantly increased expression of *Tbx5* in diabetes-exposed *Hif1a*$^{+/-}$ hearts compared to *Wt* littermates that may play a major role in the pathogenesis of reduced LV myocardial volume. Tbx5 is one of the important cardiac factors with distinct asymmetric expression, specifying the identity of the LV [42, 43]. Existing evidence supports the role of Tbx5 as a regulator of myocardial cell proliferation. Overexpression of *Tbx5* in embryonic chick heart inhibits myocardial cell proliferation [44]. Similarly, ubiquitous misexpression of *Tbx5* in the embryonic heart is associated with a thinner ventricular wall compared to the normal heart [45].

Although hypoplasia of the heart ventricles was observed in all diabetes-exposed embryos, we did not detect a significant increase in apoptotic cells at E14.5. However, a statistically significant increase in the number of apoptotic cells was detected in *Hif1a*$^{+/-}$ hearts with AVS defects. Increased apoptosis in the cardiac cushions in pre-septation stages was associated with subsequent defects of cardiac septation in TGF-β2-deficient mice [46]. Our findings of increased apoptosis at the stage where the defects are already established may reflect either a persistence of the apoptotic stimulus or abnormal hemodynamic conditions in the malformed heart, which can also lead to apoptosis [47]. However, the majority of apoptotic cells in both

malformed and normal hearts were found in physiological zones of programmed cell death associated with heart morphogenesis [48], specifically the mesenchymal cushions, valves, and interventricular septum, rather than in the myocardium of the free ventricular wall. These observations suggest that ventricular wall mass was not reduced because of increased apoptosis and are consistent with other studies, which have implicated decreased cell proliferation in the ventricular myocardium as the cause of hypoplastic myocardium in diabetes-exposed hearts [6, 7].

The proliferation of cardiomyocytes is necessary to support the increasing hemodynamic load at mid-gestation [49]. During normal heart development, the number of cardiomyocytes in the compact layer of the ventricles increases 5-fold between E12.5 and E14.5 [50]. We observed that the highly proliferative compact layer was diminished in diabetes-exposed hearts when compared to non-diabetic controls at E14.5 (Fig. 3). However, our analysis of mitotic activity showed increased proliferation in the compact ventricular myocardium of diabetes-exposed *Wt* embryos at E14.5. Since other studies have demonstrated decreased cell proliferation in the ventricular myocardium of diabetes-exposed *Wt* hearts at E13.5 [6, 7], we postulate that the proliferation of cardiomyocytes in the compact layer of the ventricles is delayed, resulting in reduced myocardial wall mass in diabetes-exposed *Wt* embryos at E14.5. Interestingly, we detected substantially reduced proliferation in the compact ventricular myocardium of diabetes-exposed *Hif1a*$^{+/-}$ embryos compared to *Wt* littermates (Fig. 4), which corresponded to the phenotype of thin ventricular compact myocardium and to the increased expression of *Tbx5*, an inhibitor of cardiomyocyte proliferation [44]. In contrast to morphological changes in the ventricular myocardium, the epicardium of diabetes-exposed hearts was characteristically spread over the myocardium, without any signs of detachment or blebbing. Since epicardial-

myocardial interactions regulate differentiation and proliferation of the ventricular wall, the possibility that epicardium-mediated signals are altered in diabetes-exposed embryos remains to be determined.

Our data demonstrate that, compared to *Wt* embryos, *Hif1a*$^{+/-}$ littermates from diabetic pregnancies with moderate hyperglycemia are more susceptible to diabetic embryopathy. To further evaluate the role of HIF-1-regulated pathways in diabetic embryopathy, we analyzed the expression of a key HIF-1 target gene, *Vegfa*, which is tightly regulated during normal embryonic development. Heterozygous *Vegfa*$^{+/-}$ mutant embryos die at E10.5, displaying abnormal vascularization. Transgenic embryos overexpressing VEGF-A also die with severe cardiac abnormalities at E12.5-E14 [37, 38, 51]. Our previous research has demonstrated that the expression of *Vegfa* is altered by the diabetic environment at E10.5 [17]. Cultured mouse embryos exposed to high glucose from E7.5 until E9.5 showed a reduction in VEGF-A levels and significant vascular abnormalities [52]. A decrease in *Vegfa* mRNA was observed in the hearts of E14 rat embryos (corresponding to E12.5 in the mouse) from diabetic pregnancies, although 25% of the analyzed embryos were not affected by the diabetic environment [53]. In contrast, an increased expression of *Vegfa* mRNA and VEGF-A protein was detected in the hearts of E13.5 mouse embryos from diabetic pregnancies [54]. In the present study, VEGF-A levels were on average increased in *Wt* but not *Hif1a*$^{+/-}$ embryos at E14.5. Our RT-qPCR analysis showed a high variability in *Vegfa* mRNA levels with a prevailing trend of decreased *Vegfa* expression in *Hif1a*$^{+/-}$ diabetes-exposed embryos at E14.5, supporting the idea that increased VEGF-A may represent an adaptive response to impaired myocardial oxygenation in diabetes-exposed embryos and that the absence of this response may increase the risk of cardiac malformations.

Additionally, we analyzed the expression of key structural and regulatory molecules important for heart development. Interestingly, the expression of *Tbx5*, *Nkx2.5*, and *Mef2c* was significantly increased in diabetes-exposed *Hif1a*$^{+/-}$ embryos but not in *Wt* littermates. Tbx5 interacts with Nkx2.5 and Tbx5 can also activate the *Nkx2.5* gene [40, 41, 45]. Additionally, Tbx5 and Nkx2.5 synergistically activate the *Nppa* gene [40]. Accordingly, we detected an increased expression of *Nppa* in the hearts of diabetes-exposed *Hif1a*$^{+/-}$ embryos but not *Wt* embryos at E14.5. This gene is also specifically expressed in the LV but not in the RV in mid-gestation similar to *Tbx5* [55]. Existing evidence strongly suggests that the levels of *Tbx5* expression in the developing heart are crucial. Overexpression of *Tbx5* in the heart is associated with abnormalities of early chamber development, hypoplasia, loss of ventricular-specific gene expression, and embryonic lethality [44, 56]. Similarly, homozygous *Tbx5*$^{-/-}$ mutants demonstrate the arrest in heart development at E9.5. Heterozygous *Tbx5*$^{+/-}$ mice show the congenital defects, including cardiac hypoplasia, atrial and ventricular septal defects, of Holt–Oram syndrome mutations in humans [40]. NKX2.5 mutations in humans are also associated with congenital heart defects similar to Holt-Oram syndrome [57]. Based on our results, we propose that the diabetic environment affects HIF-1$\alpha$ regulation in the developing heart and that haploinsufficiency of *Hif1a* alters compensatory mechanisms involving key transcriptional factors that regulate cardiac differentiation, morphogenesis, and growth.

Studies in adult mice have demonstrated that HIF-1-dependent vascularization following femoral artery ligation or cutaneous wounding is impaired in diabetic mice, which can be rescued by experimental manipulations that increase HIF-1$\alpha$ expression [58-60]. Furthermore, loss of HIF-1 activity appears to play a role in the pathogenesis of type 2 diabetes [61, 62]. Thus, environmental (maternal diabetes)

and genetic (*Hif1a* mutation) factors may each reduce HIF-1 activity in embryos and result in cardiovascular malformations if either abnormality is severe enough (*i.e.* maternal blood glucose > 30 or *Hif1a*$^{-/-}$ genotype) or when more modest abnormalities are present in combination (*i.e.* maternal blood glucose > 13 but < 30 and *Hif1a*$^{+/-}$ genotype). Clinical studies have demonstrated that polymorphisms at the *HIF1A* locus influence the presentation of ischemic heart disease [63, 64]. Taken together with the results presented here, these data raise the possibility that genetic variation at the *HIF1A* locus may also influence malformation risk for infants of diabetic mothers.

## 5. Conclusions

We used a genetic mouse model of partial HIF-1α deficiency to test our hypothesis that induction of HIF-1α in the embryonic heart represents an adaptive response to maternal diabetes and that a failure to adequately induce expression of HIF-1α and downstream target genes such as *Vegfa* increases susceptibility to the cardiac malformations that are observed in diabetic embryopathy. HIF-1α heterozygous-null and *Wt* littermate embryos were exposed to the intrauterine environment of a diabetic mother and the frequency and morphology of heart defects were analyzed. We found that the reduction in functional *Hif1a* gene dosage decreased the number of embryos per litter and increased the incidence of heart malformations, mainly AVS defects and reduced ventricular myocardial mass, in diabetes-exposed *Hif1a*$^{+/-}$ compared to *Wt* littermates. We also detected significant differences in the expression of the key cardiogenic transcription factors Tbx5, Nkx2.5, and Mef2C in diabetes-exposed *Hif1a*$^{+/-}$ and *Wt* embryonic hearts, providing a second molecular mechanism by which HIF-1α loss-of-function may increase the

risk of cardiac malformations. Taken together, these results provide compelling evidence that impairment of HIF-1$\alpha$-controlled hypoxia-response pathways may play a functionally causative role in diabetic embryopathy.

**Funding sources**

This work was funded by a Marie Curie International Reintegration Grant within the 7th European Community Framework Programme PIRG02-GA-2007–224760; grants from the Czech Ministry of Education, Youth and Sports AVOZ50520701; and the Czech Science Foundation 301/09/0117 and 302/11/1308.

**Disclosures**

None declared.

**Acknowledgments**

G.L.S. is the C. Michael Armstrong Professor at the Johns Hopkins University School of Medicine. Dr. Gabriela Pavlinkova is the guarantor of this work, had full access to all the data, and takes full responsibility for the integrity of data and the accuracy of data analysis. R.B., L.K. collected and analyzed the data. G.P. analyzed the data, wrote and reviewed the manuscript. D.S. analyzed the data, contributed to the discussion, and edited the manuscript. G.L.S. contributed to the discussion, reviewed and edited the manuscript. We also thank Jiri Truksa (Institute of Biotechnology AS CR) for help with Western blot analysis.

## References


[1] Martinez-Frias ML. Epidemiological analysis of outcomes of pregnancy in diabetic mothers: identification of the most characteristic and most frequent congenital anomalies. Am J Med Genet. 1994;51:108-13.
[2] Kucera J. Rate and type of congenital anomalies among offspring of diabetic women. The Journal of reproductive medicine. 1971;7:73-82.
[3] Wren C, Birrell G, Hawthorne G. Cardiovascular malformations in infants of diabetic mothers. Heart. 2003;89:1217-20.
[4] Corrigan N, Brazil DP, McAuliffe F. Fetal cardiac effects of maternal hyperglycemia during pregnancy. Birth Defects Res A Clin Mol Teratol. 2009;85:523-30.
[5] Correa A, Gilboa SM, Besser LM, Botto LD, Moore CA, Hobbs CA, et al. Diabetes mellitus and birth defects. American journal of obstetrics and gynecology. 2008;199:237 e1-9.
[6] Kumar SD, Dheen ST, Tay SS. Maternal diabetes induces congenital heart defects in mice by altering the expression of genes involved in cardiovascular development. Cardiovascular diabetology. 2007;6:34.
[7] Zhao Z. Cardiac malformations and alteration of TGFbeta signaling system in diabetic embryopathy. Birth Defects Res B Dev Reprod Toxicol. 2010;89:97-105.
[8] Molin DG, Roest PA, Nordstrand H, Wisse LJ, Poelmann RE, Eriksson UJ, et al. Disturbed morphogenesis of cardiac outflow tract and increased rate of aortic arch anomalies in the offspring of diabetic rats. Birth Defects Res A Clin Mol Teratol. 2004;70:927-38.
[9] Phelan SA, Ito M, Loeken MR. Neural tube defects in embryos of diabetic mice: role of the Pax-3 gene and apoptosis. Diabetes. 1997;46:1189-97.
[10] Sussman I, Matschinsky FM. Diabetes affects sorbitol and myo-inositol levels of neuroectodermal tissue during embryogenesis in rat. Diabetes. 1988;37:974-81.
[11] Reece EA, Homko CJ, Wu YK, Wiznitzer A. The role of free radicals and membrane lipids in diabetes-induced congenital malformations. J Soc Gynecol Investig. 1998;5:178-87.
[12] Yang X, Borg LA, Eriksson UJ. Altered metabolism and superoxide generation in neural tissue of rat embryos exposed to high glucose. Am J Physiol. 1997;272:E173-80.
[13] Sakamaki H, Akazawa S, Ishibashi M, Izumino K, Takino H, Yamasaki H, et al. Significance of glutathione-dependent antioxidant system in diabetes-induced embryonic malformations. Diabetes. 1999;48:1138-44.
[14] Li R, Chase M, Jung SK, Smith PJ, Loeken MR. Hypoxic stress in diabetic pregnancy contributes to impaired embryo gene expression and defective development by inducing oxidative stress. American journal of physiology Endocrinology and metabolism. 2005;289:E591-9.
[15] Wentzel P, Eriksson UJ. A diabetes-like environment increases malformation rate and diminishes prostaglandin E(2) in rat embryos: reversal by administration of vitamin E and folic acid. Birth Defects Res A Clin Mol Teratol. 2005;73:506-11.
[16] Ornoy A. Embryonic oxidative stress as a mechanism of teratogenesis with special emphasis on diabetic embryopathy. Reprod Toxicol. 2007;24:31-41.
[17] Pavlinkova G, Salbaum JM, Kappen C. Maternal diabetes alters transcriptional programs in the developing embryo. BMC Genomics. 2009;10:274.

[18] Salbaum JM, Kruger C, Zhang X, Delahaye NA, Pavlinkova G, Burk DH, et al. Altered gene expression and spongiotrophoblast differentiation in placenta from a mouse model of diabetes in pregnancy. Diabetologia. 2011;54:1909-20.
[19] Semenza GL. Oxygen sensing, homeostasis, and disease. The New England journal of medicine. 2011;365:537-47.
[20] Bardos JI, Ashcroft M. Negative and positive regulation of HIF-1: a complex network. Biochimica et biophysica acta. 2005;1755:107-20.
[21] Haddad JJ, Harb HL. Cytokines and the regulation of hypoxia-inducible factor (HIF)-1alpha. International immunopharmacology. 2005;5:461-83.
[22] Klimova T, Chandel NS. Mitochondrial complex III regulates hypoxic activation of HIF. Cell death and differentiation. 2008;15:660-6.
[23] Iyer NV, Kotch LE, Agani F, Leung SW, Laughner E, Wenger RH, et al. Cellular and developmental control of O2 homeostasis by hypoxia-inducible factor 1 alpha. Genes & development. 1998;12:149-62.
[24] Kotch LE, Iyer NV, Laughner E, Semenza GL. Defective vascularization of HIF-1alpha-null embryos is not associated with VEGF deficiency but with mesenchymal cell death. Developmental biology. 1999;209:254-67.
[25] Compernolle V, Brusselmans K, Franco D, Moorman A, Dewerchin M, Collen D, et al. Cardia bifida, defective heart development and abnormal neural crest migration in embryos lacking hypoxia-inducible factor-1alpha. Cardiovascular research. 2003;60:569-79.
[26] Krishnan J, Ahuja P, Bodenmann S, Knapik D, Perriard E, Krek W, et al. Essential role of developmentally activated hypoxia-inducible factor 1alpha for cardiac morphogenesis and function. Circulation research. 2008;103:1139-46.
[27] Yin Z, Haynie J, Yang X, Han B, Kiatchoosakun S, Restivo J, et al. The essential role of Cited2, a negative regulator for HIF-1alpha, in heart development and neurulation. Proceedings of the National Academy of Sciences of the United States of America. 2002;99:10488-93.
[28] Xu B, Doughman Y, Turakhia M, Jiang W, Landsettle CE, Agani FH, et al. Partial rescue of defects in Cited2-deficient embryos by HIF-1alpha heterozygosity. Developmental biology. 2007;301:130-40.
[29] Wikenheiser J, Wolfram JA, Gargesha M, Yang K, Karunamuni G, Wilson DL, et al. Altered hypoxia-inducible factor-1 alpha expression levels correlate with coronary vessel anomalies. Developmental dynamics : an official publication of the American Association of Anatomists. 2009;238:2688-700.
[30] Kline DD, Peng YJ, Manalo DJ, Semenza GL, Prabhakar NR. Defective carotid body function and impaired ventilatory responses to chronic hypoxia in mice partially deficient for hypoxia-inducible factor 1 alpha. Proceedings of the National Academy of Sciences of the United States of America. 2002;99:821-6.
[31] Li J, Bosch-Marce M, Nanayakkara A, Savransky V, Fried SK, Semenza GL, et al. Altered metabolic responses to intermitternt hypoxia in mice with partial deficiency of hypoxia-inducible factor 1 a. Physiol Genomics. 2006.
[32] Zhang H, Bosch-Marce M, Shimoda LA, Tan YS, Baek JH, Wesley JB, et al. Mitochondrial autophagy is an HIF-1-dependent adaptive metabolic response to hypoxia. The Journal of biological chemistry. 2008;283:10892-903.
[33] Peng YJ, Yuan G, Ramakrishnan D, Sharma SD, Bosch-Marce M, Kumar GK, et al. Heterozygous HIF-1alpha deficiency impairs carotid body-mediated systemic responses and reactive oxygen species generation in mice exposed to intermittent hypoxia. The Journal of physiology. 2006;577:705-16.

[34] Bohuslavova R, Kolar F, Kuthanova L, Neckar J, Tichopad A, Pavlinkova G. Gene expression profiling of sex differences in HIF1-dependent adaptive cardiac responses to chronic hypoxia. J Appl Physiol. 2010;109:1195-202.
[35] Ream M, Ray AM, Chandra R, Chikaraishi DM. Early fetal hypoxia leads to growth restriction and myocardial thinning. American journal of physiology Regulatory, integrative and comparative physiology. 2008;295:R583-95.
[36] Pfaffl MW. A new mathematical model for relative quantification in real-time RT-PCR. Nucleic acids research. 2001;29:e45.
[37] Carmeliet P, Ferreira V, Breier G, Pollefeyt S, Kieckens L, Gertsenstein M, et al. Abnormal blood vessel development and lethality in embryos lacking a single VEGF allele. Nature. 1996;380:435-9.
[38] Miquerol L, Langille BL, Nagy A. Embryonic development is disrupted by modest increases in vascular endothelial growth factor gene expression. Development. 2000;127:3941-6.
[39] Huang X, Gao X, Diaz-Trelles R, Ruiz-Lozano P, Wang Z. Coronary development is regulated by ATP-dependent SWI/SNF chromatin remodeling component BAF180. Developmental biology. 2008;319:258-66.
[40] Bruneau BG, Nemer G, Schmitt JP, Charron F, Robitaille L, Caron S, et al. A murine model of Holt-Oram syndrome defines roles of the T-box transcription factor Tbx5 in cardiogenesis and disease. Cell. 2001;106:709-21.
[41] Hiroi Y, Kudoh S, Monzen K, Ikeda Y, Yazaki Y, Nagai R, et al. Tbx5 associates with Nkx2-5 and synergistically promotes cardiomyocyte differentiation. Nature genetics. 2001;28:276-80.
[42] Bruneau BG, Logan M, Davis N, Levi T, Tabin CJ, Seidman JG, et al. Chamber-specific cardiac expression of Tbx5 and heart defects in Holt-Oram syndrome. Developmental biology. 1999;211:100-8.
[43] Takeuchi JK, Koshiba-Takeuchi K, Matsumoto K, Vogel-Hopker A, Naitoh-Matsuo M, Ogura K, et al. Tbx5 and Tbx4 genes determine the wing/leg identity of limb buds. Nature. 1999;398:810-4.
[44] Hatcher CJ, Kim MS, Mah CS, Goldstein MM, Wong B, Mikawa T, et al. TBX5 transcription factor regulates cell proliferation during cardiogenesis. Developmental biology. 2001;230:177-88.
[45] Takeuchi JK, Ohgi M, Koshiba-Takeuchi K, Shiratori H, Sakaki I, Ogura K, et al. Tbx5 specifies the left/right ventricles and ventricular septum position during cardiogenesis. Development. 2003;130:5953-64.
[46] Kubalak SW, Hutson DR, Scott KK, Shannon RA. Elevated transforming growth factor beta2 enhances apoptosis and contributes to abnormal outflow tract and aortic sac development in retinoic X receptor alpha knockout embryos. Development. 2002;129:733-46.
[47] Sedmera D, Hu N, Weiss KM, Keller BB, Denslow S, Thompson RP. Cellular changes in experimental left heart hypoplasia. The Anatomical record. 2002;267:137-45.
[48] Bartram U, Molin DG, Wisse LJ, Mohamad A, Sanford LP, Doetschman T, et al. Double-outlet right ventricle and overriding tricuspid valve reflect disturbances of looping, myocardialization, endocardial cushion differentiation, and apoptosis in TGF-beta(2)-knockout mice. Circulation. 2001;103:2745-52.
[49] Srivastava D, Olson EN. A genetic blueprint for cardiac development. Nature. 2000;407:221-6.

[50] Toyoda M, Shirato H, Nakajima K, Kojima M, Takahashi M, Kubota M, et al. jumonji downregulates cardiac cell proliferation by repressing cyclin D1 expression. Developmental cell. 2003;5:85-97.
[51] Dor Y, Camenisch TD, Itin A, Fishman GI, McDonald JA, Carmeliet P, et al. A novel role for VEGF in endocardial cushion formation and its potential contribution to congenital heart defects. Development. 2001;128:1531-8.
[52] Pinter E, Haigh J, Nagy A, Madri JA. Hyperglycemia-induced vasculopathy in the murine conceptus is mediated via reductions of VEGF-A expression and VEGF receptor activation. The American journal of pathology. 2001;158:1199-206.
[53] Roest PA, Molin DG, Schalkwijk CG, van Iperen L, Wentzel P, Eriksson UJ, et al. Specific local cardiovascular changes of Nepsilon-(carboxymethyl)lysine, vascular endothelial growth factor, and Smad2 in the developing embryos coincide with maternal diabetes-induced congenital heart defects. Diabetes. 2009;58:1222-8.
[54] Kumar SD, Yong SK, Dheen ST, Bay BH, Tay SS. Cardiac malformations are associated with altered expression of vascular endothelial growth factor and endothelial nitric oxide synthase genes in embryos of diabetic mice. Exp Biol Med (Maywood). 2008;233:1421-32.
[55] Zeller R, Bloch KD, Williams BS, Arceci RJ, Seidman CE. Localized expression of the atrial natriuretic factor gene during cardiac embryogenesis. Genes & development. 1987;1:693-8.
[56] Liberatore CM, Searcy-Schrick RD, Yutzey KE. Ventricular expression of tbx5 inhibits normal heart chamber development. Developmental biology. 2000;223:169-80.
[57] Schott JJ, Benson DW, Basson CT, Pease W, Silberbach GM, Moak JP, et al. Congenital heart disease caused by mutations in the transcription factor NKX2-5. Science. 1998;281:108-11.
[58] Botusan IR, Sunkari VG, Savu O, Catrina AI, Grunler J, Lindberg S, et al. Stabilization of HIF-1alpha is critical to improve wound healing in diabetic mice. Proceedings of the National Academy of Sciences of the United States of America. 2008;105:19426-31.
[59] Liu L, Marti GP, Wei X, Zhang X, Zhang H, Liu YV, et al. Age-dependent impairment of HIF-1alpha expression in diabetic mice: Correction with electroporation-facilitated gene therapy increases wound healing, angiogenesis, and circulating angiogenic cells. Journal of cellular physiology. 2008;217:319-27.
[60] Sarkar K, Fox-Talbot K, Steenbergen C, Bosch-Marce M, Semenza GL. Adenoviral transfer of HIF-1alpha enhances vascular responses to critical limb ischemia in diabetic mice. Proceedings of the National Academy of Sciences of the United States of America. 2009;106:18769-74.
[61] Cheng K, Ho K, Stokes R, Scott C, Lau SM, Hawthorne WJ, et al. Hypoxia-inducible factor-1alpha regulates beta cell function in mouse and human islets. The Journal of clinical investigation. 2010;120:2171-83.
[62] Gunton JE, Kulkarni RN, Yim S, Okada T, Hawthorne WJ, Tseng YH, et al. Loss of ARNT/HIF1beta mediates altered gene expression and pancreatic-islet dysfunction in human type 2 diabetes. Cell. 2005;122:337-49.
[63] Resar JR, Roguin A, Voner J, Nasir K, Hennebry TA, Miller JM, et al. Hypoxia-inducible factor 1alpha polymorphism and coronary collaterals in patients with ischemic heart disease. Chest. 2005;128:787-91.
[64] Hlatky MA, Quertermous T, Boothroyd DB, Priest JR, Glassford AJ, Myers RM, et al. Polymorphisms in hypoxia inducible factor 1 and the initial clinical presentation of coronary disease. American heart journal. 2007;154:1035-42.

**FIGURE LEGEND**

**Fig. 1.** Average number of embryos per litter. The average number of embryos per diabetic pregnancies (n = 52) was compared to non-diabetic pregnancies (n = 29). The number of *Wt* embryos/pregnancies was not affected by maternal diabetes in diabetic pregnancies with glucose levels > 30 mmol/L (severe hyperglycemia; n = 18 litters) or in diabetic pregnancies with blood glucose levels between 13.9 mmol/L and 30 mmol/L (moderate hyperglycemia; n = 34 litters). The number of *Hif1a*$^{+/-}$ embryos/litter was significantly decreased in diabetic pregnancies as compared to non-diabetic pregnancies. Statistical significance was assessed by one-way ANOVA (brackets at top) followed by Dunnett's post-test (all groups *vs.* non-diabetic *Wt* group). The values represent means ± SEM. *, P < 0.05; ***, P < 0.001; #, P < 0.037, *t-test*.

**Fig. 2.** External morphological changes in diabetes-exposed embryos at E14.5. The external appearances of *Wt* and *Hif1a*$^{+/-}$ embryos from non-diabetic (**A, F**) and diabetic pregnancies are compared at E14.5 (**B-E, G-J**). The most frequent defects associated with diabetic pregnancies were cardiovascular anomalies and neural tube defects. Neural tube defects were displayed mainly as neural tube closure defects (arrow in ***J*** and ***I***) and in some cases as a phenotype of zig-zag closure line of neural tube (**E**). Cardiovascular anomalies were manifested by hemorrhages (**C, G, I**), edema (**B, D, G**, arrow head), and anemic phenotype in live embryos (**H**). Scale bar: 5 mm. (**K**): Incidence of congenital defects in embryos between E10.5-E18.5 was affected by maternal diabetes. *Hif1a*$^{+/-}$ embryos from diabetic pregnancies (blood glucose levels > 13.9 mmol/L) showed an increased rate of congenital malformations

of 22% (n = 36 of 163) compared to 13% of diabetes-exposed *Wt* (n = 26 of 195; *P* = 0.03, Fisher's exact test) and to 1% of non-diabetic *Hif1a*$^{+/-}$ embryos (n = 1 of 117; P = 0.0001, Fisher's exact test). No significant effect of genotype on the incidence of congenital defects was detected in diabetic pregnancies with glucose levels > 30 mmol/L (severe hyperglycemia) with frequencies of 26% (n = 15 of 58) and 28% (n = 18 of 64; *P* = 0.8, Fisher's exact test) for *Hif1a*$^{+/-}$ and *Wt* embryos, respectively. However, the significant effect of genotype on the incidence of congenital defects was found in diabetic pregnancies with blood glucose levels between 13.9 mmol/L and 30 mmol/L (moderate hyperglycemia), in which 20% of *Hif1a*$^{+/-}$ embryos (n = 21 of 105) as compared to 6% of *Wt* embryos (n = 8 of 131, *P* = 0.002, Fisher's exact test) demonstrated congenital defects. *, P < 0.03, Fisher's exact test.

**Fig. 3.** Morphological changes in embryos exposed to maternal diabetes. H&E staining of E14.5 mouse embryonic transverse sections of E14.5 thorax demonstrated an increased rate of cardiovascular defects in diabetes-exposed embryos (**A-D**). In *Wt* (**A**) and *Hif1a*$^{+/-}$ (**C**) embryos from non-diabetic pregnancies, the right and left ventricles were separated by the interventricular septum (IVS). In diabetes-exposed embryos (**B, D**), the 65% of detected cardiovascular defects were ventricular septal defects (VSD). Ventricular myocardial walls were thinner in all diabetes-exposed compared to non-diabetic embryos at E14.5. Scale bar: 0.5 mm. RV, right ventricle; LV, left ventricle; IVS, interventricular septum; VSD, ventricular septal defect. (**E**) The relative myocardial volumes ($\mu m^3$) of compact layer of diabetes-exposed RV of *Wt* (*P* < 0.003), RV of *Hif1a*$^{+/-}$ (*P* < 0.01), and LV of *Hif1a*$^{+/-}$ (*P* < 0.001) were significantly smaller compared to non-diabetic *Wt* and *Hif1a*$^{+/-}$ hearts. The compact myocardium of diabetes-exposed *Hif1a*$^{+/-}$ LV was significantly

more affected than diabetes-exposed *Wt* LV ($P < 0.01$). The relative myocardial volume of compact layer ($\mu m^3$) was estimated from the areas of LV with length of 0.2 mm and RV with the length of 0.4 mm ($\mu m^2$) multiplied by the thickness of sections (7 µm). (**F**) Thickness of trabecular myocardium at E14.5. The average area of trabecular myocardium of both the LV ($P < 0.0004$) and RV ($P < 0.0076$) was significantly increased in the diabetes-exposed hearts of *Wt* and *Hif1a*$^{+/-}$ embryos compared to non-diabetic *Wt*. Ventricular trabecular area was quantified using ImageJ software. We analyzed compact and trabecular myocardium in 3 subsequent sections of E14.5 thorax running through the AV junction with a four chamber view from 5 embryos from 3 litters/each group. The values represent means ± STDEV. *, $P < 0.05$, **, $P < 0.01$; one-way ANOVA (brackets at top) with Bonferroni's multiple comparison post-test.

**Fig. 4.** (**A**) Apoptosis in the diabetes-exposed and non-diabetic hearts of E14.5 *Wt* and *Hif1a*$^{+/-}$ embryos. The quantitative analysis showed that the number of apoptotic cells was significantly increased in *Hif1a*$^{+/-}$ diabetes-exposed embryos with heart defects as compared to hearts from non-diabetic pregnancies (n = 3 embryos for each group and 3 slides/embryo). The values represent means ± STDEV. *, $P < 0.05$, one-way ANOVA (brackets at top) with Bonferroni's multiple comparison post-test. (**B**) Quantification of cellular proliferation in compact ventricular myocardium of the diabetes-exposed and non-diabetic hearts of E14.5 *Wt* and *Hif1a*$^{+/-}$ embryos. Heart sections (7 µm) were immunostained for phospho-histone H3 (pHH3) to detect mitotic cells and pHH3$^{+}$ cells in compact myocardium of 4 embryos per each group and 2 slides per embryo were calculated. The relative volume of compact layer was calculated from the quantified area of compact myocardium in the field of view

multiplied by the thickness of sections (7 µm). The values represent means of number $pHH3^+$ nuclei/compact layer volume ± SEM. *P < 0.05, **P < 0.01, *** P < 0.001; one-way ANOVA (brackets at top) followed by Bonferroni's multiple comparison post-test. RV, right ventricle; LV, left ventricle.

**Fig. 5.** Protein levels of HIF-1α. Western blot analysis of protein levels of HIF-1α in whole embryos and hearts at E10.5. HIF-1α protein levels were assessed by immunoblotting of total protein lysates (25 µg per lane for whole embryos; 8 µg per lane for embryonic hearts; n = 2/each group). A representative immunoblot is shown. HIF-1α protein levels were normalized to the expression of α-actin. Values are shown as percentage of α-actin levels ± SEM. *P < 0.05; one-way ANOVA followed by Dunnett's post-test (all groups *vs.* non-diabetic *Wt*).

**Fig. 6.** Diabetes-induced increase in cardiac VEGF expression. In the E14.5 heart, a diabetes-induced increase in VEGF-A expression was detected in all myocardial cells aligning the endocardial cushions of both the inflow tract and the outflow tract of the heart, in the interventricular septum, and in the ventricular myocardium of embryos. Transverse sections of embryos stained with anti-VEGF-A antibody showed increased VEGF-A expression in two of four *Wt* analyzed embryos compared to non-diabetic controls (**A, B**). In diabetes-exposed $Hif1a^{+/-}$ hearts, the expression of VEGF-A was decreased in three of four analyzed embryos (**C, D**)**.** (**A-D**): overview Scale bar: 0.2 mm, original magnification 10x. Boxed areas are shown at higher magnification, (**E**) non-diabetic *Wt* and (**F**) diabetic *Wt* (original magnification 40x). IVS, interventricular septum; LV, left ventricle; RA, right atrium; RV, right ventricle. (**G**) Quantification of VEGF-A stained area was determined as a percentage of total

tissue area of the interventricular septum and LV myocardium of the field using ImageJ software. The values represent means ± STDEV (n = 4 embryos/group). Differences in VEGF-A expression were significant between diabetic *Wt* and non-diabetic *Wt* hearts. Statistical significance was assessed by one-way ANOVA (brackets at top). *, $P < 0.05$ (Dunnett's post-test). (**H**) RT-qPCR analysis of expression of *Vegfa* mRNA in *Wt* and *Hif1a*$^{+/-}$ hearts from diabetic and normal pregnancies at E14.5. The relative expression levels were quantified using ΔΔCT method. The data represent an expression of mRNA relative to non-diabetic *Wt* expression of mRNA, normalized by the housekeeping mRNA of *Hprt1*. Differences in normalized Ct values *Wt* and *Hif1a*$^{+/-}$ from diabetic pregnancy, and non-diabetic *Hif1a*$^{+/-}$ were not significant compared to non-diabetic *Wt* (one-way ANOVA). The relative expression of *Vegfa* for each individual embryo is shown. Two *Wt* and *Hif1a*$^{+/-}$ embryos from diabetic pregnancies with severe hyperglycemia were included into the analysis (red). Horizontal bars represent average expression of *Vegfa* for each group.

**Fig. 7.** Diabetes-induced changes in the ventricular myocardium. (**A**) Confocal imaging of transverse sections of embryonic heart of stage E14.5 (green autofluorescence) stained with anti-α-SMA antibody (red) showed hypoplasia of the compact ventricular myocardium in both *Wt* and *Hif1a*$^{+/-}$ diabetes-exposed embryos. Hoechst 33342 (blue) was used as a nuclear counterstain. Images are stacked Z-plane sections from confocal microscopy. LV, left ventricle; RV, right ventricle. Scale bar: 0.1 mm. (**B**) Relative quantification of α-SMA$^{+}$ area per field is shown. Quantification of α-SMA$^{+}$ area was determined as a percentage of total tissue area of the field of view using ImageJ software. Statistical significance was assessed by one-way ANOVA with Dunnett's post-test (all groups *vs.* non-diabetic *Wt*). The values

represent means ± SEM (n = 4 embryos from 3 litters/group). *, P < 0.05, **, P < 0.01.

**Fig. 8.** Gene expression changes in *Wt* and *Hif1a*$^{+/-}$ hearts exposed to maternal diabetes at E14.5. The expression of selected genes was analyzed using RT-qPCR. The relative expression levels were quantified using ΔΔCT method. The data represent an expression of mRNA relative to non-diabetic *Wt* expression of mRNA, normalized by the housekeeping mRNA of *Hprt1*. The values represent means ± SEM (each experiment in duplicate; n = 8 per groups of diabetic *Wt* and *Hif1a*$^{+/-}$, non-diabetic *Hif1a*$^{+/-}$; n = 6 per non-diabetic *Wt*). Differences in normalized Ct values were tested for statistical significance by one-way ANOVA (brackets at top) followed by Bonferroni's multiple comparison post-test. *, P < 0.05, **, P < 0.01, ***, P < 0.001.

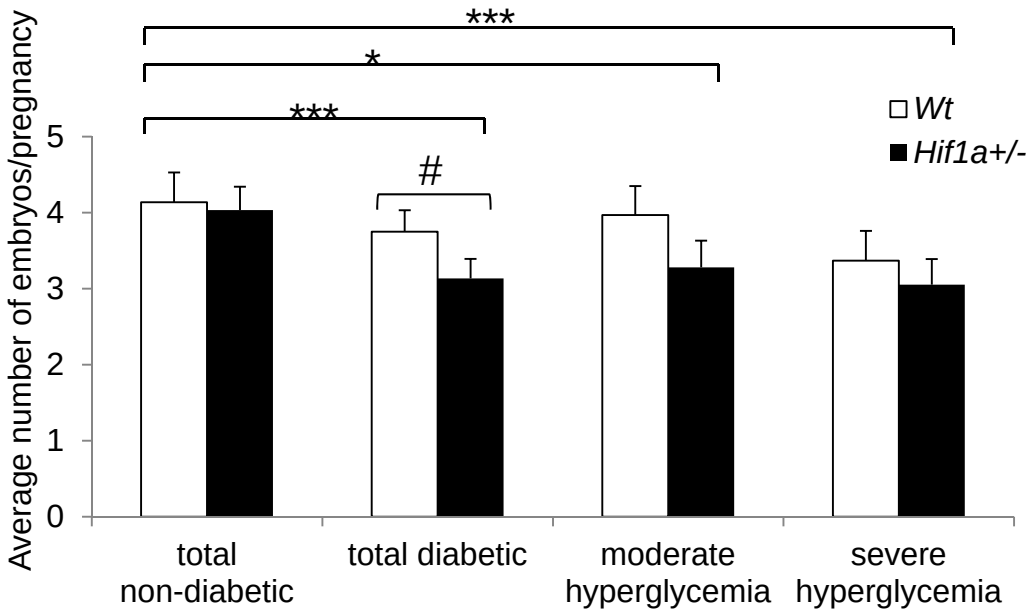


| | | | |
|---|---|---|---|
| blood glucose [mmol/L] :< 13.9 | > 13.9 | 13.9 - 30 | > 30 |

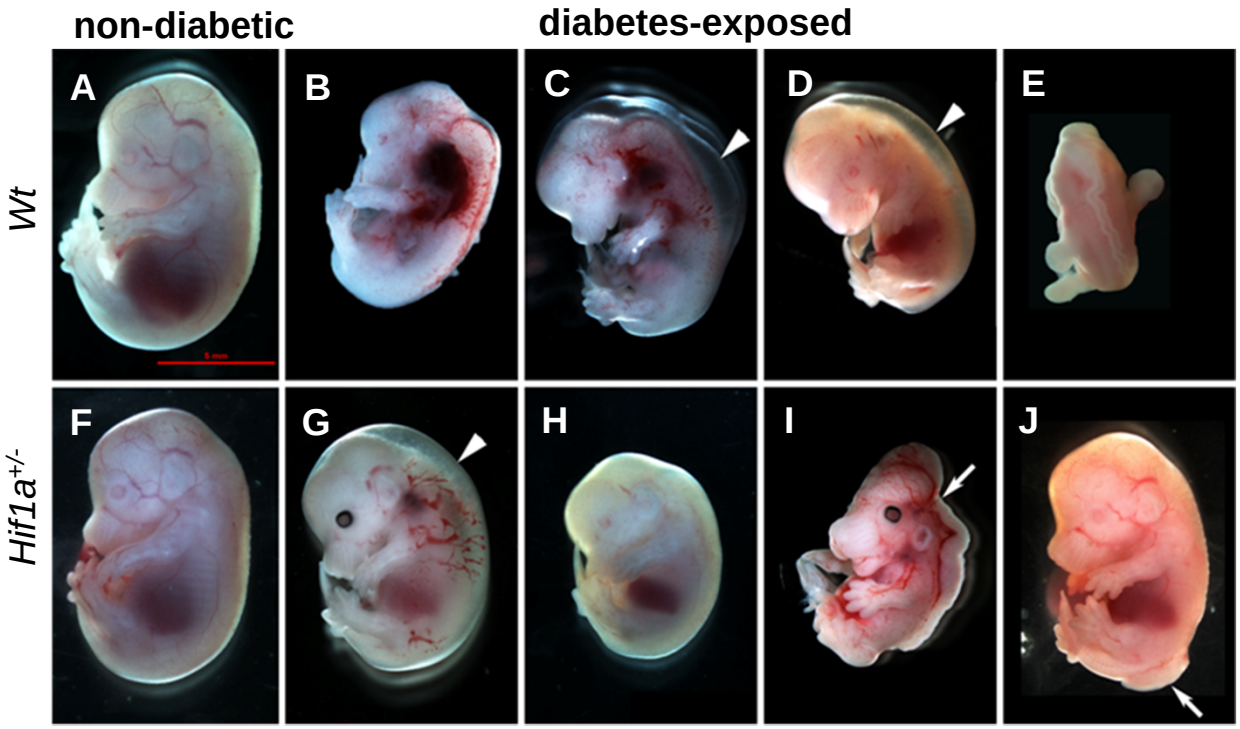
non-diabetic
diabetes-exposed
Wt
Hif1a+/-
A
B
C
D
E
F
G
H
I
J

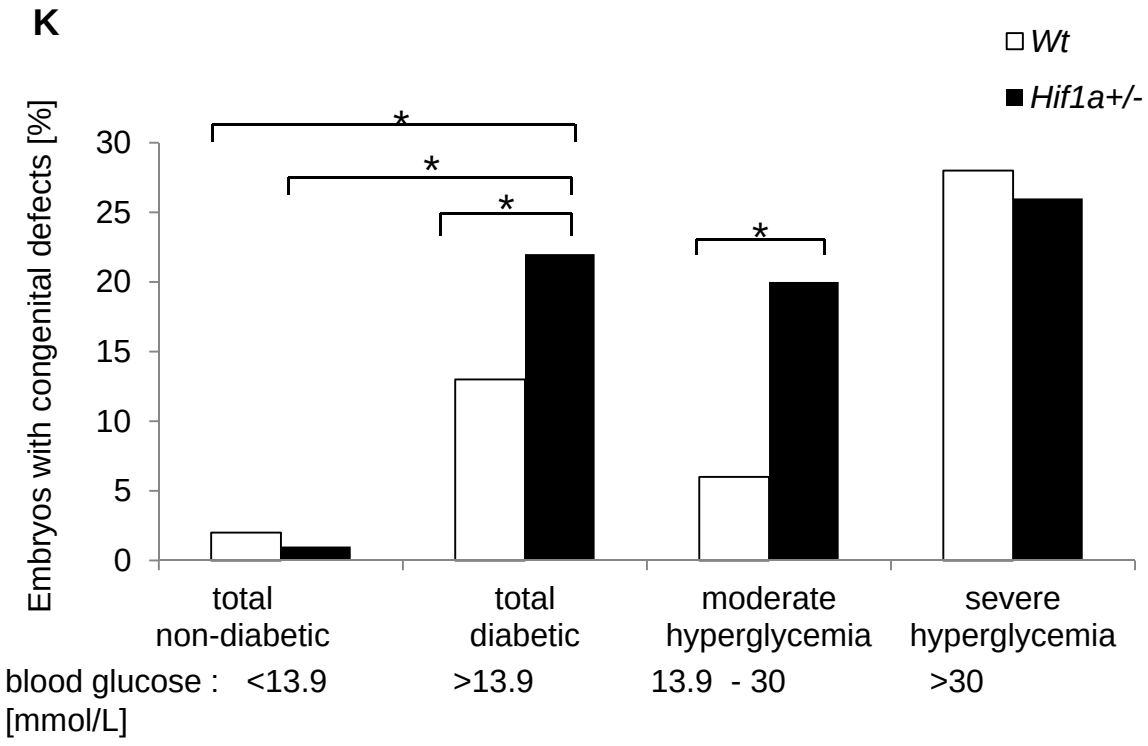
K
Wt
Hif1a+/-
Embryos with congenital defects [%]
30
25
20
15
10
5
0
*
*
*
*
total non-diabetic
total diabetic
moderate hyperglycemia
severe hyperglycemia
blood glucose : [mmol/L]
<13.9
>13.9
13.9 - 30
>30

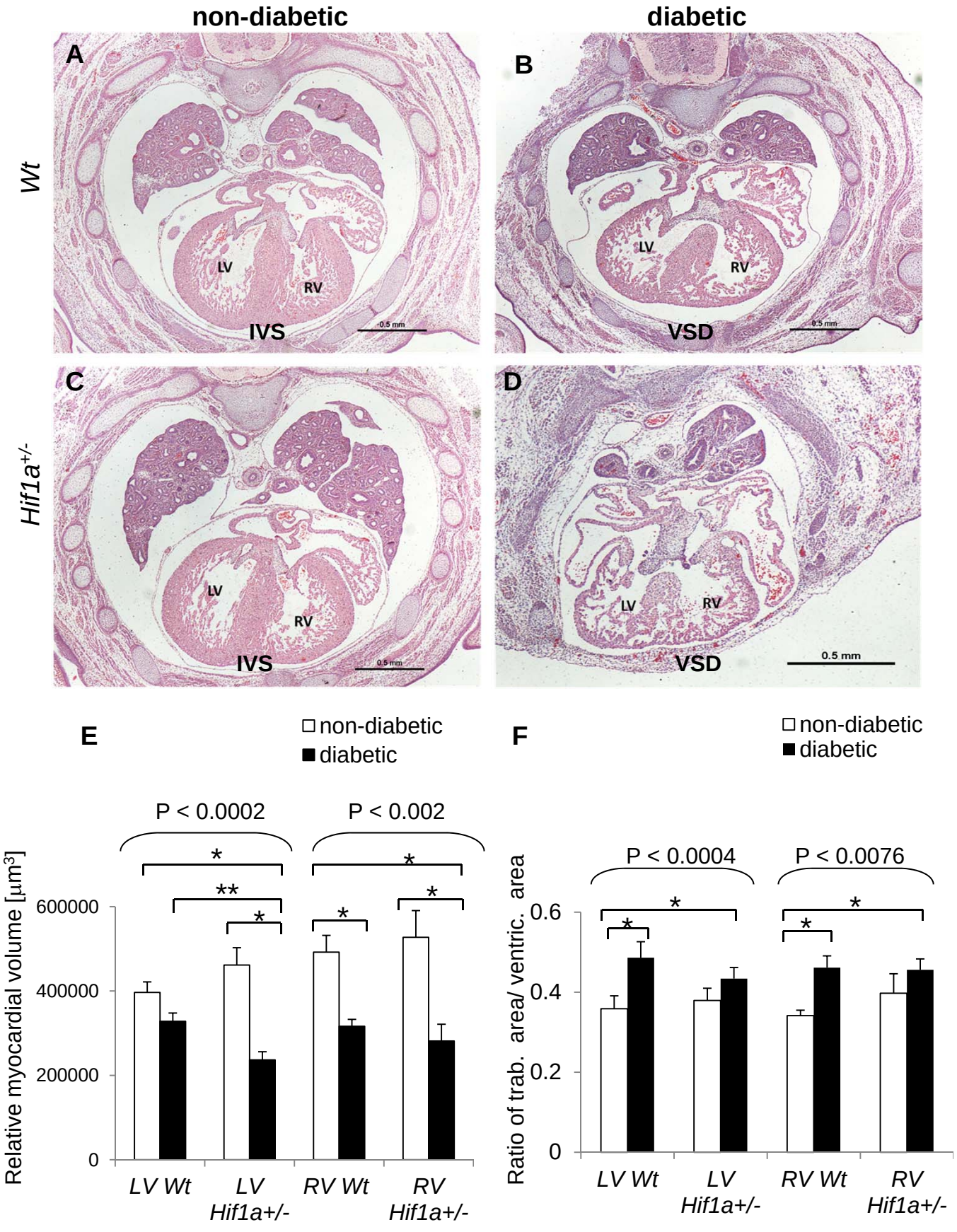
non-diabetic
diabetic
A
B
C
D
Wt
Hif1a+/-
LV
RV
IVS
VSD
0.5 mm
E
F
non-diabetic
diabetic
P < 0.0002
P < 0.002
P < 0.0004
P < 0.0076
Relative myocardial volume [µm3]
Ratio of trab. area/ ventric. area
600000
400000
200000
0
0.6
0.4
0.2
LV Wt
LV Hif1a+/-
RV Wt
RV Hif1a+/-

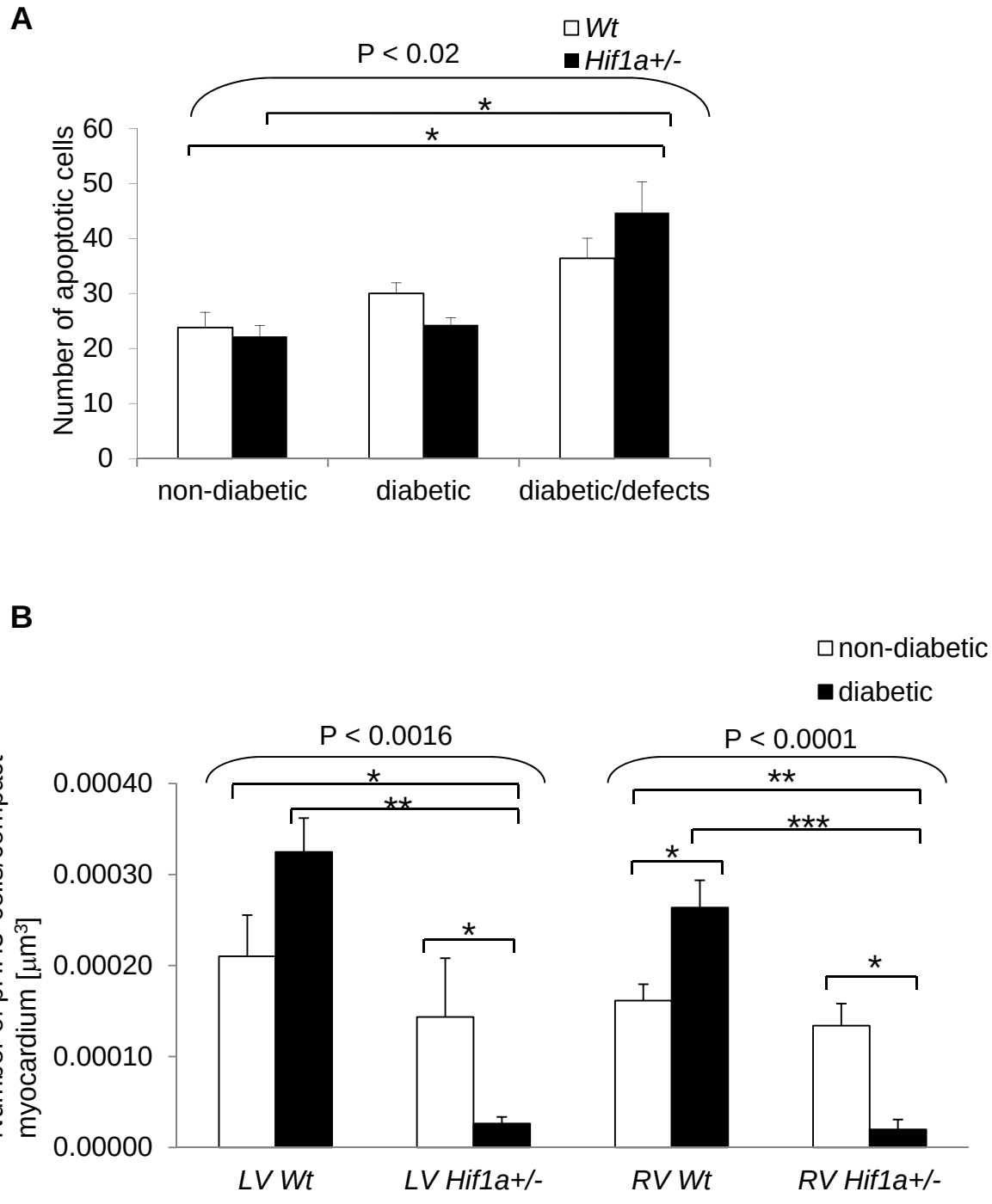
A
Wt
Hif1a+/-
P < 0.02
*
*
Number of apoptotic cells
60
50
40
30
20
10
0
non-diabetic
diabetic
diabetic/defects
B
non-diabetic
diabetic
P < 0.0016
P < 0.0001
*
**
*
**
***
*
*
*
Number of pHH3+cells/compact myocardium [µm3]
0.00040
0.00030
0.00020
0.00010
0.00000
LV Wt
LV Hif1a+/-
RV Wt
RV Hif1a+/-

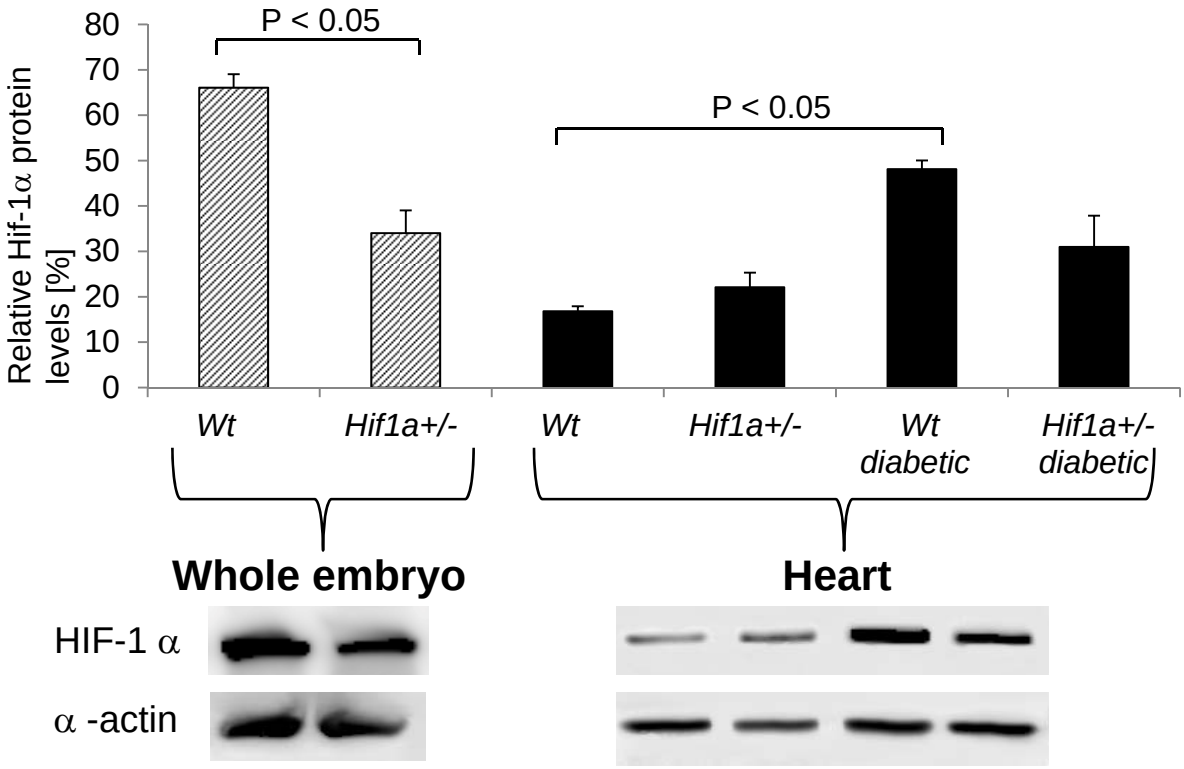
P < 0.05
P < 0.05
Relative Hif-1α protein levels [%]
80
70
60
50
40
30
20
10
0
Wt
Hif1a+/-
Wt
Hif1a+/-
Wt diabetic
Hif1a+/- diabetic
Whole embryo
Heart
HIF-1 α
α -actin

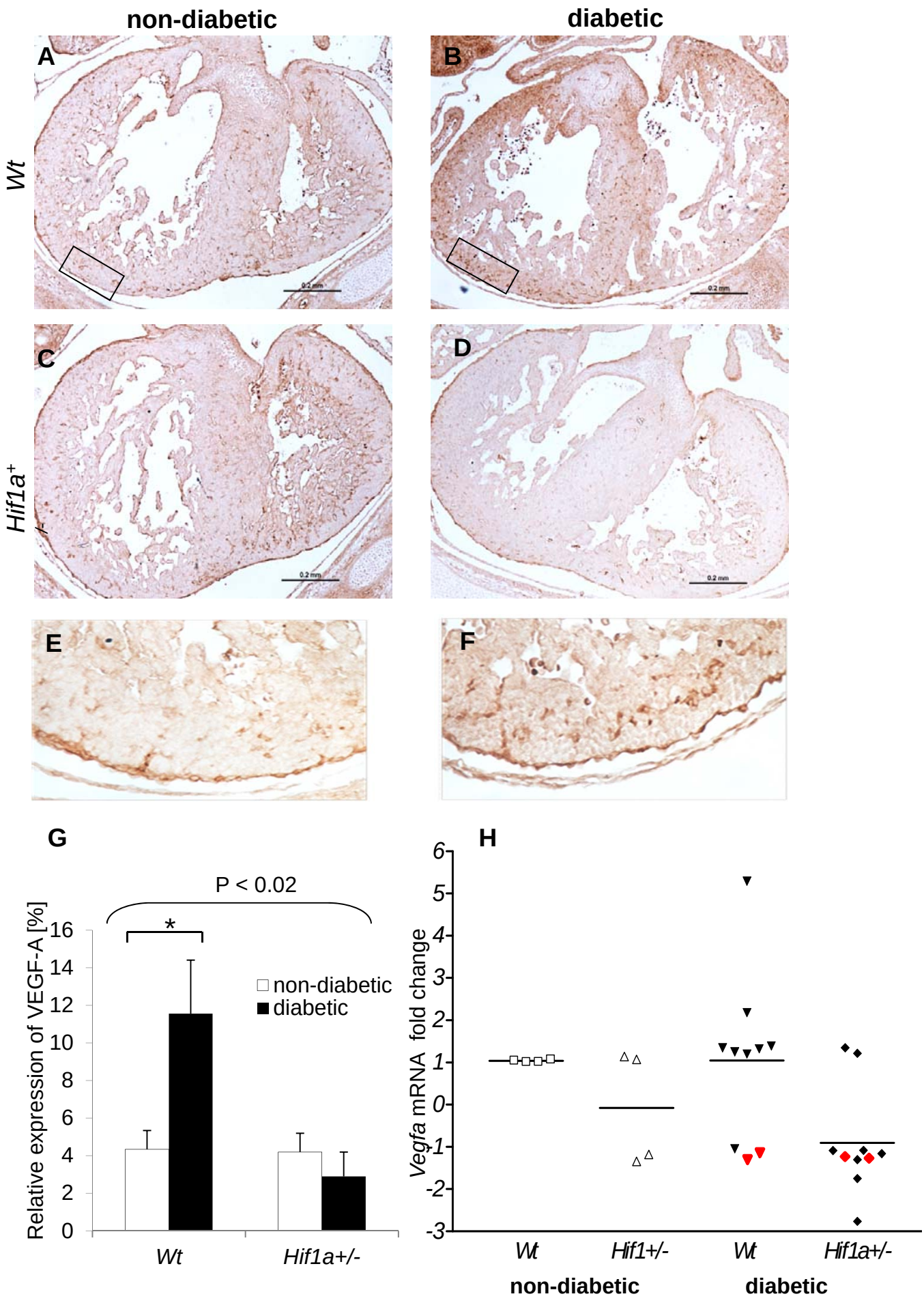
non-diabetic
diabetic
A
B
C
D
E
F
Wt
Hif1a+/-
0.2 mm
G
P < 0.02
*
Relative expression of VEGF-A [%]
16
14
12
10
8
6
4
2
0
non-diabetic
diabetic
Wt
Hif1a+/-
H
Vegfa mRNA fold change
6
5
4
3
2
1
0
-1
-2
-3
Wt
Hif1+/-
Wt
Hif1a+/-
non-diabetic
diabetic

A

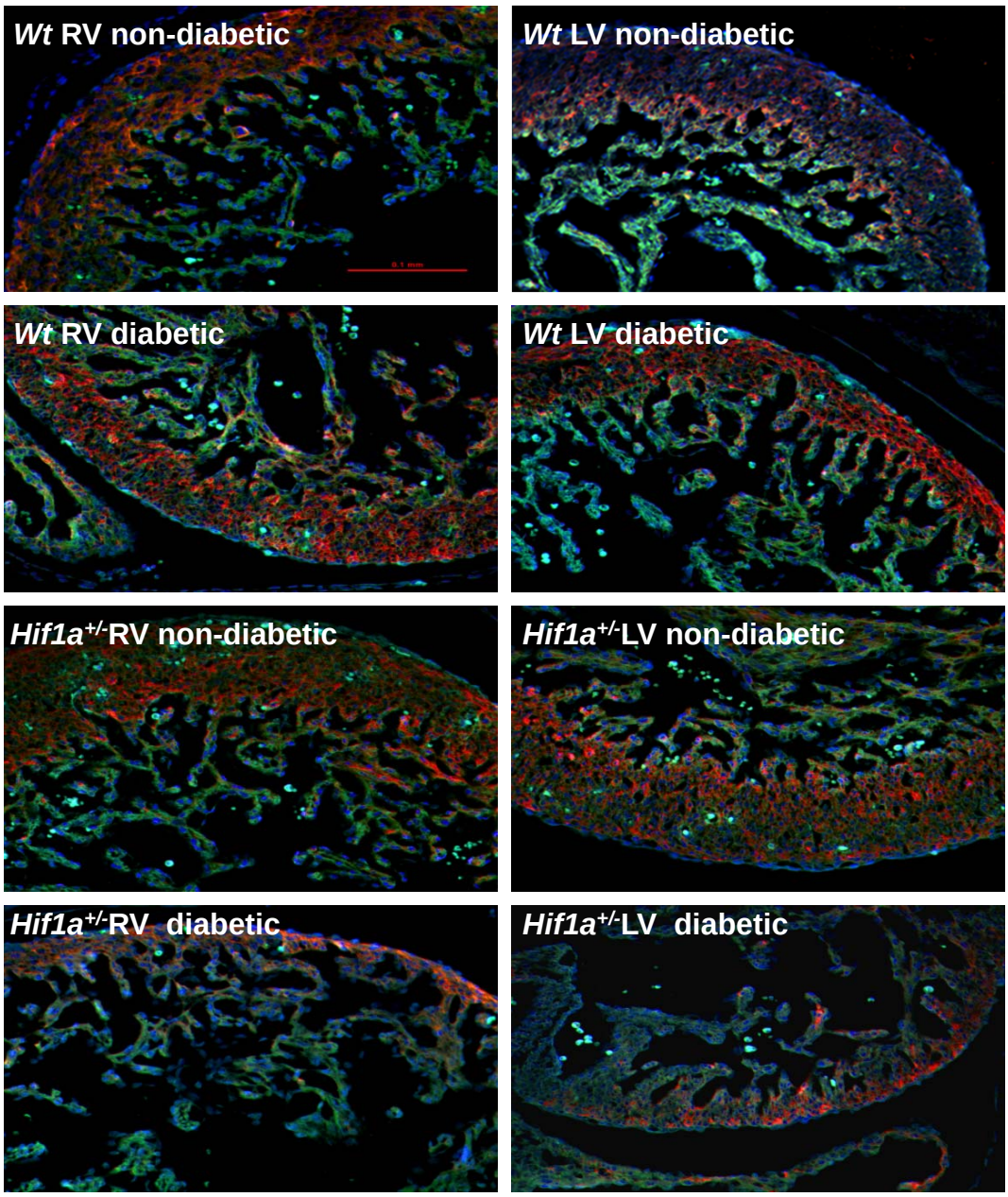
*Wt* RV non-diabetic
*Wt* LV non-diabetic
*Wt* RV diabetic
*Wt* LV diabetic
*Hif1a*$^{+/-}$RV non-diabetic
*Hif1a*$^{+/-}$LV non-diabetic
*Hif1a*$^{+/-}$RV diabetic
*Hif1a*$^{+/-}$LV diabetic

B

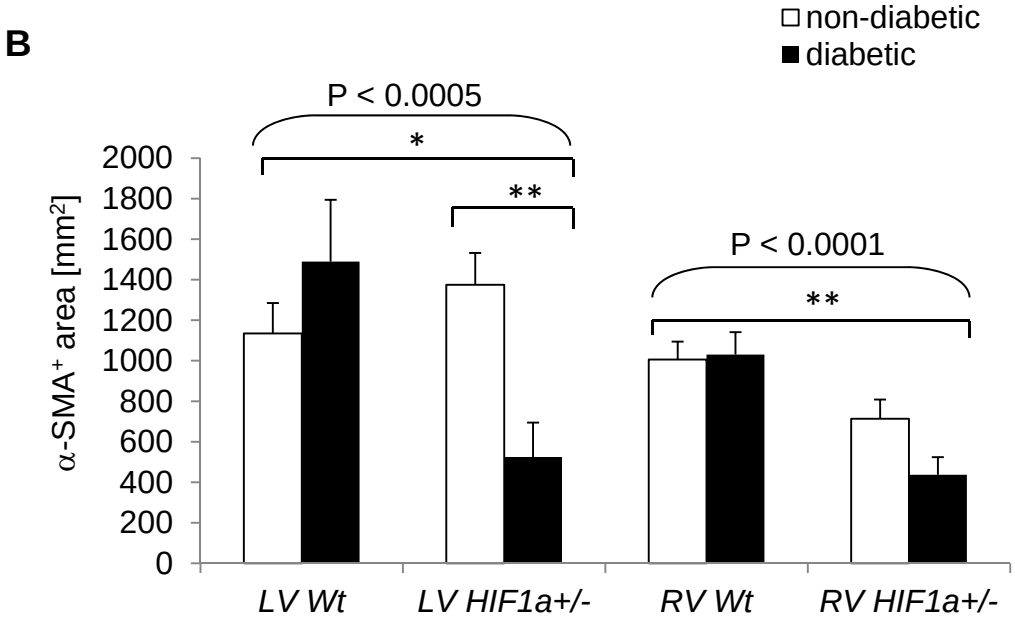
non-diabetic
diabetic
P < 0.0005
*
**
P < 0.0001
**
α-SMA⁺ area [mm²]
2000
1800
1600
1400
1200
1000
800
600
400
200
0
LV Wt
LV HIF1a+/-
RV Wt
RV HIF1a+/-

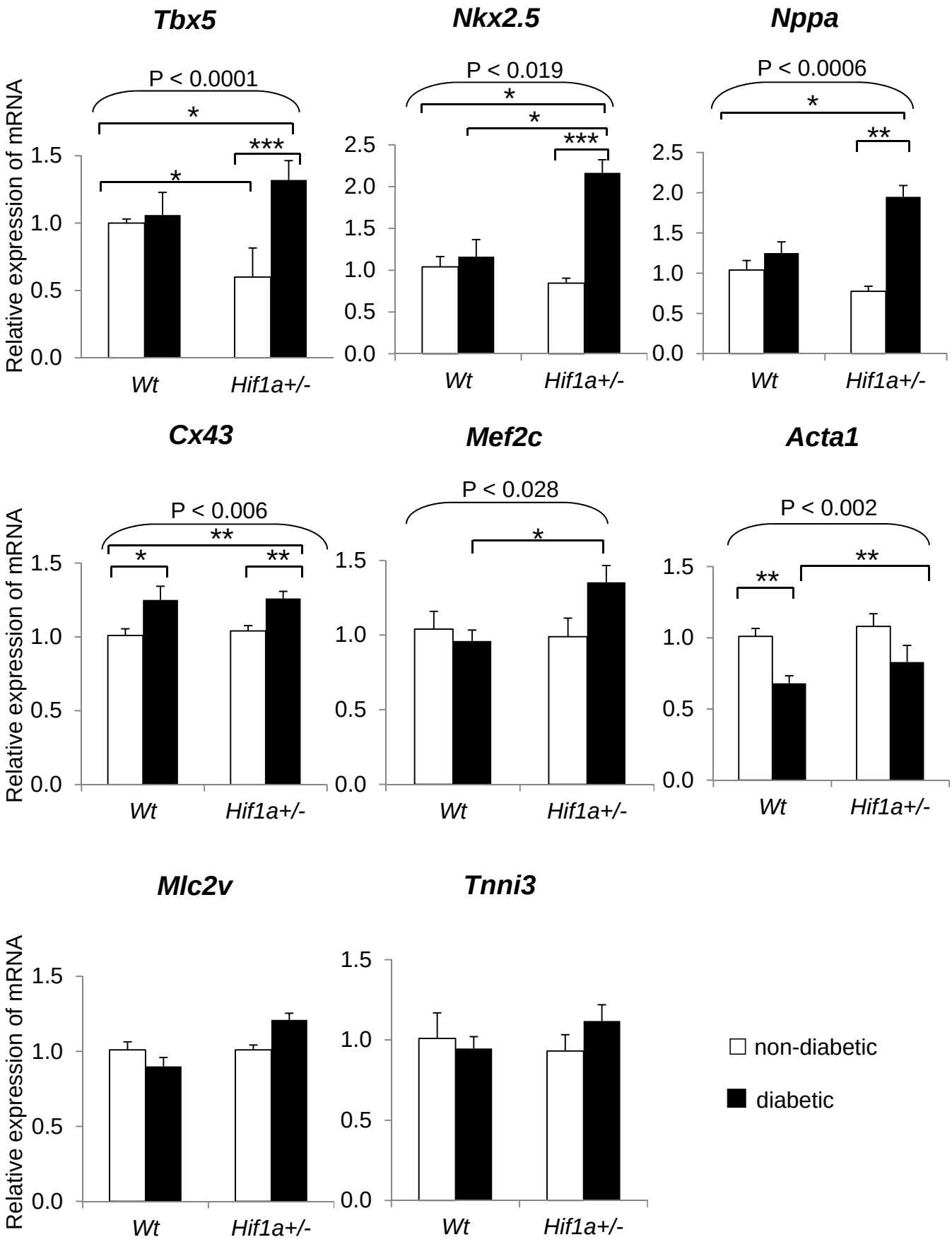
Tbx5
Nkx2.5
Nppa
Cx43
Mef2c
Acta1
Mlc2v
Tnni3
P < 0.0001
P < 0.019
P < 0.0006
P < 0.006
P < 0.028
P < 0.002
Relative expression of mRNA
Wt
Hif1a+/-
non-diabetic
diabetic

**Fig. S1**

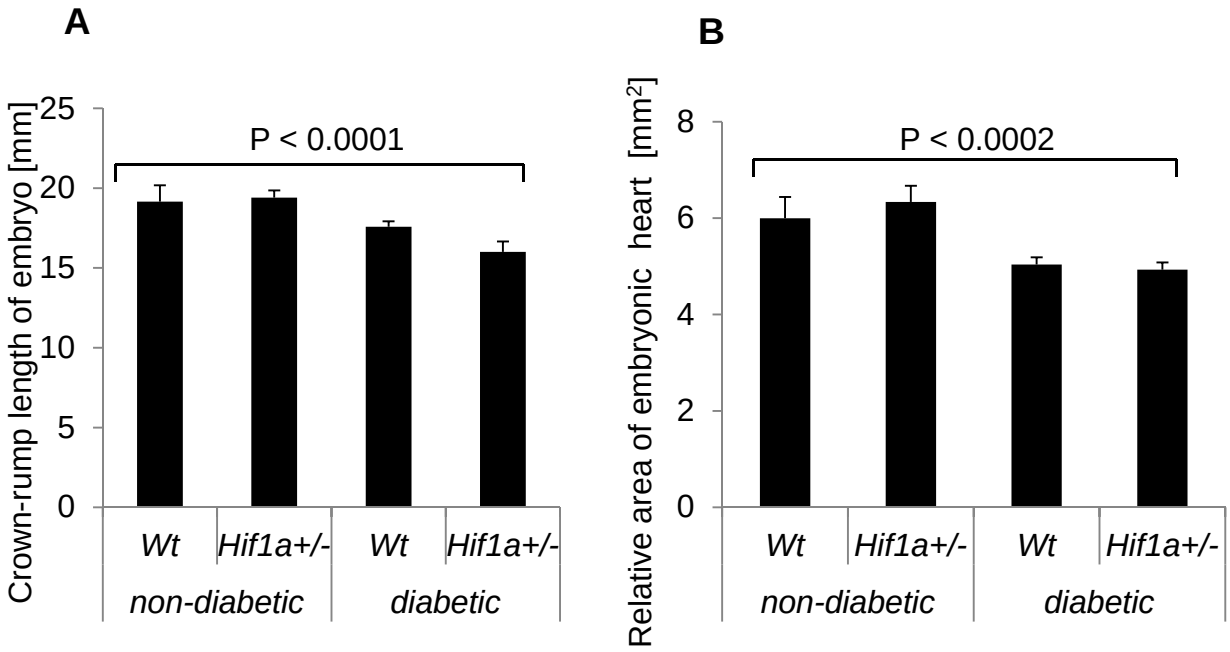
A
Crown-rump length of embryo [mm]
25
20
15
10
5
0
P < 0.0001
Wt
Hif1a+/-
Wt
Hif1a+/-
non-diabetic
diabetic
B
Relative area of embryonic heart [mm2]
8
6
4
2
0
P < 0.0002
Wt
Hif1a+/-
Wt
Hif1a+/-
non-diabetic
diabetic

# Gene expression profiling of sex differences in HIF1-dependent adaptive cardiac responses to chronic hypoxia

**Romana Bohuslavová, Frantisek Kolár, Lada Kuthanová, Jan Neckár, Ales Tichopád and Gabriela Pavlinkova**

*J Appl Physiol* 109:1195-1202, 2010. First published 15 July 2010; doi:10.1152/japplphysiol.00366.2010

*J Appl Physiol* 109: 1195–1202, 2010.
First published July 15, 2010; doi:10.1152/japplphysiol.00366.2010.

# Gene expression profiling of sex differences in HIF1-dependent adaptive cardiac responses to chronic hypoxia

**Romana Bohuslavová,[1] František Kolář,[2] Lada Kuthanová,[1] Jan Neckář,[2] Aleš Tichopád,[1,3] and Gabriela Pavlinkova[1]**

[1]*Institute of Biotechnology AS CR v.v.i, Prague;* [2]*Institute of Physiology AS CR, v.v.i., and Centre for Cardiovascular Research, Prague, The Czech Republic; and* [3]*Technical University Munich, Freising-Weihenstephan, Germany*

Submitted 6 April 2010; accepted in final form 13 July 2010

**Bohuslavová R, Kolář F, Kuthanová L, Neckář J, Tichopád A, Pavlinkova G.** Gene expression profiling of sex differences in HIF1-dependent adaptive cardiac responses to chronic hypoxia. *J Appl Physiol* 109: 1195–1202, 2010. First published July 15, 2010; doi:10.1152/japplphysiol.00366.2010.—Although physiological responses to chronic hypoxia, including pulmonary hypertension and right ventricular hypertrophy, have been well described, the molecular mechanisms involved in cardiopulmonary adaptations are still not fully understood. We hypothesize that adaptive responses to chronic hypoxia are the result of altered transcriptional regulations in the right and left ventricles. Here we report results from the gene expression profiling of adaptive responses in a chronically hypoxic heart. Of 11 analyzed candidate genes, the expression of seven and four genes, respectively, was significantly altered in the right ventricle of hypoxic male and female mice. In the transcriptional profile of the left ventricle, we identified a single expression change in hypoxic males (*Vegfa* gene). To directly test the role of HIF1, we analyzed the expression profile in *Hif1a* partially deficient mice exposed to moderate hypoxia. Our data showed that *Hif1a* partial deficiency significantly altered transcriptional profiles of analyzed genes in hypoxic hearts. The expression changes were only detected in two genes in the right ventricle of *Hif1a*$^{+/-}$ males and in one gene in the right ventricle of *Hif1a*$^{+/-}$ females. First, our results suggest that hypoxia mainly affects adaptive expression profiles in the right ventricle and that each ventricle can respond independently. Second, our findings indicate that HIF1a plays an important role in adaptive cardiopulmonary responses and the dysfunction of HIF1 pathways considerably affects transcriptional regulation in the heart. Third, our data reveal significant differences between males and females in cardiac adaptive responses to hypoxia and indicate the necessity of optimizing diagnostic and therapeutic procedures in clinical practice, with respect to sex.

hypoxia inducible factor-1α; hypoxia; gene expression profiling; vascular endothelial growth factor-A; cardiopulmonary adaptations; transcriptional regulation; quantitative RT-PCR

CHRONIC HYPOXIA is associated with many cardiopulmonary diseases or with prolonged stay at high altitude. Hypoxia induces adaptive changes at systemic and cellular levels, which have a profound effect on the morphology and function of the cardiopulmonary system, including pulmonary hypertension with the remodeling of the pulmonary arterioles and right ventricular (RV) hypertrophy. These changes may ultimately lead to heart failure. Whether the adaptive myocardial changes are beneficial or detrimental is determined by the duration and severity of hypoxic exposure.

Address for reprint requests and other correspondence: G. Pavlinkova, Institute of Physiology AS CR, v.v.i, Videnska 1083, 14220, Prague 4, CZ (e-mail: gpavlinkova@img.cas.cz).

Although physiological and pathophysiological responses to hypoxia have been described quite well (10, 23, 25), the molecular mechanisms involved in cardiac adaptations are still not fully understood. A variety of experimental studies have demonstrated that hypoxia affects many processes and pathways in the heart, including apoptosis (35), regulation of protein synthesis (9, 12), metabolism (18, 32), and transcriptional regulation, mainly by hypoxia-inducible factors (HIF) (30). HIF1 is a primary transcriptional regulator of hypoxia-induced cellular and systemic responses, and it activates a large number of target genes (~70) that are involved in many different cellular processes, such as cell proliferation, angiogenesis, metabolism, and apoptosis (31). Apart from the HIF family, hypoxia activates a number of other transcription factors (reviewed in 15), such as p53, AP-1, NF-κB, and GATA2 (37).

The regulation of gene expression and physiological responses to hypoxia are tissue specific. Hypoxia has opposite effects on systemic and pulmonary circulation, leading to vasodilatation in the systemic but vasoconstriction in the pulmonary vascular bed. Although two ventricles are influenced by tissue hypoxia, only the RV is exposed to increased pressure load. Consequently, chronic hypoxia is associated with the structural remodeling of pulmonary vessels and the development of RV hypertrophy. These adaptive changes are associated with altered gene expression within the heart (9, 12). Furthermore, clinical as well as experimental data show a significant difference between males and females in the cardiovascular responses (24, 26, 27). Although new experimental data analyzing sex differences in cardiovascular responses have recently been published, the underlying molecular mechanisms are still unknown.

To identify differences in the regulation of gene expression in the heart and differences between males and females adapted to a relatively moderate degree (12% $O_2$) of chronic continuous hypoxia (CCH), we have used mouse models and quantitative RT-PCR. To analyze the role of HIF1 pathways in responses to chronic hypoxia, we also performed gene expression profiling of *Hif1a* partially deficient male and female mice. Our results show that gene expression was differently regulated in the right and left ventricles and that it was significantly affected by hypoxia, sex, and *Hif1a* partial deficiency.

## MATERIALS AND METHODS

*Animal model.* The study was conducted in accordance with the *Guide for the Care and Use of Laboratory Animals,* published by the National Institutes of Health (NIH Publication No. 85–23, Revised 1996). The experimental protocol was approved by the Animal Care and Use Committee of the Institute of Physiology, Academy of

Sciences of the Czech Republic. All experiments were performed with male and female littermate mice that were either wild type (*wt*) or heterozygous *Hif1a* knock-out (*Hif1a*$^{+/-}$) that were on average 13 wk old at the start of the study. The heterozygous *Hif1a* mutants have the *Hif1a*$^{tm1jhu}$ mutant allele in which exon 2, encoding the bHLH domain of *Hif1a* gene, has been replaced by intragenic deletion with a neomycin resistance (*neo*$^{R}$) gene (13). The heterozygous *Hif1a* deficient mice showed a partial loss of HIF-1α protein expression levels (5, 28, 40). We obtained the *Hif1a* deficient mice on a mixed C57B6/129 genetic background from Dr. Gregg L. Semenza, Johns Hopkins University School of Medicine. To unify the genetic background, we backcrossed *Hif1a*$^{+/-}$ C57B6/129 mice onto the inbred FVB mouse strain (strain code 207, Charles River) for at least seven generations. The heterozygous *Hif1a* deficient mouse colony was bred and maintained in our laboratory. Offspring of *wt* × *Hif1a*$^{+/-}$ mating were genotyped by PCR, using genomic DNA isolated from tails and amplifying neomycin (*Neo*) and *Hif1a* exon 2 sequences (13). Both *Neo* (463 bp) and *Hif1a* (317 bp) sequences were amplified from DNA of *Hif1a*$^{+/-}$ mice, whereas only *Hif1a* sequences were amplified from DNA of *wt* mice (*Hif1a*$^{+/+}$), respectively. The sequences of *Neo* primers were 5′-ACTGGCTGCTATTGGGCGAAGTG-3′ and 5′-GTAAAGCACGAGGAAGCGGTCAG-3′. Conditions for PCR were 94°C for 30 s, 48°C for 30 s, and 72°C for 30 s, for 40 cycles. The sequences of *Hif1a* exon 2 primers were 5′-TGTAGTCTCCTGCTAAAAG-3′ and 5′-TTATTCGAGTTAAGACAAAC-3′. Conditions for PCR were 94°C for 30 s, 63°C for 30 s, and 72°C for 30 s, for 40 cycles.

*Experimental protocol.* Experimental mice were housed in a controlled environment (23°C; 12:12-h light-dark cycle) with free access to water and standard chow diet. Animals were adapted to moderate continuous normobaric hypoxia ($F_{IO_2}$ 0.12) in a small room (5.6 m$^3$) supplied with three hypoxic generators (Everest Summit, Hypoxico, NY) for 4 wk. The concentration of oxygen was continuously monitored. An access compensatory hypoxic chamber prevented the occurrence of any reoxygenation during regular animal maintenance. Normoxic controls were kept under the same conditions, with the exception of having normal room air ($F_{IO_2}$ 0.21). At the end of the adaptation period, hypoxic mice as well as normoxic controls were anesthetized with 2% isoflurane (Aerrane, Baxter SA) to measure pulmonary blood pressure. A fluid-filled catheter connected to an external pressure transducer (Bpr-02, Experimetria) was introduced into the RV via the right jugular vein. RV systolic pressure was averaged from three measurements within a 5-min interval, each comprising 10 cardiac cycles. Hematocrit was measured in the mixed venous blood taken from the RV catheter. Hearts were then rapidly excised, washed in sterile cold (0°C) saline, and dissected. The RV, the left ventricle (LV), the interventricular septum, and both atria were weighed.

*Quantitative real-time PCR.* RNA was isolated from the LV and RV of the individual hypoxic and normoxic adult mice (8 individual samples/each group) by Trizol (Invitrogen). The concentration of extracted RNA was quantified using NanoDrop. Quantitative real-time PCR (qRT-PCR) was performed using a LightCycler 480 Real-Time PCR system (Roche, Roche Applied Science, Mannheim, Germany) on cDNA samples. RNA samples (1 μg) were subjected to reverse transcription using Superscript II (Fermentas). cDNA was diluted 10×, and 4 μl was added to 6 μl of SyberGreen JumpStart Tag ReadyMix (Sigma). The PCR reactions were run with the initial AmpliTaq activation at 95°C for 10 min, followed by 40 cycles at 95°C for 15 s and for 60 s at 60°C. Values for detection above threshold level (Cq) for each gene were determined relative to measurements of a control gene in independent reactions with aliquots of the same sample. A proper reference gene was identified by running a panel of 12 potential endogenous control genes (TATAA Biocenter AB, Göteborg, Sweden) commonly used in gene expression studies, including *Gapdh, Tubb5, Actb, 18S rRNA*, etc. Hypoxanthine-guanine phosphoribosyltransferase1 (*Hprt1)* gene was selected as the best reference gene for our analyses due to its exhibiting the most constant expression among our representative test samples. Normalized Cq values ($\Delta Cq = Cq_{GENE} - Cq_{Hprt1}$) were compared between groups of hypoxia-exposed and control mice using an unpaired two-tailed *t*-test with an assumption of unequal variance (GraphPad Prism 4, GraphPad Software, San Diego, CA). The relative expression ratio of a target gene was computed, based on its real-time PCR efficiencies (*E*) and the crossing point (Cq) difference (Δ) of hypoxic sample vs. a control/normoxic sample. To compare the expression of each gene between its normoxic and hypoxic states, the ΔΔCq was determined: $\Delta\Delta Cq = \Delta Cq_{Hypoxia} - \Delta Cq_{Normoxia}$. The efficiency (E) for each reaction was derived from the slope of the linear portion of the amplification reaction (14). The relative amount of a target gene = $E^{-\Delta\Delta Cq}$. QRT-PCR data were analyzed using the GenEX5 program (http://www.multid.se/genex/). Primer sets were designed to exclude amplification of potentially contaminating genomic DNA by positioning the amplicons across exon-exon junctions. Primers were designed using the Primer 3 software (http://frodo.wi.mit.edu/primer3/). As much as possible, all primers were designed to have similar properties so that PCRs for different genes could be performed in the same run. Primers were selected according to the following parameters: length between 18 and 24 bases, melting temperature (Tm) between 58° and 60°C, and G + C content between 40 and 60% (optimal 50%). Primer sequences are presented in Table 1.

*Statistical methods.* The SAS system for Windows v. 9.2 was used to perform the statistical analysis. The proc GLM was employed to study the effect of the treatment condition (normoxia vs. hypoxia) as the main factor, also considering, however, the factors of gene deficiency (*Hif1a*$^{+/-}$ vs. *wt*), sex, and type of tissue (RV and LV). Eventually, all interactions of the main factor were also considered in the model, including interactions with sex, gene deficiency, and type of tissue. The type III sum of squares and its associated *P* value were considered for every factor and interaction within our study. The estimated least-squares means for all levels of factors and interactions were obtained and the associated *P* values calculated. To visualize the effects over all genes, for the factors of sex, genotype, and tissue type, we used a heat map (see Fig. 2).

## RESULTS

*Body and heart mass, pulmonary blood pressure, and hematocrit.* After 4 wk of CCH, the *wt* males had a significantly lower body mass than the normoxic controls, whereas the body mass of hypoxic *Hif1a*$^{+/-}$ males remained unchanged compared with the *Hif1a*$^{+/-}$ males in normoxia (Table 2). The body mass of *Hif1a*$^{+/-}$ males was significantly different compared with *wt* males (28.7 ± 0.4 g vs. 24.9 ± 0.5 g, $P < 0.001$ by unpaired *t*-test). There was no difference in body mass between *wt* and *Hif1a*$^{+/-}$ females or between females under normoxic and hypoxic conditions. Hematocrit increased in both genotypes, *Hif1a*$^{+/-}$ and *wt,* and in both sex groups; however, the differences were more significant in males ($P \leq 0.001$) than in females ($P = 0.03$; Table 2). There was no significant effect of genotype on hematocrit levels after 4 wk of hypoxia. The development of RV hypertrophy in response to CCH was significant in *wt* males ($P = 0.03$). Surprisingly, change in the RV mass of *wt* females was not significant ($P = 0.08$). Although the mass ratio of RV to LV was increased in males ($P < 0.0009$) and females ($P < 0.03$), the effect of CCH was more evident in males (Table 2). These results suggest that basic adaptive physiological responses to chronic hypoxia are, to a certain extent, significantly different between the two sexes. CCH-induced RV hypertrophy was also detected in hypoxic *Hif1a*$^{+/-}$ males ($P = 0.007$) and females ($P = 0.002$).

Table 1. *Primer sequences*

| Gene Symbol | Gene Name | RefSeq ID | Forward Primer Sequence | Reverse Primer Sequence |
|---|---|---|---|---|
| Hif1a | Hypoxia inducible factor alpha | NM_010431 | 5′-CAGTACAGGATGCTTGCCAAAA-3′ | 5′-ATACCACTTACAACATAATTCACACACACA-3′ |
| Pdgfra1 | Alpha platelet-derived growth factor receptor | NM_011058 | 5′-GTCCCCATGCTTGAAAGGAA-3′ | 5′-CATCGTCCGAAAGGAGGTTTT-3′ |
| Slc2a1 | Solute carrier family 2, facilitated glucose transporter 1 | NM_011400 | 5′-GGGCATGTGCTTCCAGTATGT-3′ | 5′-ACGAGGAGCACCGTGAAGAT-3′ |
| Casp1 | Caspase 1, apoptosis-related cysteine peptidase | NM_12362 | 5′-TGGTCTTGTGACTTGGAGGAC-3′ | 5′-AGAAACGTTTTGTCAGGGTCA-3′ |
| Prkaa1 | Protein kinase, AMP-activated, alpha 1 catalytic subunit | NM_001013367 | 5′-CCTTCGGGAAAGTGAAGGT-3′ | 5′-ATTTTTCCCACCACGTCAAG-3′ |
| Bnip3l | BCL2/adenovirus E1B interacting protein 3-like | NM_009761 | 5′-CCTCGTCTTCCATCCACAAT-3′ | 5′-TTCTTGTGGTGAAGGGCTGT-3′ |
| Ldha | Lactate dehydrogenase A | NM_010699 | 5′-GCACTGACGCAGACAAGG-3′ | 5′-TGATCACCTCGTAGGCACTG-3′ |
| Hprt1 | Hypoxanthine guanine phosphoribosyl transferase | NM_013556 | 5′-GCTTGCTGGTGAAAAGGACCTCTCGAAG-3′ | 5′-CCCTGAAGTACTCATTATAGTCAAGGGCAT-3′ |
| Gata2 | GATA binding protein 2 | NM_008090 | 5′-CCCAAGCTTCGATTCTGTGT-3′ | 5′-TTGACTCAGCACAATCGTCTC-3′ |
| Igf2 | Insulin-like growth factor 2 | NM_001122736 | 5′-CGCGGCTTCTACTTCAGC-3′ | 5′-GGGGTGGCACAGTATGTCTC-3′ |
| Flt1 | FMS-like tyrosine kinase 1 | NM_010228 | 5′-GAGGAGGATGAGGGTGTCTATAGGT-3′ | 5′-GTGATCAGCTCCAGGTTTGACTT-3′ |
| Vegfa | Vascular endothelial growth factor A | NM_001025250 | 5′-ACTGGACCCTGGCTTTACTG-3′ | 5′-TGGGACTTCTGCTCTCCTTC-3′ |

The differences in RV mass between *wt* and *Hif1a*$^{+/-}$ genotypes, adapted to hypoxia, were not significant.

To determine whether the RV hypertrophy observed in hypoxic mice was associated with pulmonary hypertension, we measured pressure in the RV (Fig. 1). RV systolic pressure was significantly increased in hypoxic *wt* males (33 ± 3.0 mmHg) and females (32.6 ± 2.9 mmHg) compared with normoxic *wt* males (26.9 ± 5.0 mmHg) and females (26.5 ± 2.5 mmHg). In contrast, there were no significant differences in RV pressure between normoxic and hypoxic *Hif1a*$^{+/-}$ mice in either sex group. The differences between *Hif1a*$^{+/-}$ and *wt* genotypes in response to moderate CCH were highly significant in males ($P = 0.005$) and females ($P = 0.02$). Our results suggest that partial deficiency of *Hif1a* significantly alters the development of hypoxia-induced pulmonary hypertension. Since *Hif1a* partial deficiency reduces the increase in RV pressure associated with hypoxia, HIF1-regulated pathways may be directly involved in the development of pulmonary hypertension. Furthermore, our data suggest that RV hypertrophy is partially regulated by different molecular mechanisms and that pulmonary hypertension is not the sole determinant of RV hypertrophy in hypoxic animals, particularly in females.

*Gene expression profiling.* To explore the tissue-specific changes induced by adaptation to hypoxia in gene expression, we analyzed the expression of selected genes, coding proteins involved in the regulation of metabolism (AMP-activated pro-

Table 2. *Changes in body and heart mass, and hematocrit*

| Group | *n* | BM, g | LV, mg | RV, mg | RV/LV | Hct, % |
|---|---|---|---|---|---|---|
| wt males | | | | | | |
| Normoxia | 10 | 27.5 ± 0.4 | 59.9 ± 1.0 | 21.1 ± 0.8 | 0.353 ± 0.012 | 44.7 ± 1.1 |
| Hypoxia | 10 | 24.9 ± 0.5* | 51.9 ± 1.5* | 24.6 ± 1.2* | 0.479 ± 0.025* | 52.9 ± 0.3* |
| wt females | | | | | | |
| Normoxia | 8 | 20.5 ± 0.5 | 49.2 ± 1.1 | 17.7 ± 0.4 | 0.363 ± 0.014 | 47.1 ± 0.6 |
| Hypoxia | 10 | 21.6 ± 0.5 | 45.0 ± 1.6 | 19.6 ± 0.9 | 0.439 ± 0.026* | 49.8 ± 0.7* |
| *Hif1a*$^{+/-}$ males | | | | | | |
| Normoxia | 9 | 27.5 ± 1.0 | 58.8 ± 2.5 | 20.7 ± 1.3 | 0.353 ± 0.016 | 46.7 ± 0.8 |
| Hypoxia | 10 | 28.7 ± 0.4 | 54.7 ± 1.3 | 24.9 ± 0.6* | 0.456 ± 0.012* | 52.0 ± 0.6* |
| *Hif1a*$^{+/-}$ females | | | | | | |
| Normoxia | 10 | 22.2 ± 0.5 | 48.2 ± 1.3 | 16.9 ± 0.5 | 0.354 ± 0.014 | 46.2 ± 1.3 |
| Hypoxia | 11 | 22.4 ± 0.8 | 45.3 ± 2.0 | 20.6 ± 1.0* | 0.460 ± 0.023* | 50.3 ± 1.0* |

Data are means ± SE from indicated number of animals (*n*) in each group. BM, body mass; LV, left ventricular mass; RV, right ventricular mass; RV/LV, right-to-left ventricular index; Hct, hematocrit; wt, wild type. Differences between hypoxia-exposed and controls were tested for statistical significance using an unpaired 2-tailed *t*-test (GraphPad Prism 4). *$P < 0.05$ vs. corresponding normoxic group.

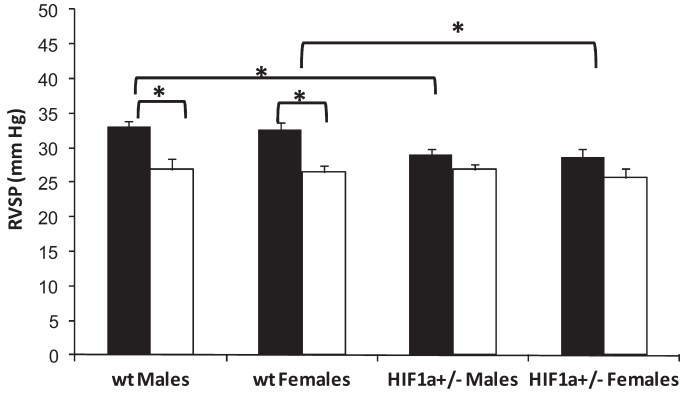


Fig. 1. Changes in right ventricular systolic pressure (RVSP) after 4 wk of continuous hypoxia. The pressure was significantly increased in *wt* males ($P < 0.0064$) and *wt* females ($P < 0.0003$) exposed to hypoxia (solid bars) compared with normoxic controls (open bars). The pressure of *Hif1a*$^{+/-}$ males and females exposed to 4 wk of hypoxia was not significantly affected compared with normoxic *Hif1a*$^{+/-}$ groups. The differences between hypoxic *Hif1a*$^{+/-}$ and *wt* males were statistically significant ($P < 0.005$). Similarly, hypoxic *Hif1a*$^{+/-}$ and *wt* females responses were significantly different ($P < 0.02$). *$P \leq 0.05$, using an unpaired 2-tailed *t*-test (GraphPad Prism 4).

tein kinase, *Prkaa*), apoptosis (caspase-1, *Casp1*), growth factor receptors (platelet-derived growth factor receptor alpha, *Pdgfra*), and transcription factors (*Hif1a*; GATA binding protein 2, *Gata2*) in the LV and RV. We also analyzed the gene expression of six HIF1 target genes, involved in glucose metabolism (lactate dehydrogenase A, *Ldha*; glucose transporter 1, *Slc2a1*), vasculogenesis and angiogenesis (vascular endothelial growth factor A, *Vegfa*; Vegf receptor-1, *Flt1*), apoptosis (BCL2/adenovirus E1B interacting protein 3-like, *Bnip3l*), and cell proliferation (insulin-like growth factor 2, *Igf2*) to directly evaluate HIF1-pathway responses to CCH. To further investigate the functional role of HIF1a, we analyzed hypoxia-induced gene expression changes in *Hif1a*$^{+/-}$ males and females. The gene expression was differentially regulated between the LV and RV of the heart (Fig. 2). In the RV, *wt* males and females responded to moderate CCH with the increased expression of the majority of the measured genes, while *Hif1a*$^{+/-}$ female and male responses were limited to one and two genes, respectively. In contrast to the RV expression patterns, in the LV, the largest increase in RNA levels was detected in *Hif1a*$^{+/-}$ males and the smallest expression changes were detected in *wt* males adapted to CCH. The significant interaction of sex and gene deficiency under hypoxic conditions was detected, with $P < 0.001$ and $P < 0.0001$, respectively (SAS system, proc GLM). Our results show that gene expression regulation in chronically hypoxic hearts was tissue specific and was significantly influenced by sex and *Hif1a* partial deficiency.

*Sex differences.* To test whether gene expression in the heart is regulated by CCH in a sex-dependent manner, the gene expression profiles in the RV and LV of female and male mice, adapted to CCH, were compared. On average, the relative expression of the measured genes was higher in males than in females, after 4 wk of hypoxia (Fig. 3). Of 11 measured genes, the expression of seven genes was significantly altered in hypoxic *wt* males, while the expression of four genes was significantly changed by hypoxia in the RV of *wt* females. The CCH transcriptional adaptive responses in the RV of *Hif1a* deficient females and males were detected in one and two genes, respectively (Fig. 3). Unexpectedly, *Hif1a*$^{+/-}$ male and female mutants responded to hypoxia with major transcription changes in the LV. The expression of nine genes was significantly altered in the *Hif1a*$^{+/-}$ male LV, whereas four genes were affected in the LV of *Hif1a*$^{+/-}$ females. The main difference between male and female responses to CCH was the expression of *Vegfa* mRNA. We designed the *Vegfa* primers for our qRT-PCR experiments to detect all primary *Vegfa* isoforms: VEGF 120, VEGF 164, and VEGF 188. Our results show that males responded to CCH with a significant downregulation of *Vegfa* mRNA in the RV, after 4 wk of adaptation. However, none of the hypoxic female groups showed any significant changes in *Vegfa* mRNA levels compared with the normoxic groups. Our results suggest that the expression of *Vegfa* in CCH exposure is also differently regulated based on sex.

*Effect of genotype on gene expression changes induced by hypoxia.* Similar to the smaller physiological changes, the transcriptional responses of *Hif1a* heterozygous mutants in the RV were less significant than in *wt* males, after 4-wk adaptation to CCH. Of 11 measured genes, the expression of seven genes was significantly altered by hypoxia in *wt* males, while the expression of two genes was significantly altered in hypoxic *Hif1a*$^{+/-}$ males. Of seven affected genes in the RV of *wt* hypoxic males, five genes were HIF1-mediated target genes (*Ldha, Flt1, Slc2a1, Igf2,* and *Vegfa*). In contrast, only one HIF1 target gene (*Vegfa*) was altered by 4-wk hypoxia in the RV of *Hif1a*$^{+/-}$ males (Fig. 3). Interestingly, the largest hypoxia-induced expression changes were detected in the LV of *Hif1a*$^{+/-}$ males. The mRNA expression of nine genes was significantly altered by hypoxia in the LV of *Hif1a*$^{+/-}$ males, whereas significantly altered response was detected in only one gene of 11 analyzed genes in the of *wt* male LV. The *Hif1a*$^{+/-}$ females responded to hypoxia with an increased expression of mRNA of just one gene, *Casp1*, in the RV, whereas *wt* females showed significant increase in the expression of four genes in the RV after CCH adaptation. Intriguingly, the *Hif1a*$^{+/-}$ males and females responded to hypoxia with increased *Casp1* expression, although the levels of *Casp1* mRNA were not significantly affected in hypoxic *wt* mice. The expression of *Casp1* was significantly increased, 1.5-fold on average, in the two heart ventricles of *Hif1a*$^{+/-}$ by CCH compared with normoxic *Hif1a*$^{+/-}$ controls. These results show that the regulation of gene expression is significantly affected by *Hif1a* deficiency and that the hypoxic responses are differently regulated in the two heart ventricles.

## DISCUSSION

*Gene expression profiling of adaptive responses to hypoxia.* In the present study, we found that an adaptation to moderate CCH was associated with a substantially differential response between the RV and LV myocardium. Although we analyzed relatively a small number of genes, we established that the expression of the majority of investigated genes (with a specific focus on HIF1 pathways) increased only in the RV compared with the LV of *wt* males and females. This differential expression can be attributed to the fact that both heart ventricles are exposed to different changes of workload under conditions of chronic hypoxia, while only the RV is challenged

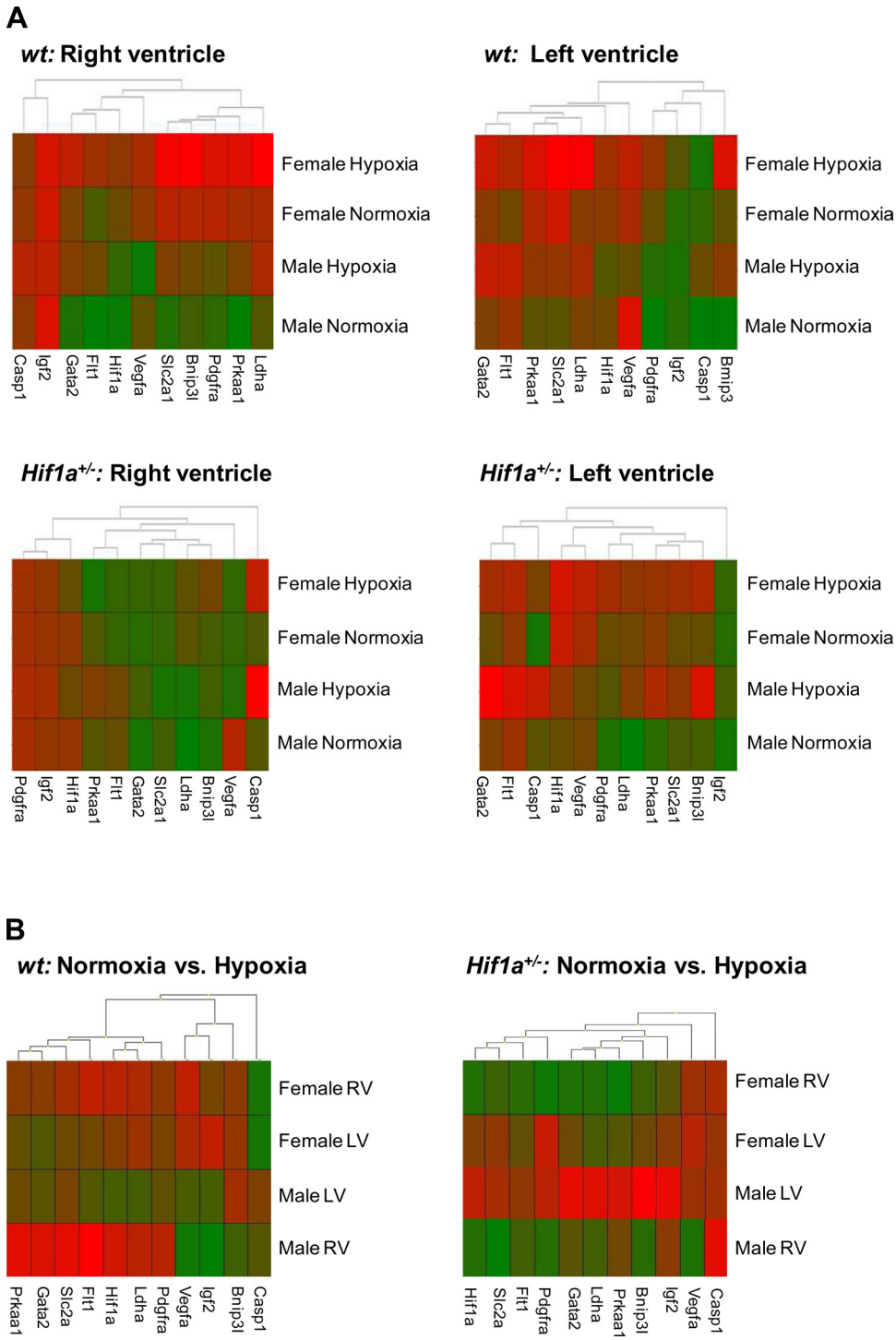


Fig. 2. Gene expression profiles/heat map. An expression profile of 11 individual genes (columns) across different groups of samples (rows) was visualized through hierarchical agglomerate clustering (GenEx5). The expression levels of each gene were measured in 8 different individual samples for each group, and their averages were displayed as a single cell in the heat map. *A*: the colors used in the *A* heat maps correspond to the ΔCq, which is the value for detection above threshold level (Cq) for each gene normalized to the levels of a reference gene (*Hprt1)* in the same sample. Boxes in bright red represent samples expressing genes at the highest levels; bright green represents genes with the lowest expression. *B*: the colors used in the *B* heat maps correspond to changes in gene expression between normoxic and hypoxic conditions. Boxes in bright red represent samples with the largest increase in gene expression; bright green represents genes with the largest decrease in gene expression between normoxia and hypoxia. These graphic representations show that expression profiles differ considerably between the right (RV) and left ventricles (LV) and are significantly affected by sex and *Hif1a* partial deficiency. Abbreviations: lactate dehydrogenase A (*Ldha*), BCL2/adenovirus E1B interacting protein 3-like (*Bnip3l*), hypoxia-inducible factor 1a (*Hif1a*), insulin-like growth factor 2 (*Igf2*), Vegf receptor-1 (*Flt1*), platelet derived growth factor receptor alpha (Pdgfra), protein kinase AMP-activated (*Prkaa*), glucose transporter 1 (*Slc2a1*), Caspase-1 (*Casp1*), GATA binding protein 2 (*Gata2*), vascular endothelial growth factor A (*Vegfa*).

by pulmonary hypertension. Therefore, our data suggest that the majority of analyzed genes were regulated by pressure load. In our model, the adaptation to moderate CCH was associated with the transcriptional upregulation of metabolic genes in the RV myocardium of *wt* males and females, including glycolytic enzyme *Ldha*, glucose transporter *Slc2a1*, and cardiac metabolism regulator *Prkaa* (Fig. 3). The reprogramming of cardiac energy metabolism to facilitate glucose utilization has been associated with the development of myocardial hypertrophy (1, 18, 32). We also identified adaptive changes in the transcriptional profiles of nonmetabolic genes involved in the regulation of cell proliferation (*Igf2*), apoptosis (*Bnip3l*), vasculogenesis and angiogenesis (*Vegfa* and *Flt1*), and transcription (*Gata2*). The transcription factor GATA2 is one of the regulatory elements required for a functional hypoxia-responsive element. The complementing roles of GATA2 and HIF1a in transcriptional regulation and their functional and physical relationship have been shown in previous reports (34, 37). In our experiments, *Gata2* mRNA was upregulated in the RV of hypoxic *wt* males and females, suggesting an increased

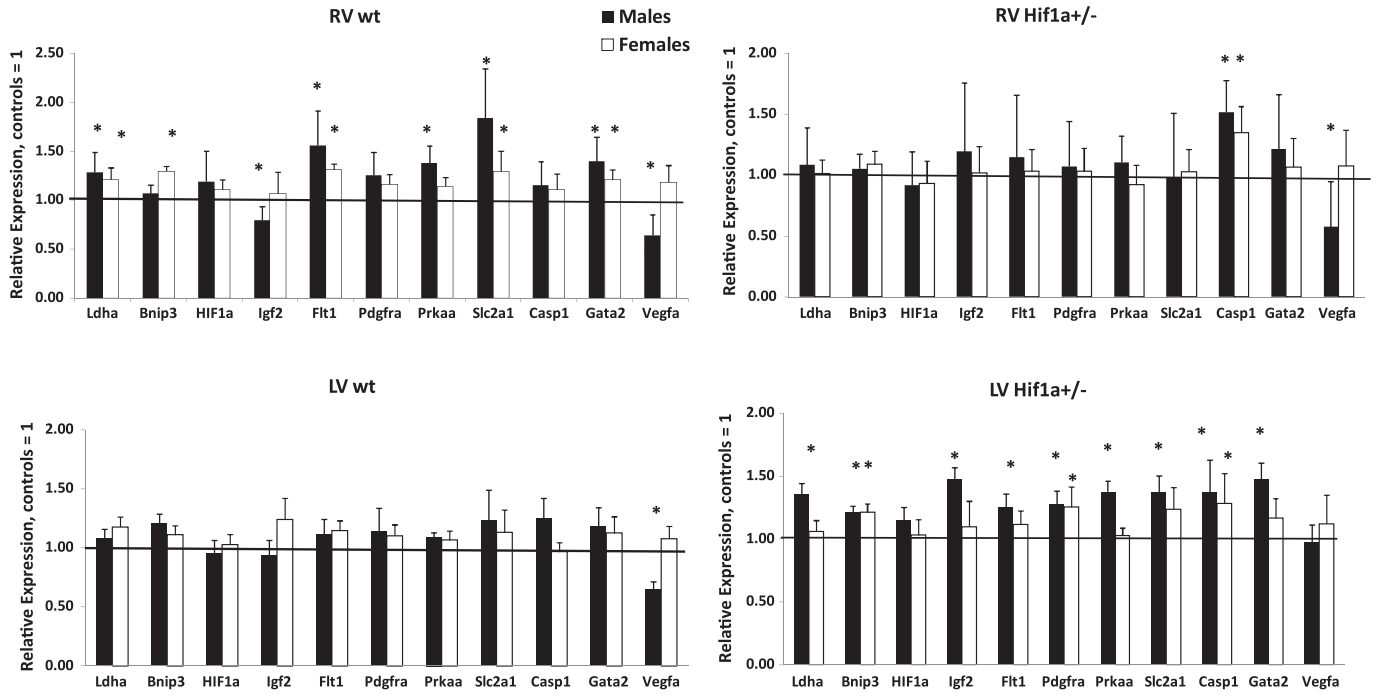


Fig. 3. Quantitative real-time PCR analysis of expression profiles in chronically hypoxic hearts of males and females. Total RNA was extracted from the LV and RV of *wt* and *Hif1a*$^{+/-}$ males and females after 4 wk of continuous hypoxia. Specific mRNAs were quantified, as described in MATERIALS AND METHODS. The data represent an expression of mRNA relative to normoxic controls, normalized by the housekeeping mRNA of *Hprt1*. Results are expressed as means ± SE (each experiment in duplicate; $n = 8$ per group). Differences in normalized Ct values between hypoxia-exposed and controls were tested for statistical significance using an unpaired 2-tailed *t*-test (GraphPad Prism 4). *Significant difference between normoxic and hypoxic groups at $P < 0.05$.

level of activation of HIF pathways via hypoxia-responsive element. Although the expression of *Hif1a* mRNA was not significantly increased in the analyzed hypoxic hearts, increased HIF1 transcriptional activity was evidenced through the altered mRNA expression of HIF1 transcriptional targets (*Flt1, Bnip3l, Ldha, Slc2a1, Igf2, Vegfa*). Our data are supported by several in vivo studies which show that *Hif1a* mRNA levels are only transiently increased in response to hypoxia, returning to basal levels within 24 h, and that the oxygen-sensitive α-subunit of HIF1 is predominantly regulated at the level of protein stability (3, 4, 36, 38). Furthermore, our findings suggest that persistent pulmonary hypertension primarily affects gene expression adaptive profile in the RV and that each ventricle can respond independently. Our data underscore the crucial importance of analyzing changes in gene expression separately from different regions of the heart because analyses of changes in the whole heart lead, by necessity, to inaccurate results and conclusions.

*Vegfa mRNA expression changes.* In our studies, significant changes were observed in the gene expression of *Vegfa*, a key target gene of local adaptation to hypoxia. Systemic hypoxia is one of the stimuli for in vivo induction of *Vegfa* expression, which affects vasculogenesis and angiogenesis in many organs. The expression of *Vegfa* is differentially regulated, based on the specific cell type, specific organ, severity of hypoxia, time of hypoxic exposure, and species reaction (22, 29). In addition, our results show that the expression of *Vegfa* in CCH exposure is also differently regulated based on sex. The time kinetics of *Vegfa* expression during hypoxic exposure is based on the formation of new capillaries, which cause an increase in oxygenation with a correlated downregulation of *Vegfa* expression, thus limiting the hypoxic stimulus (22). Previous studies have shown that initial increase in the expression of *Vegfa* mRNA in hypoxia is followed by the downregulation of *Vegfa* expression (7, 22), which corresponds with our current data. Furthermore, of 11 analyzed genes, *Vegfa* was the only gene with significant expression changes detected in both heart ventricles. These data suggest that the reduction of *Vegfa* mRNA in *wt* males after 4 wk of CCH was not regulated through an increased pressure load, but through other compensatory mechanisms, which were affected by sex.

*Differences between male and female responses to hypoxia.* On average, the relative expression of measured genes was smaller in *wt* females than in *wt* males. These smaller changes in gene expression may be correlated with a smaller effect of CCH on the body mass and the development of RV hypertrophy in *wt* females. These significant sex differences in adaptation to hypoxia may reflect the different sensitivity of males and females to oxygen deprivation and other stresses. Sex dependence in the development of cardiac hypertrophy and the reduced risk for cardiovascular diseases in females have also been reported in both epidemiological and experimental studies (reviewed in 24, 26). An additional possibility is that the temporal gene expression profile of hypoxic females may be different from the temporal profile of hypoxic males. This assumption is supported by recent studies, using neonatal mice (12). In this model, the fold change of the measured genes was also higher in males than females after 4-wk hypoxia; however, the relative gene expression was higher in females after 1-wk hypoxia (12). Taken together, our data reveal significant differences between males and females in cardiac adaptive responses to hypoxia and lend support to the necessity of opti-

mizing diagnostic and therapeutic procedures in clinical practice with respect to sex.

*Changes associated with Hif1a deficiency.* Several in vitro and animal studies have shown that HIF1 is crucial for the maintenance of normal cardiac functions and that activation of HIF1-regulated pathways plays a cardiovascular protective role (2, 6, 8, 11, 16). In contrast, the chronic activation of these pathways may contribute to cardiac degeneration and progression toward heart failure, as reported for mice with cardiac myocyte-specific deletion of the von Hippel-Lindau protein (21). The chronicity and intensity of HIF1 pathways activation are major determinants of whether the responses are pathological or beneficial. In this study, *Hif1a*$^{+/-}$ males and females adapted well to relatively moderate CCH with significantly altered gene expression profiles compared with hypoxic *wt* mice. In contrast to hypoxic *wt*, the transcriptional responses were significantly increased in the majority of analyzed genes in the *Hif1a*$^{+/-}$ LV, whereas the expression changes induced by hypoxia were only detected in two genes in the RV of *Hif1a*$^{+/-}$ males and in one gene in the RV of *Hif1a*$^{+/-}$ females. This striking difference between gene expression of *wt* and *Hif1a* deficient mutant mice exposed to moderate CCH was an unexpected finding. Based on our data, sustained hypoxia activates predominantly adaptive transcriptional responses in the RV of *wt*, whereas gene expression in the LV is essentially maintained at the normoxic levels. Thus the significantly smaller pressure load on the RV of *Hif1a*$^{+/-}$ and/or the limited availability of *Hif1a* may result in normoxic mRNA levels in the RV of *Hif1a*$^{+/-}$ as a means of adaptation to CCH. However, we can only speculate about the conditions that primarily affect gene expression in the LV of hypoxic *Hif1a*$^{+/-}$ mice. It is unlikely that the expression changes in the partially *Hif1a* deficient LV are related to pressure load conditions as CCH may decrease rather than increase systemic peripheral resistance and blood pressure. This indication is in agreement with the unchanged LV mass in hypoxic *Hif1a*$^{+/-}$. Therefore, the potential compensatory mechanisms associated with dysfunction of HIF1 pathways, inducing the CCH-adaptive expression pattern in the hypoxic *Hif1a*$^{+/-}$ LV, remain to be identified.

Along with small changes in the adaptive expression profiles of analyzed genes in the RV, the changes in body mass and RV systolic pressure were significantly smaller in hypoxic *Hif1a*$^{+/-}$ than in hypoxic *wt*. Using *Hif1a* deficient mice, other studies have also shown that CCH induces a significantly smaller degree of pulmonary hypertension (33, 39) and impaired ventilatory responses (17) compared with *wt* mice. Heterozygous deficient *Hif1a* mice were protected against hypoxia-induced pulmonary vascular remodeling, resulting in the decreased muscularization of pulmonary arterioles (39). An important signal in eliciting cardiorespiratory responses to hypoxia, including pulmonary remodeling, is the release of reactive oxygen species (19, 20). Interestingly, the production of reactive oxygen species is impaired in *Hif1a*$^{+/-}$ mice exposed to hypoxia (28), which may also contribute to the observed phenotype.

Taken together with other studies, our results indicate that HIF1 plays an important role in the development of hypoxic pulmonary hypertension. Since the development of severe pulmonary hypertension is linked to eventual heart failure, the downregulation of *Hif1a* expression could play an important beneficial role and it could influence existing therapies. We have shown that dysfunction of HIF1 pathways massively affects transcriptional profiles of analyzed genes in hypoxic hearts of *Hif1a*$^{+/-}$ mutants. With an increasing knowledge of HIF1 function, HIF1 therapeutical potential is evident and, therefore, the modulation of HIF1 activity is a high-priority target for cardiac treatments. Thus a detailed understanding of HIF1 regulation in the heart is of clinical importance.

## ACKNOWLEDGMENTS

We thank Gregg L. Semenza, M.D., Ph.D. for providing us with *Hif1a*$^{+/-}$ mutant mice.

## GRANTS

This study was supported by a Marie Curie International Reintegration Grant within the 7th European Community Framework Programme PIRG02-GA-2007–224760; grants from Ministry of Education, Youth and Sports AVOZ50520701; and the Czech Science Foundation 301/09/0117.

## DISCLOSURES

No conflicts of interest, financial or otherwise, are declared by the authors.

## REFERENCES

1. **Adrogue JV, Sharma S, Ngumbela K, Essop MF, Taegtmeyer H.** Acclimatization to chronic hypobaric hypoxia is associated with a differential transcriptional profile between the right and left ventricle. *Mol Cell Biochem* 278: 71–78, 2005.
2. **Bao W, Qin P, Needle S, Erickson-Miller CL, Duffy KJ, Ariazi JL, Zhao S, Olzinski AR, Behm DJ, Pipes GT, Jucker BM, Hu E, Lepore JJ, Willette RN.** Chronic inhibition of hypoxia-inducible factor (HIF) prolyl 4-hydroxylase improves ventricular performance, remodeling and vascularity following myocardial infarction in the rat. *J Cardiovasc Pharmacol* 2010 April 17 (doi:10.1097/FJC.0b013e3181e2bfef).
3. **Belaiba RS, Bonello S, Zahringer C, Schmidt S, Hess J, Kietzmann T, Gorlach A.** Hypoxia up-regulates hypoxia-inducible factor-1alpha transcription by involving phosphatidylinositol 3-kinase and nuclear factor kappaB in pulmonary artery smooth muscle cells. *Mol Biol Cell* 18: 4691–4697, 2007.
4. **Bianciardi P, Fantacci M, Caretti A, Ronchi R, Milano G, Morel S, von Segesser L, Corno A, Samaja M.** Chronic in vivo hypoxia in various organs: hypoxia-inducible factor-1alpha and apoptosis. *Biochem Biophys Res Commun* 342: 875–880, 2006.
5. **Bosch-Marce M, Okuyama H, Wesley JB, Sarkar K, Kimura H, Liu YV, Zhang H, Strazza M, Rey S, Savino L, Zhou YF, McDonald KR, Na Y, Vandiver S, Rabi A, Shaked Y, Kerbel R, Lavallee T, Semenza GL.** Effects of aging and hypoxia-inducible factor-1 activity on angiogenic cell mobilization and recovery of perfusion after limb ischemia. *Circ Res* 101: 1310–1318, 2007.
6. **Cai Z, Zhong H, Bosch-Marce M, Fox-Talbot K, Wang L, Wei C, Trush MA, Semenza GL.** Complete loss of ischaemic preconditioning-induced cardioprotection in mice with partial deficiency of HIF-1 alpha. *Cardiovasc Res* 77: 463–470, 2008.
7. **Deindl E, Kolar F, Neubauer E, Vogel S, Schaper W, Ostadal B.** Effect of intermittent high altitude hypoxia on gene expression in rat heart and lung. *Physiol Res* 52: 147–157, 2003.
8. **Eckle T, Kohler D, Lehmann R, El Kasmi K, Eltzschig HK.** Hypoxia-inducible factor-1 is central to cardioprotection: a new paradigm for ischemic preconditioning. *Circulation* 118: 166–175, 2008.
9. **Fan C, Iacobas DA, Zhou D, Chen Q, Lai JK, Gavrialov O, Haddad GG.** Gene expression and phenotypic characterization of mouse heart after chronic constant or intermittent hypoxia. *Physiol Genomics* 22: 292–307, 2005.
10. **Gilbert RD, Pearce WJ, Longo LD.** Fetal cardiac and cerebrovascular acclimatization responses to high altitude, long-term hypoxia. *High Alt Med Biol* 4: 203–213, 2003.
11. **Hyvarinen J, Hassinen IE, Sormunen R, Maki JM, Kivirikko KI, Koivunen P, Myllyharju J.** Hearts of hypoxia-inducible factor prolyl 4-hydroxylase-2 hypomorphic mice show protection against acute ischemia-reperfusion injury. *J Biol Chem* 285: 13646–13657.

12. **Iacobas DA, Fan C, Iacobas S, Haddad GG.** Integrated transcriptomic response to cardiac chronic hypoxia: translation regulators and response to stress in cell survival. *Funct Integr Genomics* 8: 265–275, 2008.
13. **Iyer NV, Kotch LE, Agani F, Leung SW, Laughner E, Wenger RH, Gassmann M, Gearhart JD, Lawler AM, Yu AY, Semenza GL.** Cellular and developmental control of $O_2$ homeostasis by hypoxia-inducible factor 1 alpha. *Genes Dev* 12: 149–162, 1998.
14. **Karlen Y, McNair A, Perseguers S, Mazza C, Mermod N.** Statistical significance of quantitative PCR. *BMC Bioinformatics* 8: 131, 2007.
15. **Kenneth NS, Rocha S.** Regulation of gene expression by hypoxia. *Biochem J* 414: 19–29, 2008.
16. **Kido M, Du L, Sullivan CC, Li X, Deutsch R, Jamieson SW, Thistlethwaite PA.** Hypoxia-inducible factor 1-alpha reduces infarction and attenuates progression of cardiac dysfunction after myocardial infarction in the mouse. *J Am Coll Cardiol* 46: 2116–2124, 2005.
17. **Kline DD, Peng YJ, Manalo DJ, Semenza GL, Prabhakar NR.** Defective carotid body function and impaired ventilatory responses to chronic hypoxia in mice partially deficient for hypoxia-inducible factor 1 alpha. *Proc Natl Acad Sci USA* 99: 821–826, 2002.
18. **Krishnan J, Suter M, Windak R, Krebs T, Felley A, Montessuit C, Tokarska-Schlattner M, Aasum E, Bogdanova A, Perriard E, Perriard JC, Larsen T, Pedrazzini T, Krek W.** Activation of a HIF1alpha-PPARgamma axis underlies the integration of glycolytic and lipid anabolic pathways in pathologic cardiac hypertrophy. *Cell Metab* 9: 512–524, 2009.
19. **Kumar GK, Rai V, Sharma SD, Ramakrishnan DP, Peng YJ, Souvannakitti D, Prabhakar NR.** Chronic intermittent hypoxia induces hypoxia-evoked catecholamine efflux in adult rat adrenal medulla via oxidative stress. *J Physiol* 575: 229–239, 2006.
20. **Lachmanova V, Hnilickova O, Povysilova V, Hampl V, Herget J.** *N*-acetylcysteine inhibits hypoxic pulmonary hypertension most effectively in the initial phase of chronic hypoxia. *Life Sci* 77: 175–182, 2005.
21. **Lei L, Mason S, Liu D, Huang Y, Marks C, Hickey R, Jovin IS, Pypaert M, Johnson RS, Giordano FJ.** Hypoxia-inducible factor-dependent degeneration, failure, and malignant transformation of the heart in the absence of the von Hippel-Lindau protein. *Mol Cell Biol* 28: 3790–3803, 2008.
22. **Marti HH, Risau W.** Systemic hypoxia changes the organ-specific distribution of vascular endothelial growth factor and its receptors. *Proc Natl Acad Sci USA* 95: 15809–15814, 1998.
23. **Martin D, Windsor J.** From mountain to bedside: understanding the clinical relevance of human acclimatisation to high-altitude hypoxia. *Postgrad Med J* 84: 622–627; quiz 626, 2008.
24. **Murphy E, Steenbergen C.** Gender-based differences in mechanisms of protection in myocardial ischemia-reperfusion injury. *Cardiovasc Res* 75: 478–486, 2007.
25. **Ostadal B, Kolar F.** Cardiac adaptation to chronic high-altitude hypoxia: beneficial and adverse effects. *Respir Physiol Neurobiol* 158: 224–236, 2007.
26. **Ostadal B, Netuka I, Maly J, Besik J, Ostadalova I.** Gender differences in cardiac ischemic injury and protection - experimental aspects. *Exp Biol Med (Maywood)* 234: 1011–1019, 2009.
27. **Ostadal B, Prochazka J, Pelouch V, Urbanova D, Widimsky J.** Comparison of cardiopulmonary responses of male and female rats to intermittent high altitude hypoxia. *Physiol Bohemoslov* 33: 129–138, 1984.
28. **Peng YJ, Yuan G, Ramakrishnan D, Sharma SD, Bosch-Marce M, Kumar GK, Semenza GL, Prabhakar NR.** Heterozygous HIF-1alpha deficiency impairs carotid body-mediated systemic responses and reactive oxygen species generation in mice exposed to intermittent hypoxia. *J Physiol* 577: 705–716, 2006.
29. **Sandner P, Gess B, Wolf K, Kurtz A.** Divergent regulation of vascular endothelial growth factor and of erythropoietin gene expression in vivo. *Pflügers Arch* 431: 905–912, 1996.
30. **Semenza GL.** Hypoxia-inducible factor 1 (HIF-1) pathway. *Sci STKE* 2007 (407): cm8, 2007.
31. **Semenza GL.** Targeting HIF-1 for cancer therapy. *Nat Rev Cancer* 3: 721–732, 2003.
32. **Sharma S, Taegtmeyer H, Adrogue J, Razeghi P, Sen S, Ngumbela K, Essop MF.** Dynamic changes of gene expression in hypoxia-induced right ventricular hypertrophy. *Am J Physiol Heart Circ Physiol* 286: H1185–H1192, 2004.
33. **Shimoda LA, Manalo DJ, Sham JS, Semenza GL, Sylvester JT.** Partial HIF-1alpha deficiency impairs pulmonary arterial myocyte electrophysiological responses to hypoxia. *Am J Physiol Lung Cell Mol Physiol* 281: L202–L208, 2001.
34. **Simon MP, Tournaire R, Pouyssegur J.** The angiopoietin-2 gene of endothelial cells is up-regulated in hypoxia by a HIF binding site located in its first intron and by the central factors GATA-2 and Ets-1. *J Cell Physiol* 217: 809–818, 2008.
35. **Webster KA, Graham RM, Bishopric NH.** BNip3 and signal-specific programmed death in the heart. *J Mol Cell Cardiol* 38: 35–45, 2005.
36. **Wiener CM, Booth G, Semenza GL.** In vivo expression of mRNAs encoding hypoxia-inducible factor 1. *Biochem Biophys Res Commun* 225: 485–488, 1996.
37. **Yamashita K, Discher DJ, Hu J, Bishopric NH, Webster KA.** Molecular regulation of the endothelin-1 gene by hypoxia. Contributions of hypoxia-inducible factor-1, activator protein-1, GATA-2, AND p300/CBP. *J Biol Chem* 276: 12645–12653, 2001.
38. **Yu AY, Frid MG, Shimoda LA, Wiener CM, Stenmark K, Semenza GL.** Temporal, spatial, and oxygen-regulated expression of hypoxia-inducible factor-1 in the lung. *Am J Physiol Lung Cell Mol Physiol* 275: L818–L826, 1998.
39. **Yu AY, Shimoda LA, Iyer NV, Huso DL, Sun X, McWilliams R, Beaty T, Sham JS, Wiener CM, Sylvester JT, Semenza GL.** Impaired physiological responses to chronic hypoxia in mice partially deficient for hypoxia-inducible factor 1alpha. *J Clin Invest* 103: 691–696, 1999.
40. **Zhang X, Liu L, Wei X, Tan YS, Tong L, Chang R, Ghanamah MS, Reinblatt M, Marti GP, Harmon JW, Semenza GL.** Impaired angiogenesis and mobilization of circulating angiogenic cells in HIF-1alpha heterozygous-null mice after burn wounding. *Wound Repair Regen* 18: 193–201, 2010.

*J Appl Physiol* 111: 625, 2011;
doi:10.1152/japplphysiol.zdg-9724-corr.2011.

**Corrigendum**

*Vol. 109, October 2010*

**Bohuslavová R, Kolář F, Kuthanová L, Neckář J, Tichopád A, Pavlinkova G**. Gene expression profiling of sex differences in HIF1-dependent adaptive cardiac responses to chronic hypoxia. *J Appl Physiol* 109: 1195–1202, 2010. First published July 15, 2010; doi:10.1152/japplphysiol.00366.2010.—The address for correspondence of G. Pavlinkova is incorrect. The correct address should be Institute of Biotechnology AS CR, v. v. i., Prague, The Czech Republic.

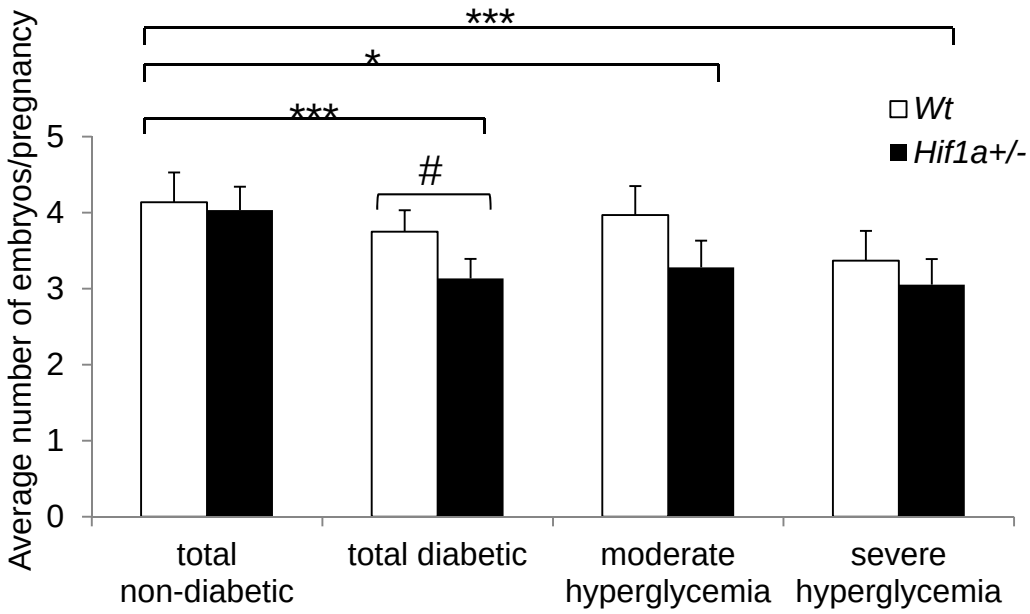


| | | | |
|---|---|---|---|
| blood glucose [mmol/L] :< 13.9 | > 13.9 | 13.9 - 30 | > 30 |

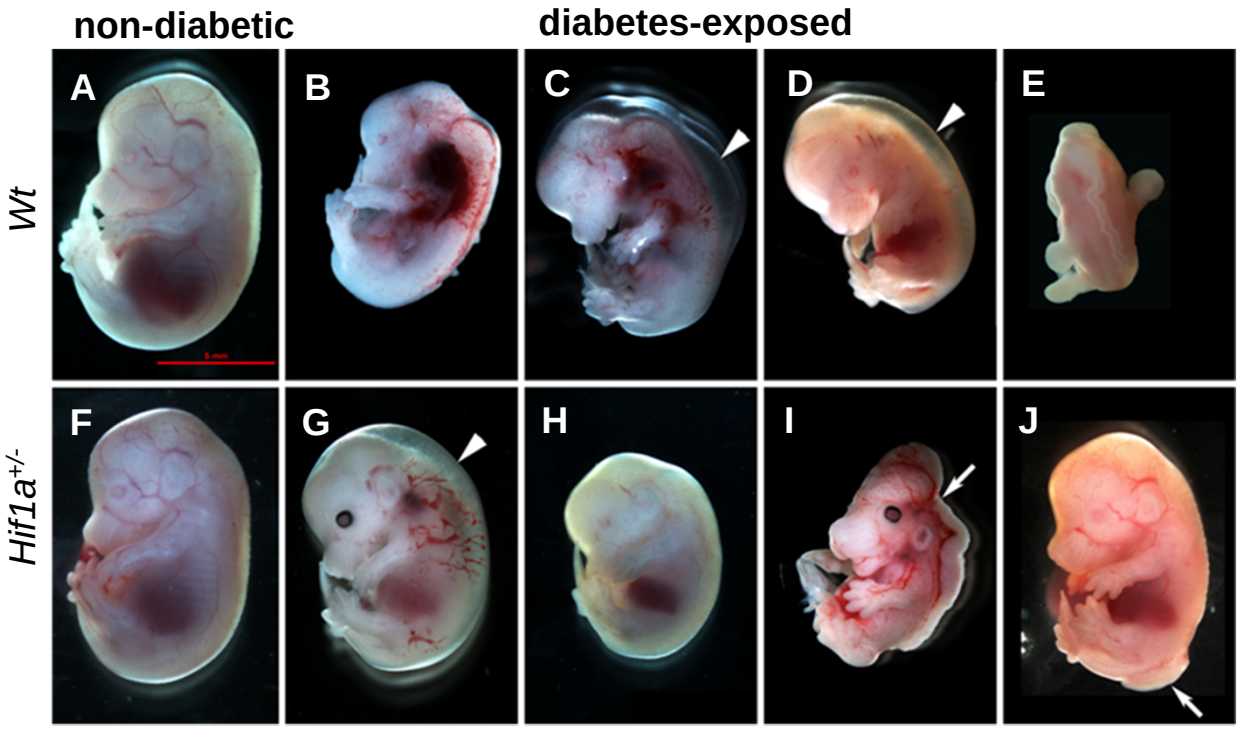
non-diabetic
diabetes-exposed
Wt
Hif1a+/-
A
B
C
D
E
F
G
H
I
J

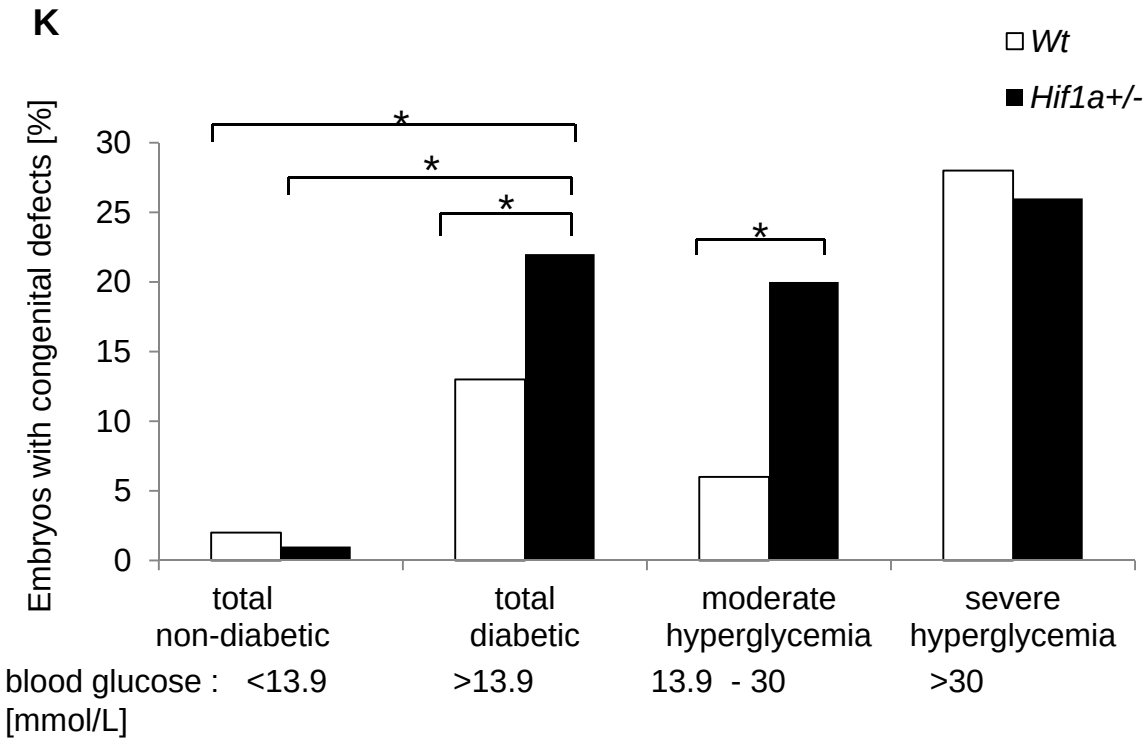
K
Wt
Hif1a+/-
Embryos with congenital defects [%]
30
25
20
15
10
5
0
*
*
*
*
total non-diabetic
total diabetic
moderate hyperglycemia
severe hyperglycemia
blood glucose : [mmol/L]
<13.9
>13.9
13.9 - 30
>30

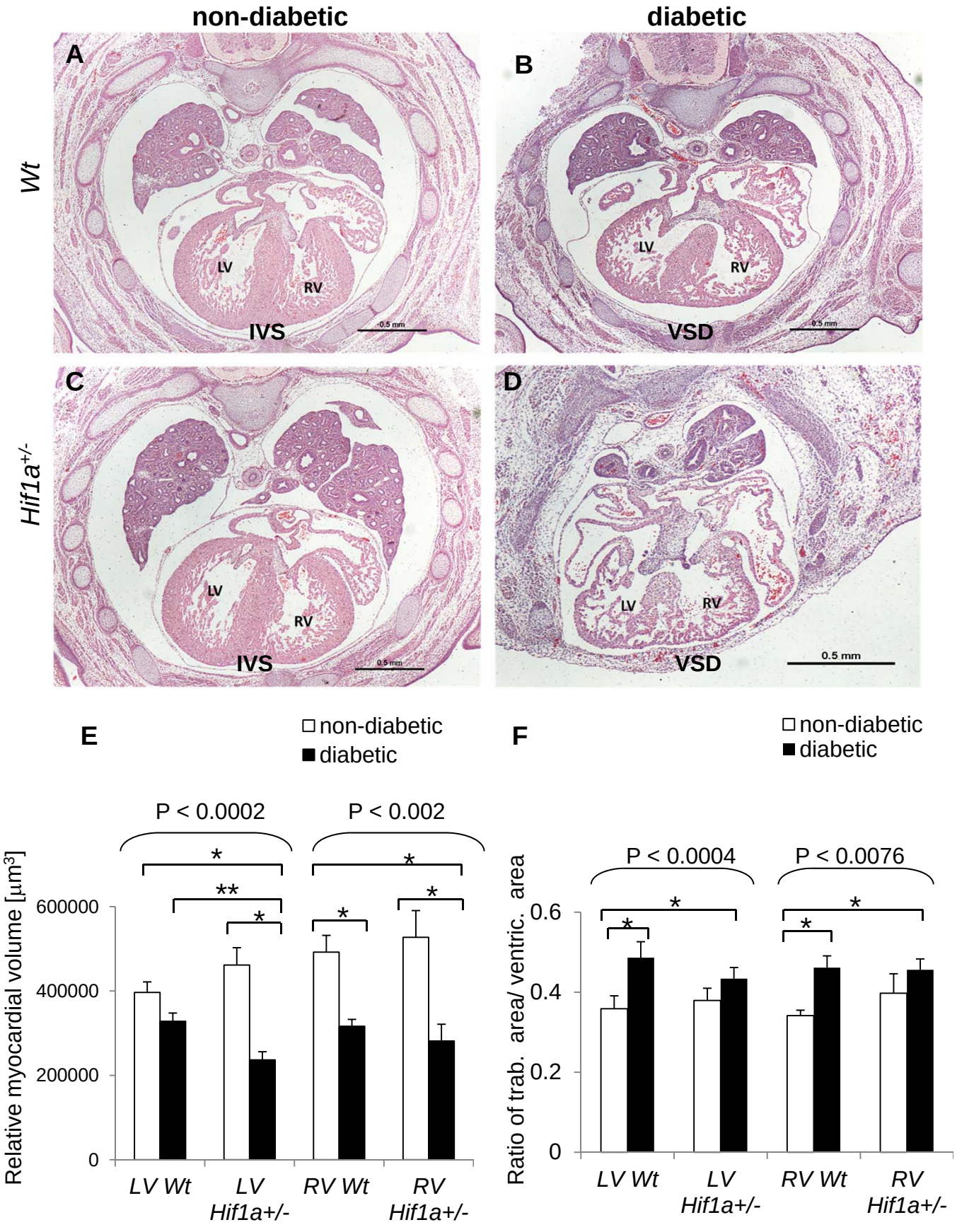
non-diabetic
diabetic
A
B
C
D
Wt
Hif1a+/-
LV
RV
IVS
VSD
0.5 mm
E
F
non-diabetic
diabetic
P < 0.0002
P < 0.002
P < 0.0004
P < 0.0076
Relative myocardial volume [µm3]
Ratio of trab. area/ ventric. area
600000
400000
200000
0
0.6
0.4
0.2
LV Wt
LV Hif1a+/-
RV Wt
RV Hif1a+/-

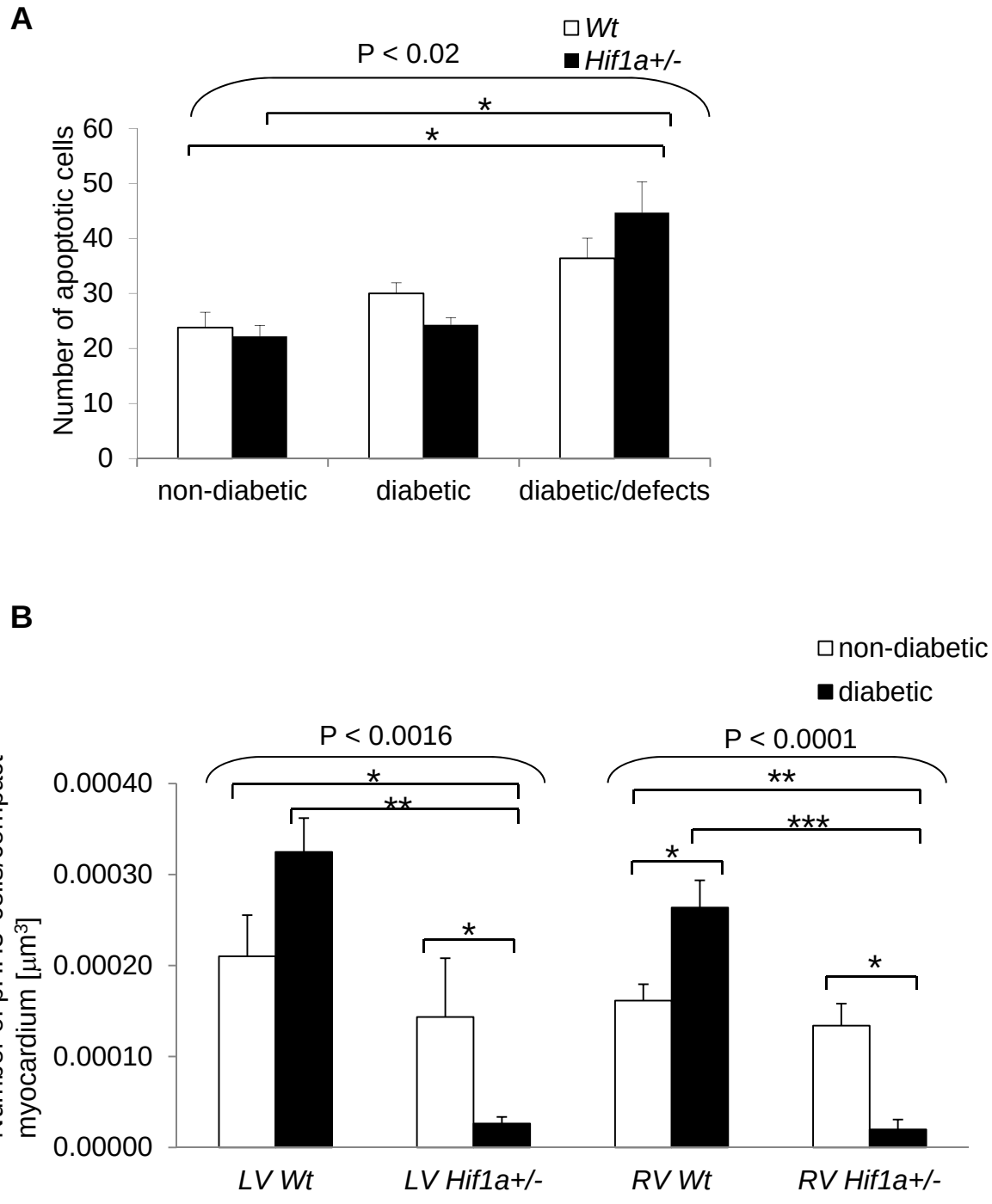
A
Wt
Hif1a+/-
P < 0.02
*
*
Number of apoptotic cells
60
50
40
30
20
10
0
non-diabetic
diabetic
diabetic/defects
B
non-diabetic
diabetic
P < 0.0016
P < 0.0001
*
**
*
**
***
*
*
*
Number of pHH3+cells/compact myocardium [µm3]
0.00040
0.00030
0.00020
0.00010
0.00000
LV Wt
LV Hif1a+/-
RV Wt
RV Hif1a+/-

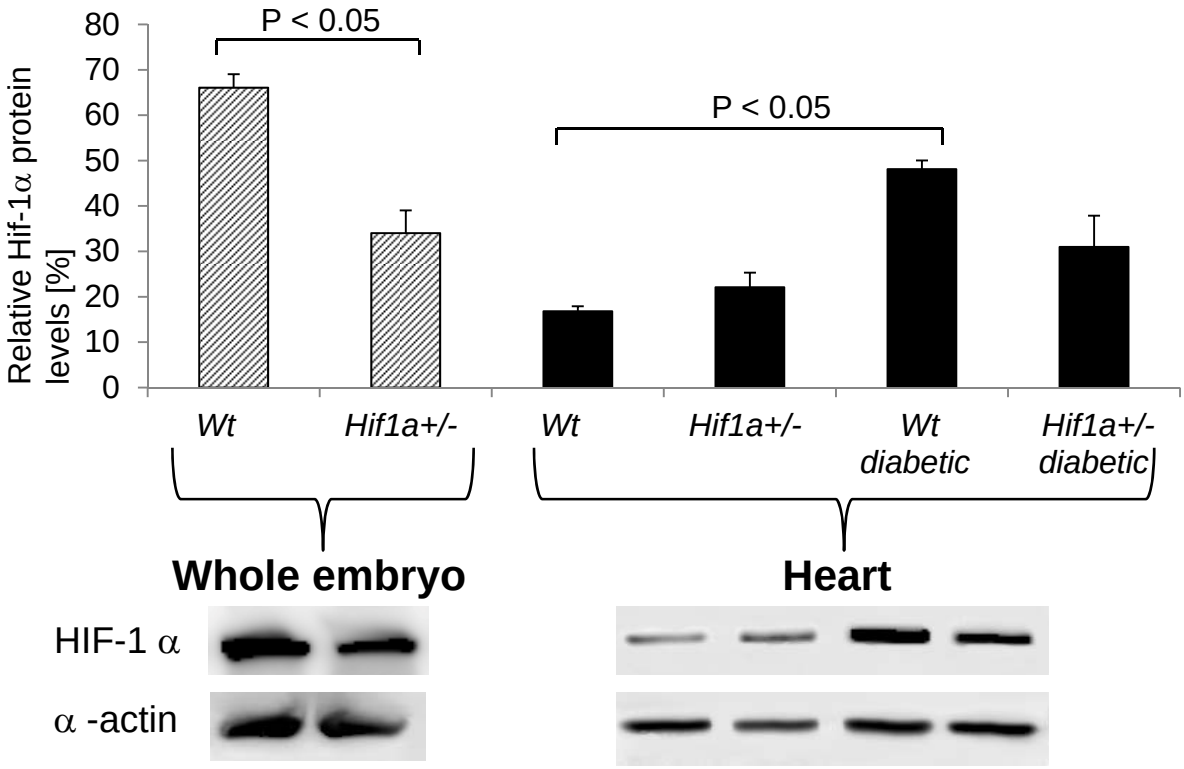
P < 0.05
P < 0.05
Relative Hif-1α protein levels [%]
80
70
60
50
40
30
20
10
0
Wt
Hif1a+/-
Wt
Hif1a+/-
Wt diabetic
Hif1a+/- diabetic
Whole embryo
Heart
HIF-1 α
α -actin

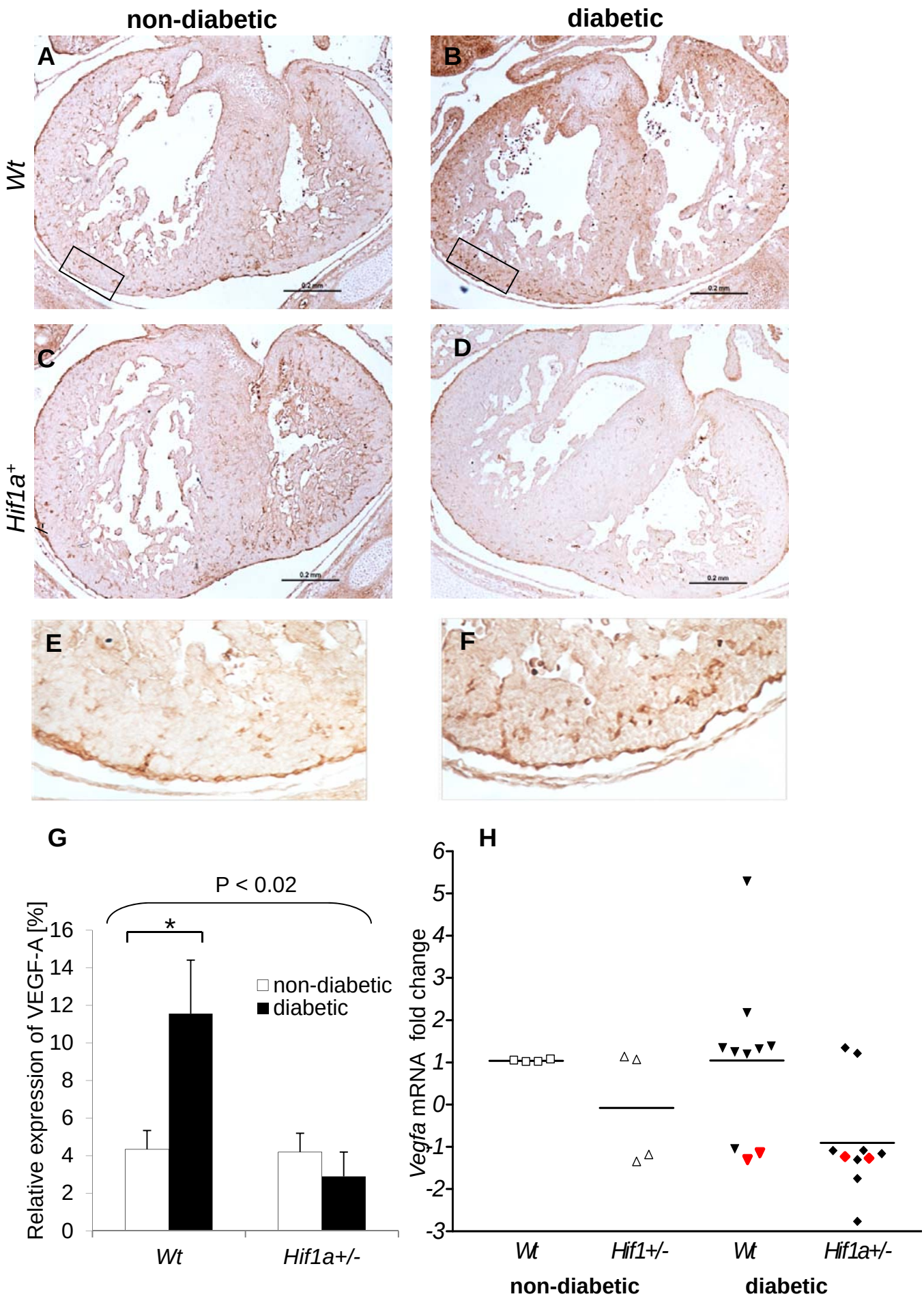
non-diabetic
diabetic
A
B
C
D
E
F
Wt
Hif1a+/-
0.2 mm
G
P < 0.02
*
Relative expression of VEGF-A [%]
16
14
12
10
8
6
4
2
0
non-diabetic
diabetic
Wt
Hif1a+/-
H
Vegfa mRNA fold change
6
5
4
3
2
1
0
-1
-2
-3
Wt
Hif1+/-
Wt
Hif1a+/-
non-diabetic
diabetic

A

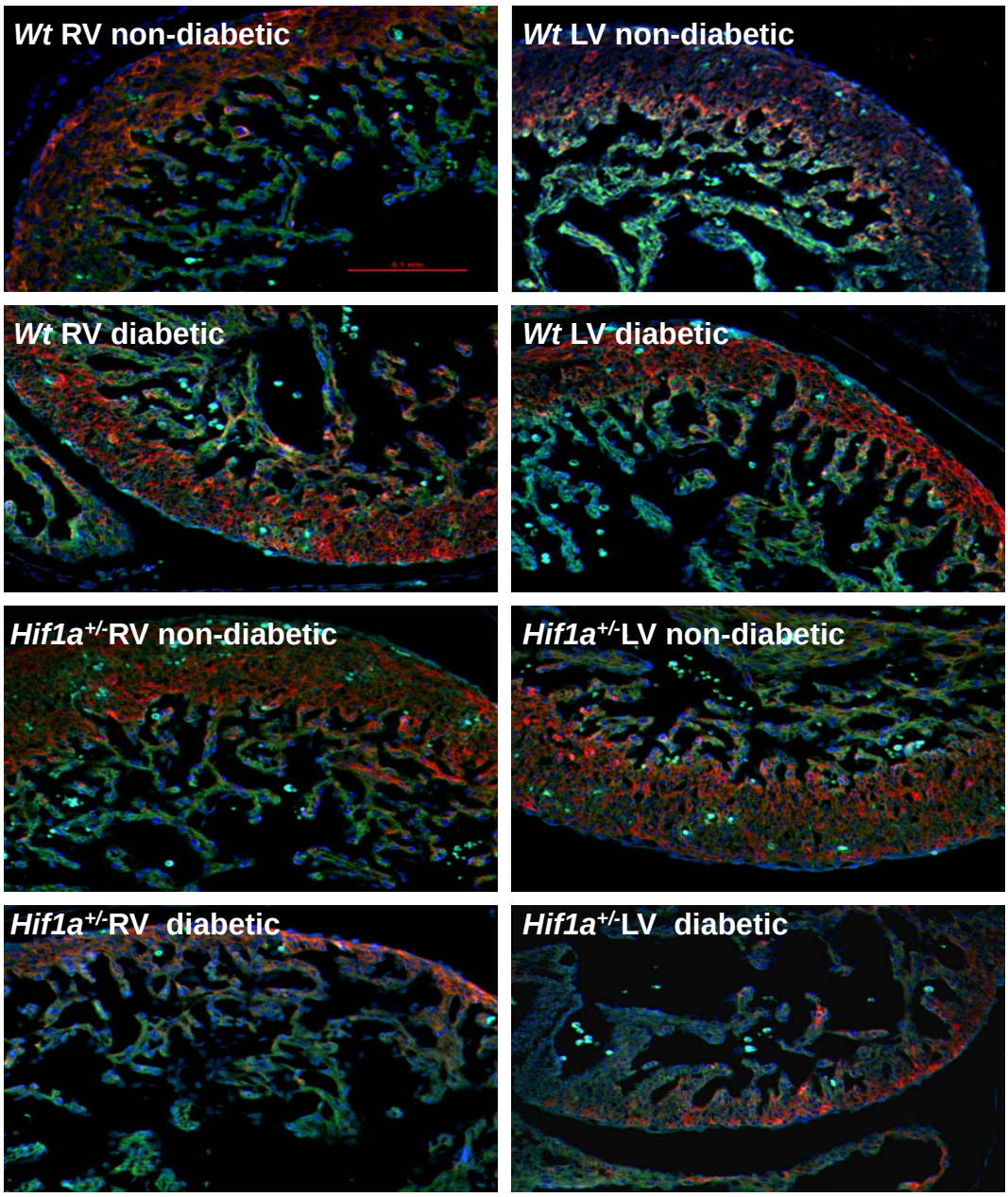
*Wt* RV non-diabetic
*Wt* LV non-diabetic
*Wt* RV diabetic
*Wt* LV diabetic
*Hif1a*$^{+/-}$RV non-diabetic
*Hif1a*$^{+/-}$LV non-diabetic
*Hif1a*$^{+/-}$RV diabetic
*Hif1a*$^{+/-}$LV diabetic

B

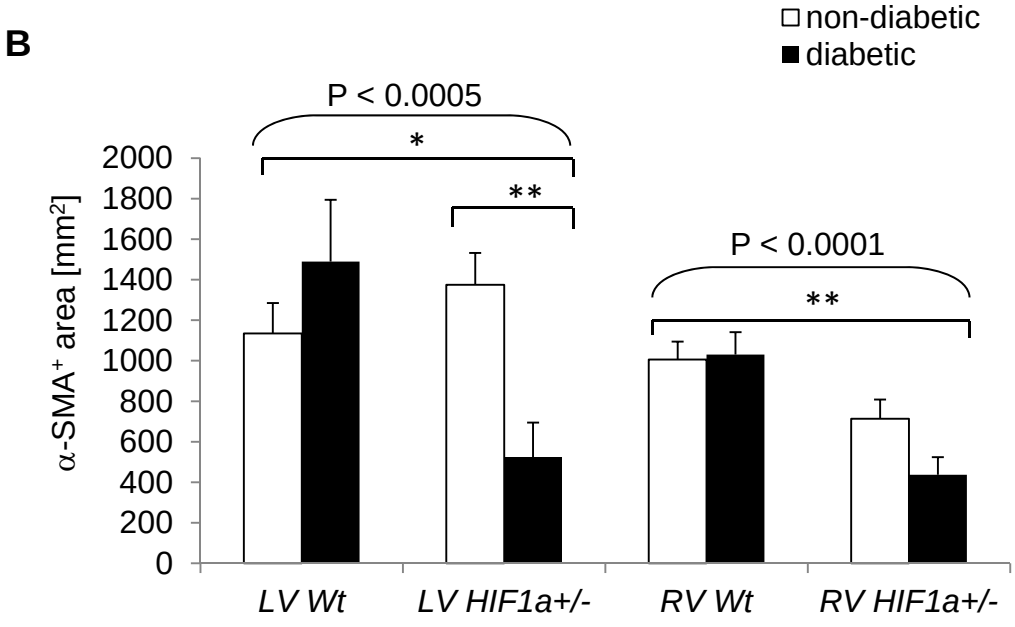
non-diabetic
diabetic
P < 0.0005
*
**
P < 0.0001
**
α-SMA⁺ area [mm²]
2000
1800
1600
1400
1200
1000
800
600
400
200
0
LV Wt
LV HIF1a+/-
RV Wt
RV HIF1a+/-

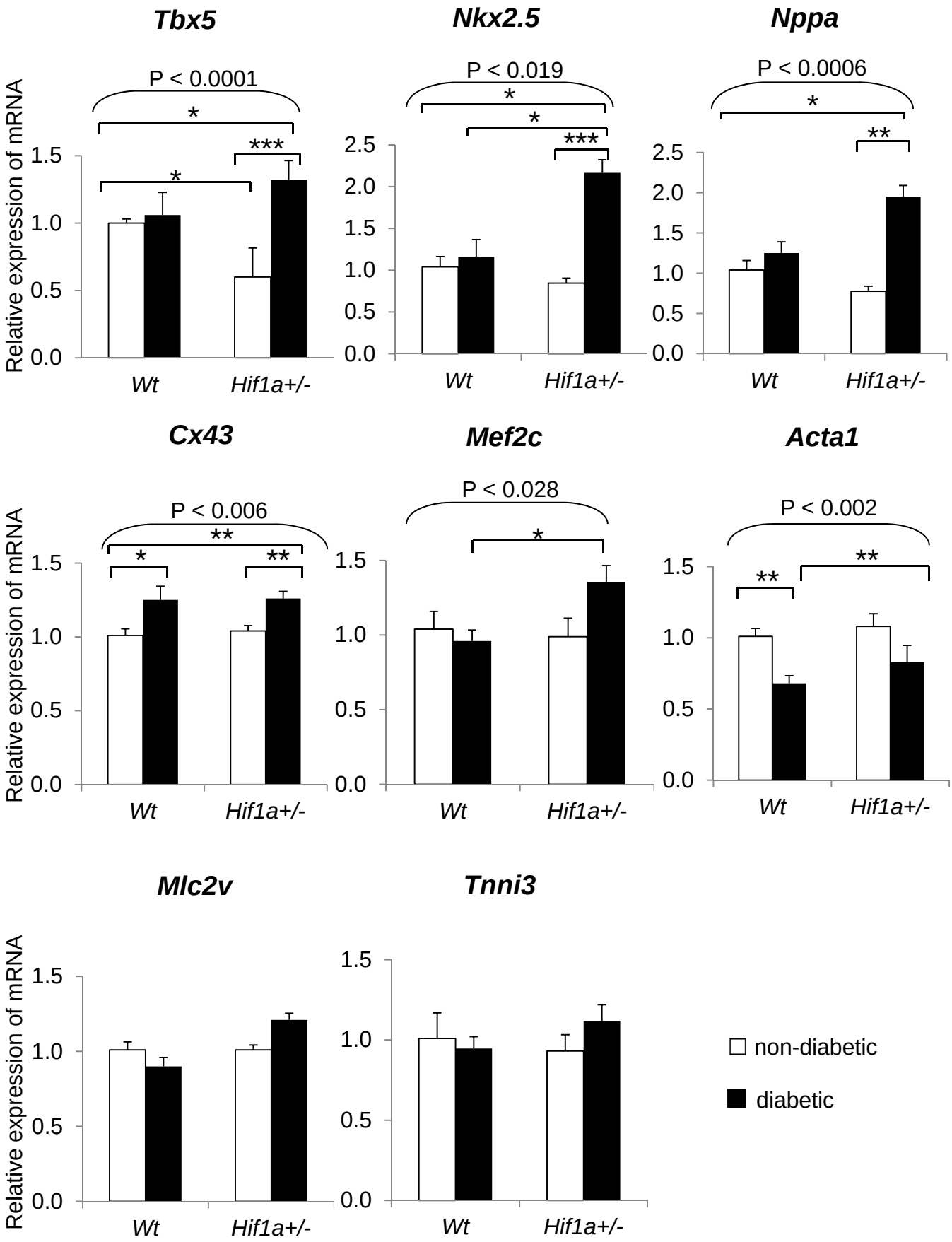
Tbx5
Nkx2.5
Nppa
Cx43
Mef2c
Acta1
Mlc2v
Tnni3
P < 0.0001
P < 0.019
P < 0.0006
P < 0.006
P < 0.028
P < 0.002
Relative expression of mRNA
Wt
Hif1a+/-
non-diabetic
diabetic

**Fig. S1**

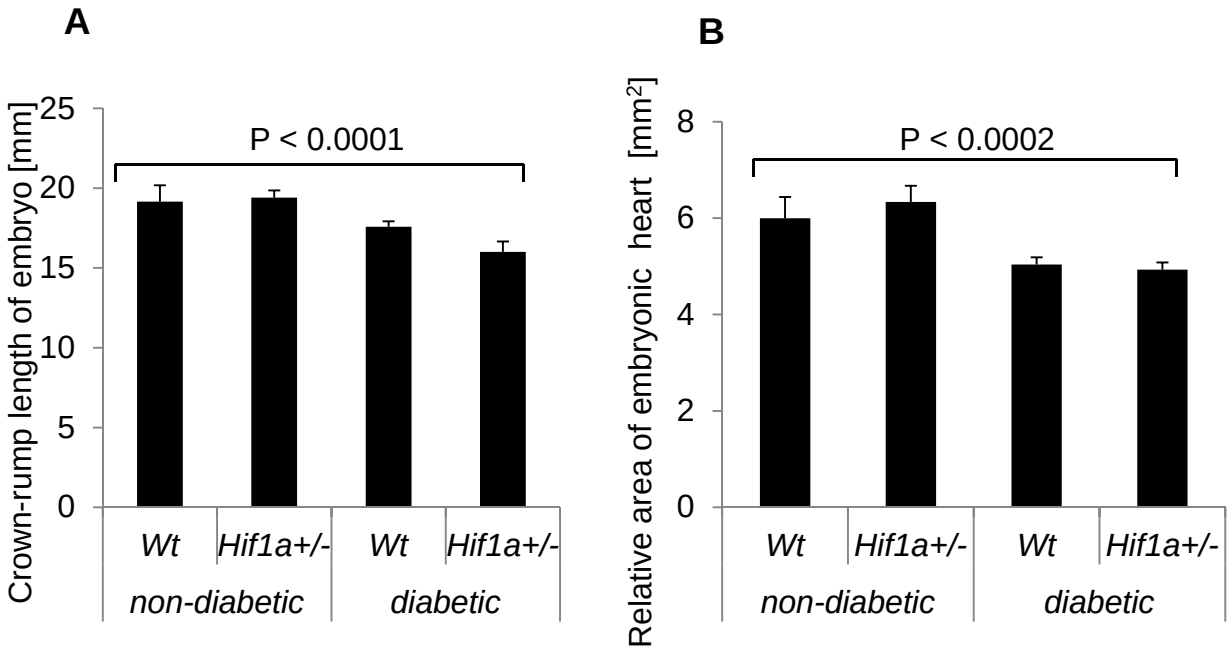
A
Crown-rump length of embryo [mm]
25
20
15
10
5
0
P < 0.0001
Wt
Hif1a+/-
Wt
Hif1a+/-
non-diabetic
diabetic
B
Relative area of embryonic heart [mm2]
8
6
4
2
0
P < 0.0002
Wt
Hif1a+/-
Wt
Hif1a+/-
non-diabetic
diabetic